شیمی وب، شبکه دوستداران شیمی

@ShimiWeb

Solutions to Problems

Chapter 1

1.1. a. A dipolar resonance structure has aromatic character in both rings and would be expected to make a major contribution to the overall structure.

b. The "extra" polarity associated with the second resonance structure would contribute to the molecular structure but would not be accounted for by standard group dipoles.

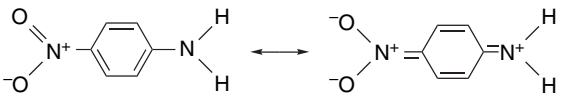

c. There are three major factors contributing to the overall dipole moments: (1) the σ-bond dipole associated with the C−O and C−N bonds; (2) the π-bond dipole associated with delocalization of π electrons from the heteroatom to the ring; and (3) the dipole moment associated with the unshared electron pair (for O) or N−H bond (for N). All these factors have a greater moment toward rather than away from the heteroatom for furan than for pyrrole. For pyrrole, the C−N π dipole should be larger and the N−H moment in the opposite direction from furan. These two factors account for the reversal in the direction of the overall dipole moment. The AIM charges have been calculated.

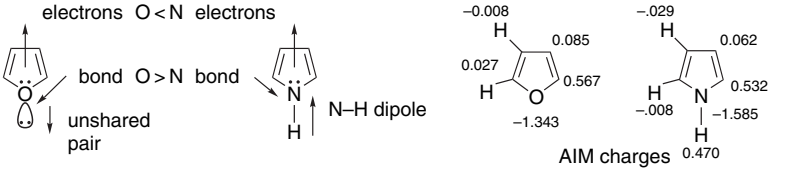

1.2. a. The nitrogen is the most basic atom.

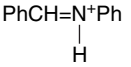

b. Protonation on oxygen preserves the resonance interaction with the nitrogen unshared electron pair.

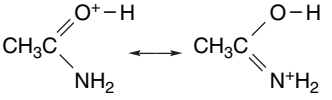

c. Protonation on nitrogen limits conjugation to the diene system. Protonation on C(2) preserves a more polar and more stable conjugated iminium system. Protonation on C(3) gives a less favorable cross-conjugated system.

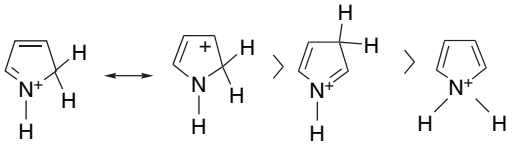

d. Protonation on the ring nitrogen preserves conjugation with the exocyclic nitrogen unshared electrons.

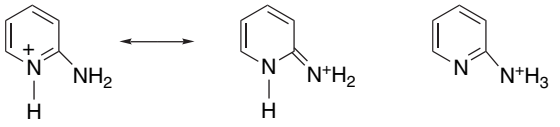

charge can be delocalized

charge is localized on exocyclic nitrogen

1.3. a. The dipolar resonance structure containing cyclopentadienide and pyridinium rings would be a major resonance contributor. The dipole moments and bond lengths would be indicative. Also, the inter-ring "double bond" would have a reduced rotational barrier.

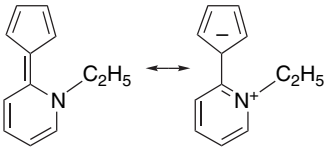

b. The dipolar oxycyclopropenium structure contributes to a longer C−O bond and an increased dipole moment. The C=O vibrational frequency should be shifted toward lower frequency by the partial single-bond character. The compound should have a larger pK_a for the protonated form, reflecting increased electron density at oxygen and aromatic stabilization of the cation.

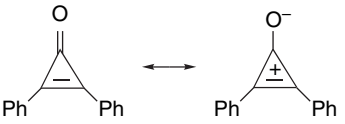

c. There would be a shift in the UV spectrum, the IR C=O stretch, and NMR chemical shifts, reflecting the contribution from a dipolar resonance structure.

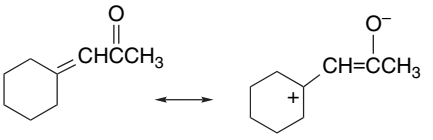

1.4. a. Amides prefer planar geometry because of the resonance stabilization. The barrier to rotation is associated with the disruption of this resonance. In MO terminology, the orbital with the C=O π^* orbital provides a stabilized delocalized orbital. The nonplanar form leads to isolation of the nitrogen unshared pair from the C=O system.

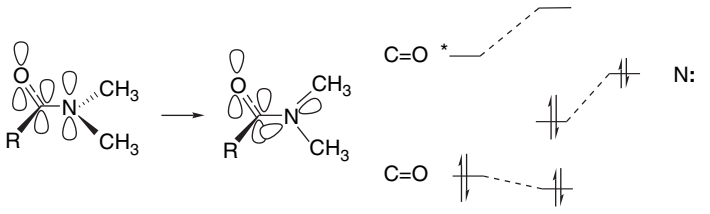

b. The delocalized form is somewhat more polar and is preferentially stabilized in solution, which is consistent with the higher barrier that is observed.

c. Amide resonance is reduced in the aziridine amide because of the strain associated with sp^2 hybridization at nitrogen.

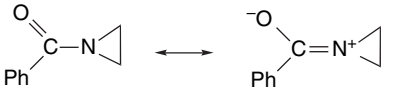

The bicyclic compound cannot align the unshared nitrogen electron pair with the carbonyl group and therefore is less stable than a normal amide.

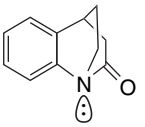

1.5. a. The site of protonation should be oxygen, since it has the highest negative charge density.

b. The site of reaction of a hard nucleophile should be C(1), the carbonyl carbon, as it has the most positive charge.
c. A soft nucleophile should prefer the site with the highest LUMO coefficient. The phenyl group decreases the LUMO coefficient, whereas an alkyl group increases it. Reaction would be anticipated at the alkyl-substituted carbon.

1.6. The gross differences between the benzo[b] and benzo[c] derivatives pertain to all three heteroatoms. The benzo[b] compounds are more stable, more aromatic, and less reactive than the benzo[c] isomers. This is reflected in both ΔH_f and the HOMO-LUMO gap. Also the greater uniformity of the bond orders in the benzo[b] isomers indicates they are more aromatic. Furthermore benzenoid aromaticity is lost in the benzo[b] adducts, whereas it increases in the benzo[c] adducts, and this is reflected in the TS energy and $\Delta H^{\ddagger}$. The order of $\Delta H^{\ddagger}$ is in accord with the observed reactivity trend O > NH > S. Since these dienes act as electron donors toward the dienophile, the HOMO would be the frontier orbital. The HOMO energy order, which is NH > S > O, does not accord with the observed reactivity.

1.7. The assumption of the C−H bond energy of 104 kcal/mol, which by coincidence is the same as the H−H bond energy, allows the calculation of the enthalpy associated with the center bond. Implicit in this analysis is the assumption that all of the energy difference resides in the central bond, rather than in strain adjustments between the propellanes and bicycloalkanes. Let BE_c be the bond energy of the central bond:

$$\Delta H = 2(\text{C}{-}\text{H}) - \text{BE}_c - \text{H}{-}\text{H} = 208 - \text{BE}_c - 104 = 104 - \text{BE}_c$$
$$\text{BE}_c[2.2.1]\text{propellane} = 104 - 95 = 5$$
$$\text{BE}_c[2.1.1]\text{propellane} = 104 - 73 = 31$$
$$\text{BE}_c[1.1.1]\text{propellane} = 104 - 39 = 65$$

This result indicates that while rupture of the center bond in [2.2.1]propellane is nearly energy neutral, the bond energy increases with the smaller rings. The underlying reason is that much more strain is released by the rupture of the [2.2.1]propellane bond than in the [1.1.1]propellane bond.

1.8. The various ΔH_{H2} values allow assigning observed ΔH_{H2} and ΔH_{isom} as in the chart below. Using the standard value of 27.4 kcal/mol for a *cis*-double bond allows the calculation of the heats of hydrogenation and gives a value for the "strain" associated with each ring. For example, the ΔH_{H2} of *cis*-cyclooctene is only 23.0 kcal/mol, indicating an increase of $27.4 - 23.0 = 4.4$ kcal/mol of strain on going to cyclooctane. The relatively high $\Delta \text{H}_{\text{H2}}$ for *trans*-cyclooctene reflects the release of strain on reduction to cyclooctane. The "strain" for each compound is a combination of total strain minus any stabilization for conjugation. The contribution of conjugation can be seen by comparing the conjugated 1,3-isomer with the unconjugated 1,4- and 1,5-isomers of cyclooctadiene and is about 4 ± 1 kcal/mol. Since the "strain" for cyclooctatetraene is similar to the other systems, there is no evidence of any major stabilization by conjugation.

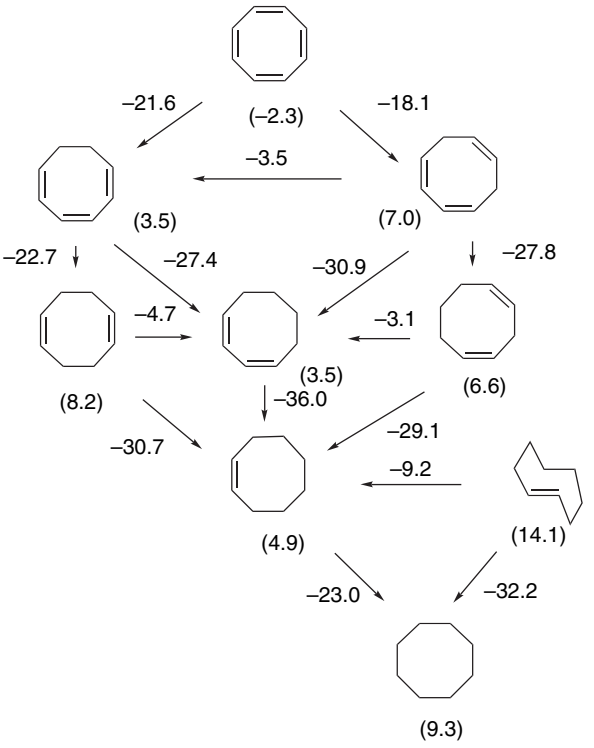

1.9. By subtracting the value for X=H from the other values, one finds the "additional" resonance stabilization associated with the substituent. There is some stabilization associated with the methyl and ethyl groups and somewhat more for ethenyl and ethynyl. This is consistent with the resonance concept that the unsaturated functional groups would "extend" the conjugation. The stabilization for amino is larger than for the hydrocarbons, suggesting additional stabilization associated with the amino group. The stabilizations calculated are somewhat lower than for the values for groups directly on a double bond.

1.10. The gas phase ΔG gives the intrinsic difference in stabilization of the anion, relative to the corresponding acid. The reference compound, CH_3CO_2H, has the highest value and therefore the smallest intrinsic relative stabilization. The differential solvation of the anion and acid can be obtained from p. 5 by subtracting the solvation of the acid from the anion. The numbers are shown below. The total stabilization favoring aqueous ionization, relative to acetic acid, is the sum of the intrinsic stabilization and the solvation stabilization. These tend to be in opposite directions, with the strongest acids having high intrinsic stabilization, but negative relative solvation.

X	Net solvation	Intrinsic	total	Δ
CH_3	$77.58 - 7.86 = 69.72$	345.94	$345.94 - 69.72 = 276.22$	–
H	$77.10 - 8.23 = 68.87$	342.49	$342.49 - 68.87 = 273.62$	−2.60
$ClCH_2$	$70.57 - 10.61 = 59.96$	333.50	$333.50 - 59.96 = 273.54$	−2.68
$NCCH_2$	$69.99 - 14.52 = 55.47$	327.66	$327.66 - 55.47 = 272.19$	−4.03
$(CH_3)_3C$	$72.42 - 6.70 = 65.72$	341.71	$341.71 - 65.72 = 275.99$	+0.23

We see that the final stabilization relative to acetic acid gives the correct order of pK_a. Interestingly, the solvation of the stronger acids is less than that of the weaker acids. This presumably reflects the effect of the stronger internal stabilization. These data suggest that intrinsic stabilization dominates the relative acidity for this series, with solvation differences being in the opposite direction.

1.11. These observations are the result of hyperconjugation between the nitrogen unshared electron pair and the axial C−H bonds. The chair conformation of the piperidine ring permits the optimal alignment. The weaker C−H bond reflects N :→ σ* delocalizations. The greater shielding of the axial hydrogen is also the result of increased electron density in the C−H bond. The effect of the axial methyl groups is one of raising the energy of the unshared electrons on nitrogen and stabilizing the radical cation.

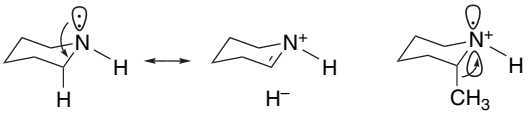

1.12. a–c. Each of these substitutions involves extending the conjugated system and results in an MO pattern analogous to allyl for fluoroethene and to butadiene for propenal and acrylonitile, respectively.

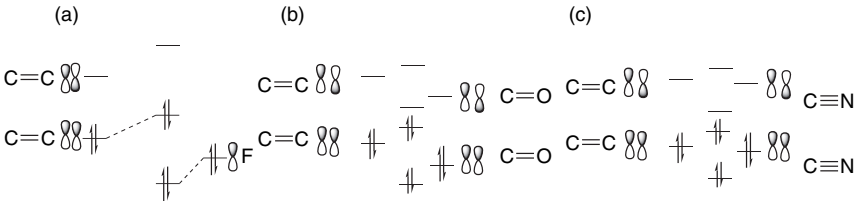

d. The addition of the methyl group permits σ → π* and π → σ* interactions that can be depicted by the π-type methyl orbitals. The σ orbitals can be depicted as the *symmetry-adapted* pairs shown. As a first approximation, one of each pair will be unperturbed by interaction of the adjacent π orbital because of the requirement that interacting orbitals have the same symmetry.

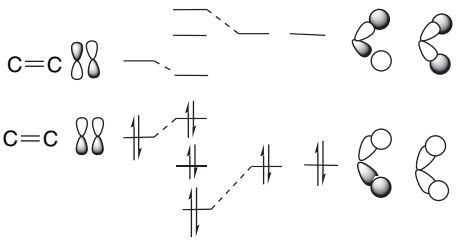

e–f. The substituents add an additional *p* orbital converting the conjugated system to a benzyl-like system. In the benzyl cation, the ψ_4 orbital is empty, resulting in a positive charge. In fluorobenzene, the p_z orbital on fluorine

will be conjugated with the π system and ψ_4 will be filled. This results in delocalization of some π-electron density from fluorine to the ring. The electronegative character of fluorine will place the orbitals with F participation at somewhat lower energy than the corresponding orbitals in the benzyl system. As a first approximation, the two benzene orbitals with nodes at C(1) will remain unchanged.

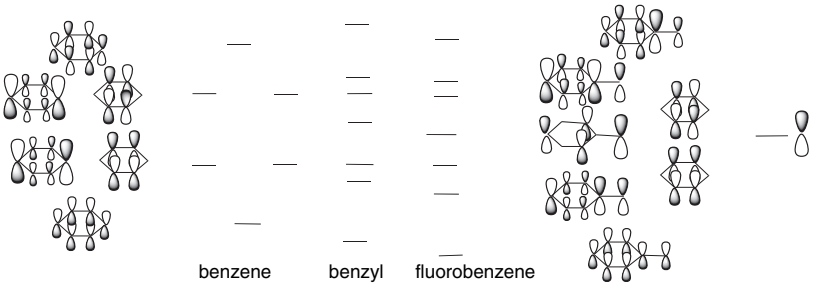

Comment. With the availability of suitable programs, these orbitals could be calculated.

1.13. a. The resonance interactions involve $\sigma \rightarrow \pi^*$ hyperconjugation in the case of methyl and $n \rightarrow \pi^*$ conjugation in the case of NH_2, OH, and F, as depicted below.

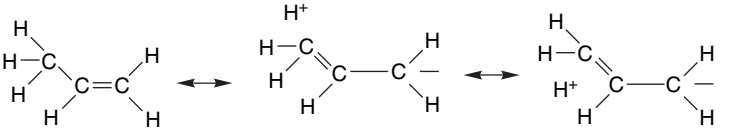

$CH_2=CH-X: \longleftrightarrow {}^{-}CH_2-CH=X^{+}$

VB description of interaction
with donor substituents

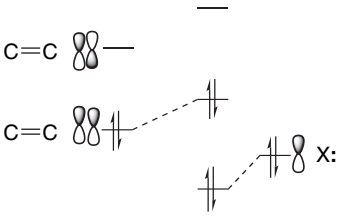

MO description of interaction
with donor substituents

b. There are two major stabilizing factors at work. One is the π delocalization depicted for both the methyl group and heteroatoms. The order of this effect should be $NH_2 > OH > CH_3$, which is in accord with the observed order of the increase in stability. The other factor is the incremental polarity of the bonds, where an increment in stability owing to the electronegativity difference should occur. This should be in the order $F > OH > NH_2$, but this order seems to be outweighed by the effect of the π-electron delocalization.

c. The NPA charges are in qualitative agreement with the resonance/polar dichotomy. The electron density on the unsubstituted carbon C(2) increases, as predicted by the resonance structures indicating delocalization of the heteroatom unshared electron pair. The charge on the substituted carbon C(1) increases with the electronegativity of the substituent. As is characteristic (and based on a different definition of atomic charge), the AIM charges are dominated by electronegativity differences. There is some indication of the π-donor effect in that C(2) is less positive in the order $NH_2 < OH < F$.

1.14. a. In the strict HMO approximation, there would be two independent π and π^* orbitals, having energies that are unperturbed from the isolated double bonds, which would be $\alpha + \beta$ in terms of the HMO parameters.

b. There would now be four combinations. The geometry of the molecule tilts the orbitals and results in better overlap of the *endo* lobes. ψ_1 should be stabilized, whereas ψ_2 will be somewhat destabilized by the antibonding interactions between C(2) and C(6) and C(3) and C(5). ψ_3 should be slightly stabilized by the cross-ring interaction. The pattern would be similar to that of 1,3-butadine, but with smaller splitting of ψ_1 and ψ_2 and ψ_3 and ψ_4.

c. The first IP would occur from ψ_2, since it is the HOMO and the second IP would be from ψ_1. The effect of the donor substituent is to lower both IPs, but IP_1 is lowered more than IP_2. The electron-withdrawing substituent increases both IPs by a similar amount. The HOMO in the case of methoxy will be dominated by the substituted double bond, which becomes more electron rich as a result of the methoxy substituent. The cyano group reduces the electron density at both double bonds by a polar effect and conjugation.

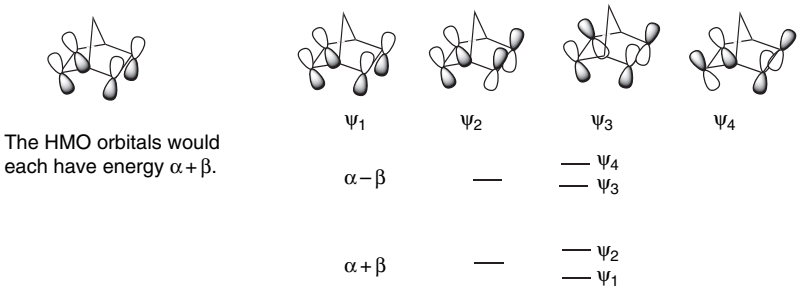

1.15. a. Since there are four π electrons in the pentadienyl cation, ψ_2 will be the HOMO.

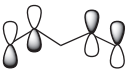

b. From the coefficients given, the orbitals are identified as ψ_2 and ψ_3, shown below. ψ_2 is a bonding orbital and is antisymmetric. ψ_3 is a nonbonding orbital and is symmetric.

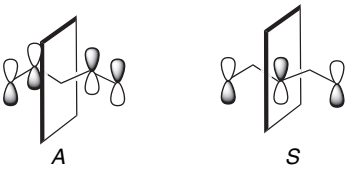

1.16. The positive charge on the benzylic position increases with the addition of the EWG substituents, which is consistent with the polarity of these groups. There is relatively little change at the ring positions. All the cations show that a substantial part of the overall cationic charge is located on the hydrogens. There is a decrease in the positive charge at the *para* position, which is consistent with delocalization to the substituent. All the structures show very significant bond length alterations that are consistent with the resonance structures for delocalization of the cation charge to the ring, especially the *para* position.

1.17. a. In terms of x the four linear homogeneous equations for butadiene take the form:

$$\begin{aligned} a_1x + a_2 &= 0 \\ a_1 + a_2x + a_3 &= 0 \\ a_2 + a_3x + a_4 &= 0 \\ a_3 + a_4x &= 0 \end{aligned}$$

where $x = -1.62$, -0.618, 0.618, and 1.62.

For ψ_1, $x = -1.62$, and we obtain

$$\begin{aligned} -1.62a_1 + a_2 &= 0 \\ a_1 - 1.62a_2 + a_3 &= 0 \\ a_2 - 1.62a_3 + a_4 &= 0 \\ a_3 - 1.62a_4 &= 0 \end{aligned}$$

The first equation yields

$$a_2 = 1.62a_1$$

Substitution of this value for a_2 into the second equation gives

$$a_1 - 1.62(1.62a_1) + a_3 = 0$$

or

$$a_3 = 1.62a_1$$

From the last equation, we substitute the a_3 in terms of a_1 and obtain

$$\begin{aligned} 1.62a_1 - 1.62a_1 &= 0 \\ a_4 &= a_1 \end{aligned}$$

We must normalize the eigenfunction:

$$a_1^2 + a_2^2 + a_3^2 + a_4^2 = 1$$

Making the appropriate substitutions gives

$$a_1{}^2 + 2.62a_1{}^2 + 2.62a_1{}^2 + a_1{}^2 = 1$$

$$a_1 = \frac{1}{\sqrt{7.24}}$$

$$a_1 = 0.372$$

$$a_2 = 0.602$$

$$a_3 = 0.602$$

$$a_4 = 0.372$$

and

$$\psi_1 = 0.372p_1 + 0.602p_2 + 0.602p_3 + 0.272p_4$$

To obtain the coefficients for ψ_2 we use the value of x, $x = -0.618$, and carry out the same procedure that is illustrated above. The results are:

$$a_2 = 0.618a_1$$

$$a_3 = -0.618a_1$$

$$a_4 = -a_1$$

and

$$a_1{}^2 + 0.382a_1{}^2 + 0.382a_1{}^2 + a_1{}^2 = 1$$

$$a_1 = \frac{1}{\sqrt{2.76}}$$

$$a_1 = 0.602$$

$$a_2 = 0.372$$

$$a_3 = 0.372$$

$$a_4 = 0.602$$

and

$$a_1{}^2 + 0.382a_1{}^2 + 0.382a_1{}^2 + a_1{}^2 = 1$$

$$a_1 = \frac{1}{\sqrt{2.76}}$$

$$a_1 = 0.602$$

$$a_2 = 0.372$$

$$a_3 = 0.372$$

$$a_4 = 0.602$$

$$\psi_2 = 0.602p_1 + 0.372p_2 - 0.372p_3 - 0.602p_4$$

Using the values $x = 0.618$ and 1.62, we repeat the same procedure for ψ_3 and ψ_4. The four eigenfunctions for butadiene are:

$$\psi_1 = 0.372p_1 + 0.602p_2 - 0.602p_3 - 0.372p_4$$
$$\psi_2 = 0.602p_1 + 0.372p_2 - 0.372p_3 - 0.602p_4$$
$$\psi_3 = 0.602p_1 + 0.372p_2 - 0.372p_3 - 0.602p_4$$
$$\psi_4 = 0.372p_1 + 0.602p_2 - 0.602p_3 - 0.372p_4$$

b.

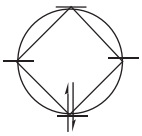

The MO diagram can be constructed using the Frost Circle. The energy of the occupied orbital is $\alpha + 2\beta$, so there is a stabilization of 2β, nominally the same as benzene, suggesting substantial stabilization for this ion.

c. The longest UV-VIS band should correspond to the HOMO-LUMO gap. For 1,3,5,7-octatetraene and 1,3,5-hexatriene the HMO orbitals are as follows:

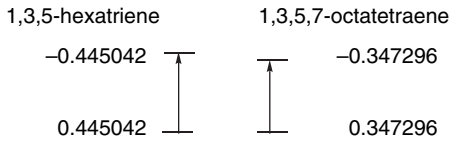

The energy gap decreases with the length of the conjugated system, and therefore the 1,3,5,7-octatetraene absorption should occur at longer wavelengths.

1.18. a. The additional strain in spiropentane relative to cyclopropane is due to the fact that there can be no relief of strain by rehybridization of the spiro carbon. By symmetry it is tetrahedral and maintains sp^3 hybridization.

b. These values provide further indication of the strain in spiropentane. The internal angle is close to that of an equilateral triangle (as in cyclopropane). The 137° value indicates considerable strain from the ideal 109° for an sp^3 carbon. This strain induces rehybridization in the C(2) and C(3) carbons.

c. Using 0.25 as the *s* character in the spiro carbon, we find the *s* character in the C(1)−C(2) bond to be $20.2 = 550(0.25)(x)$. The *s* character is 14.5%. For the C(2)−C(3) bond, $7.5 = 550(x^2)$. The fractional s character is 11.7%.

1.19. a. This reaction would be expected to be unfavorable, since cyclopropane is more acidic than methane. The increased *s* character of the cyclopropane C−H bond makes it more acidic. A gas phase measurement indicates a difference in ΔH of about 5 kcal/mol.

b. This comparison relates to the issue of whether a cyano group is stabilizing (delocalization) or destabilizing (polar) with respect to a carbocation (see p. 304). The results of a HF/3-21G calculation in the cited reference indicate a net destabilization of about 9 kcal/mol, in which case the reaction will be exothermic in the direction shown.

c. The polar effects of the fluorine substituents should strongly stabilize negative charge on carbon, suggesting that the reaction will be exothermic. An MP4SDTQ/6-31++(d,p) calculation finds a difference of ~ 45 kcal/mol.

1.20. a. Because of the antiaromaticity of the cyclopentadienyl cation (p. 31), the first reaction would be expected to be the slower of the two. The reaction has not been observed experimentally, but a limit of $< 10^{-5}$ relative to cyclopentyl iodide has been placed on its rate.

b. The cyclopropenyl anion is expected to be destabilized (antiaromatic). Therefore, K should be larger for the first reaction. An estimate based on the rate of deuterium exchange has suggested that the pK difference is at least 3 log units.

c. The second reaction will be the fastest. The allylic cation is stabilized by delocalization, but the cyclopentadienyl cation formed in the first reaction is destabilized.

1.21. The diminished double-bond character indicates less delocalization by conjugation in the carbene, which may be due to the electrostatic differences. In the carbocation, delocalization incurs no electrostatic cost, since the net positive charge of 1 is being delocalized. However in **B**, any delocalization has an electrostatic energy cost, since the localized sp^2 orbital represents a negative charge in the overall neutral carbene.

1.22. The results are relevant to a significant chemical issue, namely the stability of imines. It is known that imines with N-π-donor substituents, such as oximes (YX=HO) and hydrazones (YX = H_2N), are more stable to hydrolysis than alkyl (YX = H_3C). The classical explanation is ground state resonance stabilization:

The stabilization is greatest for the F > OH > NH_2 series of substituents. The silyl group (ERG) is destabilizing, and the conjugated EWG groups are moderately stabilizing. The most significant structural change is in the bond angle, which implies a change in hybridization at nitrogen. The NPA charges show a buildup of charge on carbon for NH_2, OH, and F of about the same magnitude for each. This could result from the π delocalization. The charges on N are negative (except for F, where it is neutral) and seem to be dominated by the electronegativity of the substituent atom with the order being Si > C > N > O > F. These results indicate that as the substituent becomes more electronegative, the unshared pair orbital has more s character. (Results not shown here for X = Li and Na indicate that the lone pair is p in these compounds.) At least part of the stabilization would then be due to the more stable orbital for the unshared electron pair. A second factor in the stabilization may be a bond strength increment from the electronegativity difference between X and N.

1.23. The NPA charges indicate that the planar (conjugated) structures have characteristics associated with amide resonance. The oxygen charge in formamide is -0.710 in the planar form and -0.620 in the twisted form. For the NH_2 group, the charge is -0.080 in the planar form and -0.182 in the twisted form. These differences indicate more N to O charge transfer in the planar form. For 3-aminacrolein, the corresponding numbers are $O_{(planar)}: -0.665$, $O_{(twisted)}: -0.625$ and $NH_{2(planar)}: -0.060$, $NH_{2(twisted)}: -0.149$. These values indicate somewhat

less polarization associated with the (vinylic) resonance in this compound. For squaramide, the magnitude of the charges is similar $O(1)_{(planar)}$: −0.655; $O(1)_{(twisted)}$: −0.609 and $NH_{2(planar)}$: −0.001, $NH_{2(twisted)}$: −0.095. The differences in the ^{17}O chemical shifts and the rotational barrier also indicate greater resonance interaction in formamide than in 3-aminoacrolein and squaramide. The interaction maps show that the nitrogen is repulsive toward a positive charge in the planar forms, but becomes attractive in the twisted form. The attractive region is associated with the lone pair on the nitrogen atom in the twisted form.

Chapter 2

2.1. a. diastereomers; b. enantiomers; c. enantiomers; d. diastereomers; e. enantiomers; f. enantiomers.

2.2. a. *S*; $CH(C)_2 > CH_2CH(C)_2 > CH_2CH_2 > H$
b. *R*; Si > O > C > H
c. *R*; O > C=O > $C(C)_3$ > H
d. *R*; O > $C(C)_3$ > CH_2 > H
e. *S*; O > $C(C)_3C(C)_2H > C(C)_3C(C)H_2 > C(C)_2H$
f. *R*; N > $C(O)_3$ > $C(C)_2H$ > $C(C)H_2$
g. *R*; O > $C(C)_3$ > CH_3 > : (electron pair)

2.3.

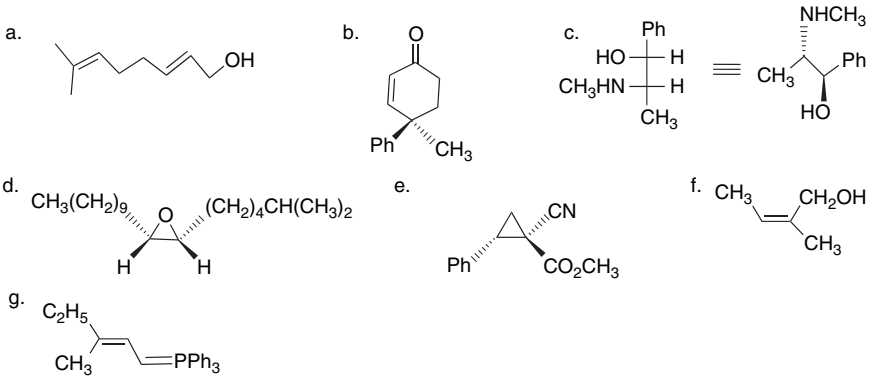

2.4.

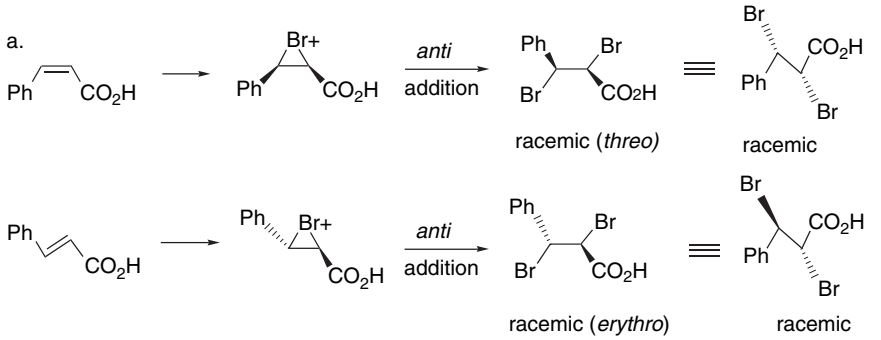

b.

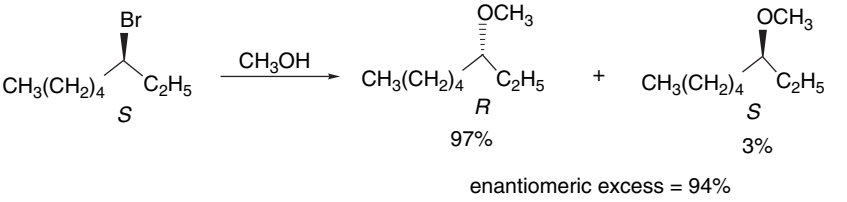

enantiomeric excess = 94%

c.

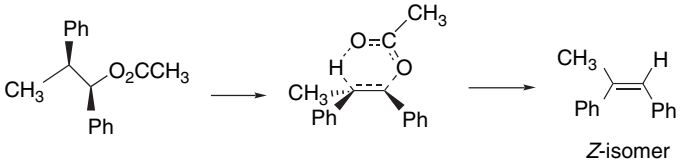

Z-isomer

d.

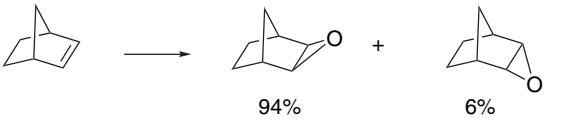

94% 6%

2.5. The solution to this problem lies in recognizing that there are steric differences for the phenyl group in the axial and equatorial conformations. In the equatorial position, the phenyl group can adopt an orientation that is more or less "perpendicular" to the cyclohexane ring, which minimizes steric interactions with the 2,6-equatorial hydrogens. In the axial conformation, the phenyl group is forced to rotate by about 90°, which adds to the apparent $-\Delta G_c$ for the phenyl group. When a 1-methyl substituent is present, the favorable "perpendicular" is no longer available and this destabilizes the equatorial orientation relative to phenylcyclohexane.

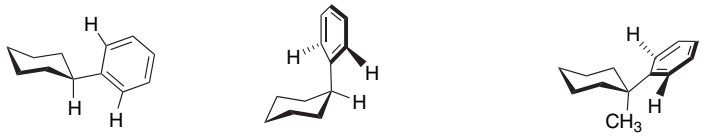

preferred conformation of *eq* 1-phenylcyclohexane

preferred conformation of *ax* 1-phenycyclohexane

methyl group precludes preferred conformation and adds a destabilizing interaction with 2,6-*eq* hydrogens

Comment. This is a challenging question but can be approached effectively by MM modeling, as was done in the original and subsequent references.

2.6. As discussed on p. 148, the preferred conformation of acetone is the C−H/C=O eclipsed conformation. This is stabilized by a $\sigma \rightarrow \pi^*$ interaction. For 2-butanone the C(4)/C=O eclipsed is preferred, as discussed on p. 148 and illustrated by Figure 2.12. For 3-methyl-2-butanone, four distinct conformations arise. The maxima at 60° and 180° represent the CH_3/CH_3 eclipsed conformations, which give rise to a barrier of about 2.5 kcal/mol. This is somewhat less than for the CH_3/CH_3 eclipsed conformation of butane and presumably reflects the absence of additional H/H eclipsing. An analysis of the 3-methyl-2-butanone spectrum is available in Ref. 36, p. 149.

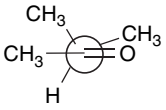

0°; 240° CH_3/C=O eclipsed

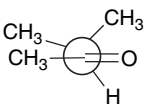

60°, 180°, staggered CH_3/CH_3 eclipsed

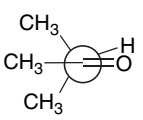

120°, H/C = O eclipsed

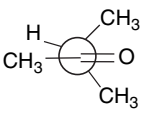

300°, staggered CH_3/H eclipsed

2.7. The stereochemistry of all of these reactions is governed by steric approach control.

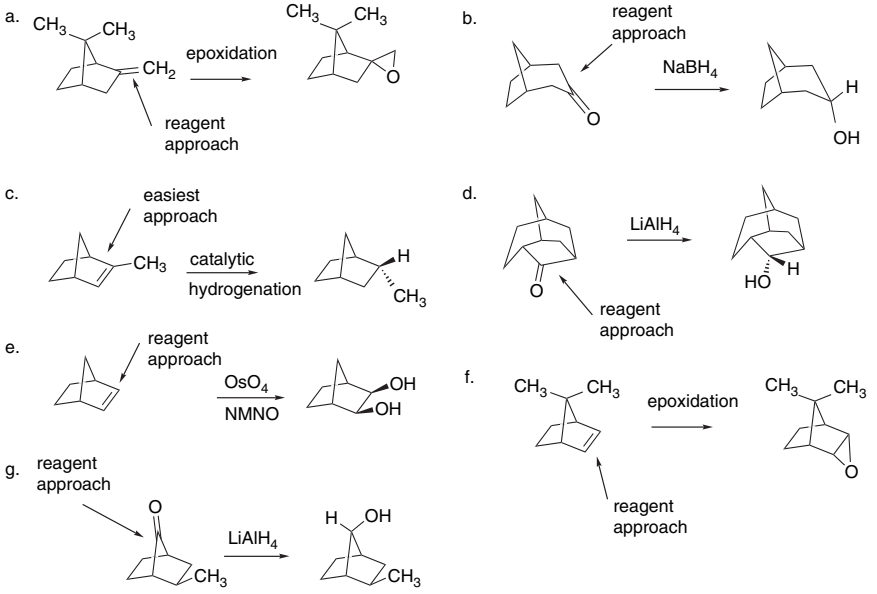

2.8. a, b. The conformers of 2-methylbutane differ by one "double" *gauche* interaction. The conformation of 2-methylbutane that avoids this interaction is favored by 0.9 kcal. There is good agreement between experimental and ab initio results. Surprisingly, the two conformations of 2,3-dimethylbutane are virtually equal in energy, by experimental, MM, and ab initio results. The qualitative "double" gauche argument fails in this case.

c. This is an example of the 3-alkyl ketone effect (p. 161), by which the conformational free energy of a 3-alkyl substituent is smaller than that in cyclohexane. The ΔG_c has been estimated as 0.55 kcal/mol.

Comment. Assuming availability of a suitable program, this question can framed as an exercise to calculate and compare the energies of the two conformations of each compound.

2.9. An estimate can be made by assuming additive ΔG_c and adding an increment (3.7 kcal/mol) for 1,3-diaxial interactions between methyl groups. The reference takes a somewhat different approach, summing *gauche* interaction terms to estimate the energy differences.

$-\Delta G = 3.4 - 1.7 = 1.7$

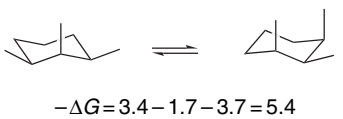

$-\Delta G = 3.4 - 1.7 - 3.7 = 5.4$

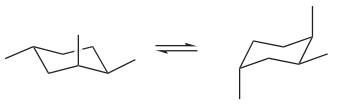

$-\Delta G = 3.4 - 1.7 = 1.7$

$-\Delta G = 3.7 + 3.4 - 1.7 = 5.4$

Comment. This problem would be amenable to an MM approach.

2.10. The conformation equilibria shown below have been measured.

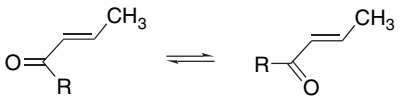

R	K
CH_3	0.45
C_2H_5	0.79
C_3H_7	1.00
i-C_4H_9	1.22
i-C_3H_7	2.3
t-C_4H_9	>100

The trend is a rather modest increase with size for the primary groups through isobutyl. There is a slightly larger change with the secondary isopropyl group, followed by a very large factor favoring the *s-cis* conformer for *t*-butyl. The very large increase on going to *t*-butyl occurs because there is no longer a hydrogen that can occupy the position eclipsed with the β-C−H in the *s-trans* conformation.

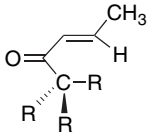

2.11. The product stereochemistry can be predicted on the basis of the Felkin model.

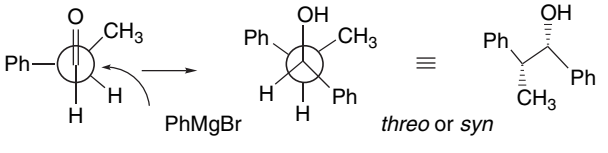

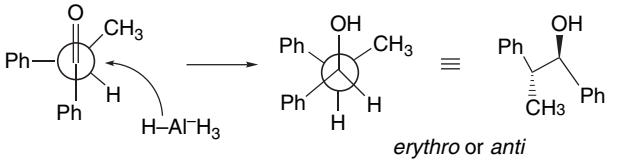

Comment. The reference is an early formulation of Cram's rule and uses an alternative conformation of the reactant.

2.12. The α, β-double bond is held in proximity to the catalyst center by the acetamido substituent, while the γ, δ-double bond is not brought near the coordination center.

2.13.

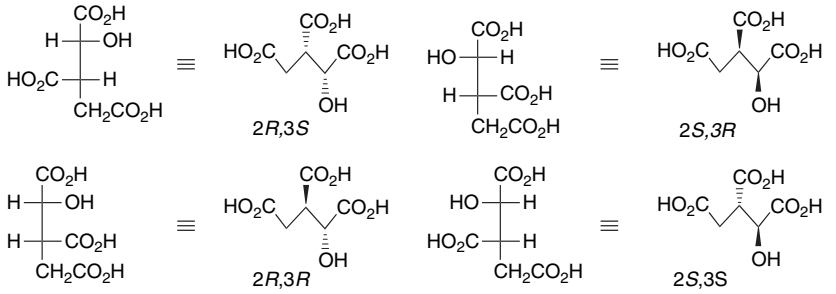

2.14. a.

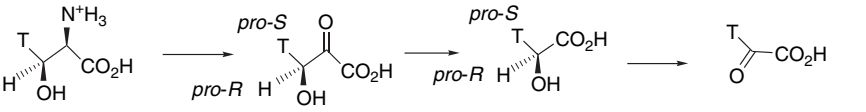

b.

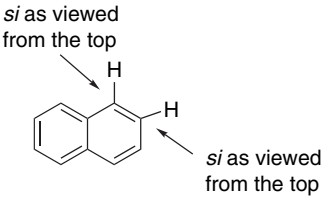

c. The reaction proceeds with retention of configuration at C(3). Inversion occurs at C(2).

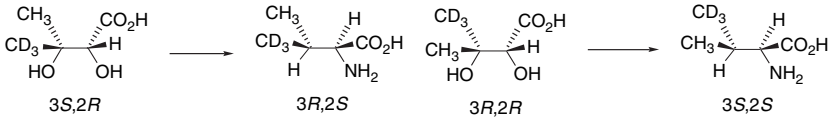

d.

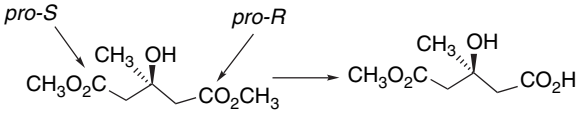

2.15. An achiral tetramer with a center of symmetry results if the two enantiomeric dimers nonactic acids are combined in a structure that contains a center of symmetry.

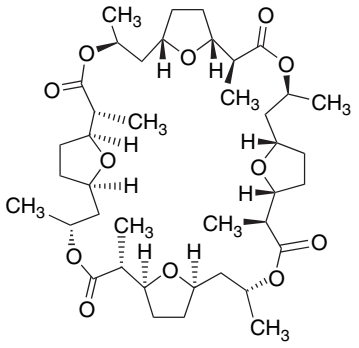

2.16. a. (a) The *cis* isomer is achiral while the *trans* isomer is chiral. The chirality of the *trans*-substituted ring system makes the benzyl hydrogens *diastereotopic* and nonequivalent. This results in the observation of geminal coupling and the appearance of an AB quartet. (b) Hyperconjugation with the nitrogen lone pair moves axial hydrogens to high field in piperidines. The *trans* isomer has one equatorial hydrogen, which appears near 2.8 ppm. In the *cis* isomer, only axial hydrogens are present and they appear upfield of the range shown.

b. Isomer **A** is the *cis*,*cis*-2,6-dimethyl isomer. The benzyl singlet indicates that there is no stereogenic center in the ring and the relatively narrow band at 3.4 indicates that there is only eq-ax coupling to the C(1) hydrogen. Isomer **B** is the *trans*, *trans*-2,6-dimethyl isomer. The benzyl singlet indicates an achiral structure but now the larger ax-ax coupling that would be present in this isomer is seen. Isomer **C** is the chiral *cis*, *trans*-2,6-dimethyl isomer. The AB quartet pattern of the benzyl hydrogens indicates that the ring system is the chiral *cis*, *trans* isomer. The splitting of the signal at 3.0 is consistent with one equatorial and one axial coupling.

2.17. The data allows calculation of $-\Delta G_c$. The interpretation offered in the reference is that hydrogen-bonding solvents (the last two entries) increase the effective size of the hydroxy group. The potential donor solvents dimethoxyethane and tetrahydrofuran seem to have little effect.

2.18. This result seems to be due to $\pi \rightarrow \sigma^*$ and $\sigma \rightarrow \pi^*$ hyperconjugation between the oximino and chloro substituents. Since hyperconjugation is also present in the ketone, the issue is raised as to why the oximino ethers are more prone to the diaxial conformation. The fact that the oximino ethers adopt the diaxial conformation indicates that the hyperconjugative stabilization is greater for the oximes than the ketones. This implies that the $\pi \rightarrow \sigma^*$ component must be dominant, since a greater donor capacity is anticipated for the oxime ethers.

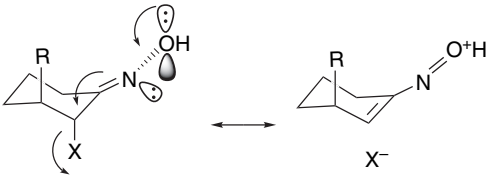

Comment. This question is amenable to MO analysis of the relative energies of the conformers and to NPA charge transfer analysis.

2.19. There is a significant barrier to rotation at the biaryl bond and this gives rise to the temperature dependence as well as introducing a stereogenic feature. In the *trans* isomer **19-A**, the two methyl groups are equivalent but the two conformers are *diastereomers*, and therefore not of equivalent energy. This is evident in the low-temperature spectrum from the unequal ratio. In the *cis* isomer **19-B**, the two conformations are enantiomeric but the methyl groups are nonequivalent. In the high-temperature spectrum, the nonequivalent signals are averaged.

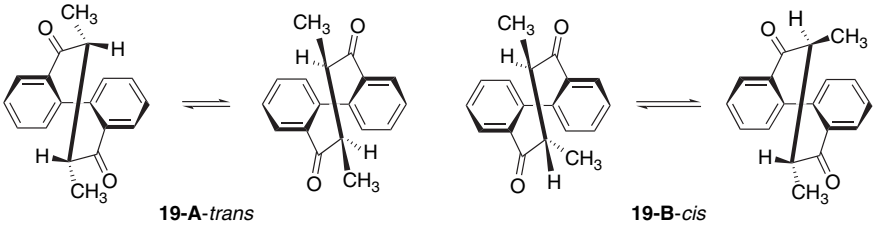

19-A-*trans* **19-B**-*cis*

2.20. The thermal isomerization of the alcohol involves a conformational change that allows the two aryl ring to "slip" by one another. This generates a diastereomer. Oxidation of the diastereomer then leads to the enantiomer of **20-B**.

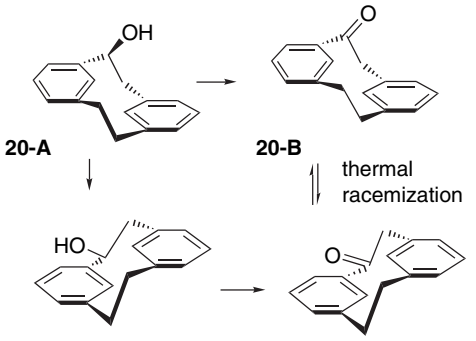

2.21. Product **21-A** is a straightforward oxazoline derivative. Specifying the *R* configuration of the new stereogenic center should be possible on steric grounds. Product **21-B** is the achiral *meso* dimer. According to the reference, other epimeric dimers are 8–15 kcal/mol higher in energy on the basis of MNDO calculations.

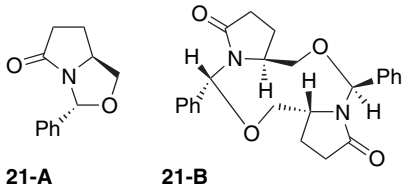

The structure of **21-B** can be assigned on the basis of its dimeric composition, and recognition that it must have an achiral structure. Note that **21-B** is achiral as the result of a center of symmetry.

2.22. The major factor appears to be dipole-dipole repulsion between the C−X and C=O bond, which is at a maximum at 0°. This repulsion is reduced somewhat

in a more polar environment, accounting for the shift toward more of the *syn* conformation. There does not seem to be stabilization of the 90° conformation, which would presumably optimize C-X → π* hyperconjugation. The anomalous behavior of the nitro group is attributed to the somewhat different spatial orientation of the substituent.

2.23. a. The stereoselectivity is consistent with a chelated TS.

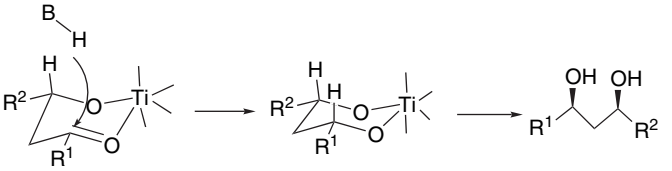

b. The observed stereoselectivity is consistent with a Felkin-Ahn model.

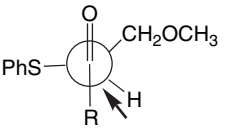

2.24. Application of the oxazaborolidine (p. 196) and $(Ipc)_2BCl$ (p. 194) models correctly predict the *R* configuration of the chiral center.

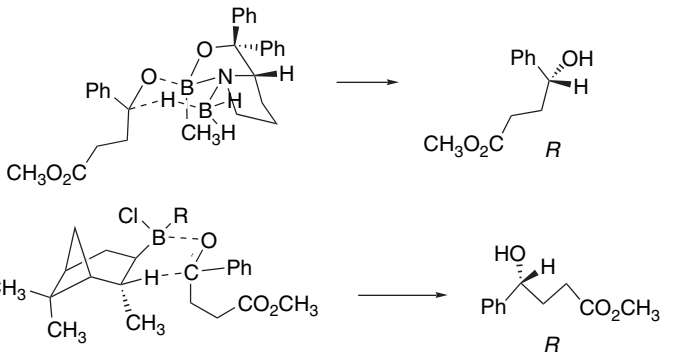

2.25. a. The two methyl groups are enantiotopic.

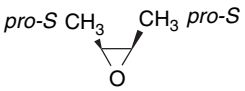

b. The two methyl groups are enantiotopic.

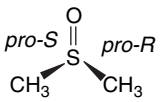

c. The methyls in the *i*-propyl group are diastereotopic.

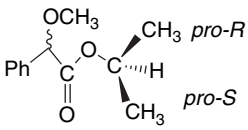

d. The two methyl groups are diastereotopic.

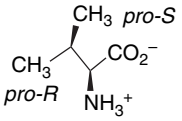

e. Both the benzyl and glycyl methylene hydrogens are diastereotopic.

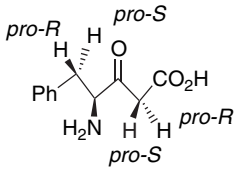

f. The ethoxy methylenes hydrogens are diastereotopic. The bromomethylene hydrogens are enantiotopic.

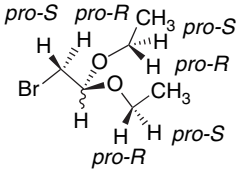

2.26. (a) chiral; (b) chiral, but note that inversion of the configuration of the methyl groups on one ring would give a molecule with a center of symmetry; (c) chiral; (d) achiral, plane of symmetry dissecting any ring and a ring junction; (e) achiral, center of symmetry and a plane of symmetry; (f) chiral; (g) chiral by virtue of helicity; (h) chiral; (i) chiral; (j) chiral; (k) chiral; (l) achiral, plane of symmetry aligned with the two C=O bonds; (m) chiral.

2.27. The following predictions are made by fitting the alkenes to the TS model in Figure 2.27.

(a) DHQD (*R*); DHQ (*S*)
(b) DHQD (*S*); DHQ (*R*)
(c) DHQD (*R*,*R*); DHQ (*S*,*S*)
(d) DHQD (*R*,*R*); DHQ (*S*,*S*)

2.28. a. The TS model on page 196 predicts *R* configuration.

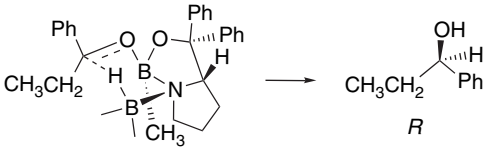

b. The TS model on page 194 predicts *R* configuration.

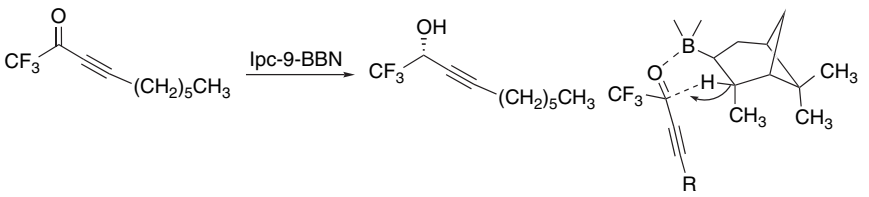

c. The empirical predictive scheme on p. 198 predicts that the 2*R*,3*S*-epoxide will be formed.

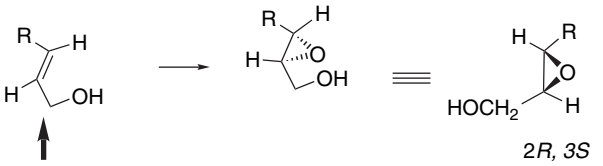

2.29. (a) Classical resolution; (b) kinetic resolution; (c) chiral chromatography; (d) enantioselective synthesis.

2.30. The original reference analyzed the barrier in terms of σ-π hyperconjugation. However, as suggested by the analysis of ethane in Topic 1.1, the rotational barrier is affected by adjustments in molecular geometry, which will lead to changes in all components of the total energy. The analysis of the acetaldehyde rotational barrier given on p. 148 shows that nuclear-nuclear and electron-electron, and nuclear-electron interactions all contribute to the overall barrier.

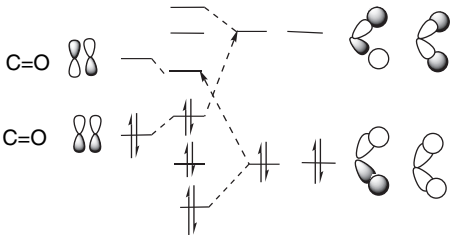

The dashed arrows indicate the attractive hyperconjugative interactions.

2.31. These observations can be accounted for by a rapid equilibration of the monochlorophosphonates, followed by diastereoselective reaction with 4-nitrophenol.

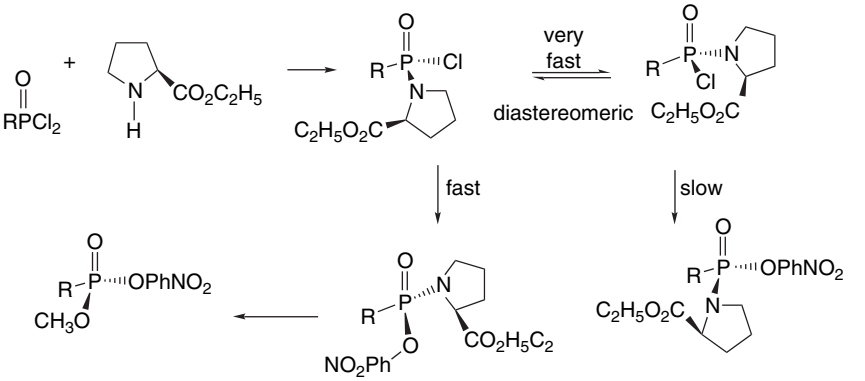

kinetic resolution is achieved at this stage of the reaction

2.32. In the cited reference the experimental ratios are reported to be 96:4; 99.5:0.5, and 99.9:0.1 This is in order of expectation of the steric interference with *endo* hydroboration. The complication is that the experimental values may include some hydroboration by the monoalkylborane, which would accentuate the steric factor.

2.33. The 1,3-dimethylcycloalkenes would be expected to have the 3-methyl substituent in a pseudoaxial position to avoid $A^{1,3}$ allylic strain. This directs the hydroboration to the opposite face. The *syn* addition then results in the formation of the *trans*, *trans*-2,6-dimethylcycloalkanol.

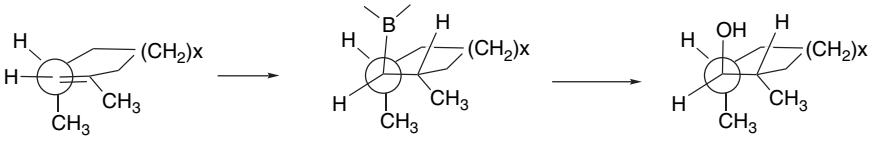

2.34. The stereoselectivity in the protected derivatives is governed by steric factors with the relatively large silyloxy group favoring hydrogenation from the opposite face. The Crabtree catalyst is known to be responsive to *syn*-directive effects by the hydroxy group. The noticeable decrease in stereoselectivity of the carbomethoxy derivative may be due to competing complexation at the ester carbonyl.

Chapter 3

3.1. a. The difference in ΔH_f between cyclohexene and cyclohexane gives the ΔH_{H2} for cyclohexene as 28.4 kcal/mol. A rough estimate of the heat of hydrogenation of cyclohexa-1,3,5-triene would be three times this value or 85.2 kcal/mol. The difference of 36.8 kcal/mol is an estimate of the stabilization of benzene relative to cyclohexa-1,3,5-triene. This estimate makes no allowance for the effect of conjugation in cyclohexa-1,3,5-triene, since it uses the isolated double bond cyclohexene as the model.

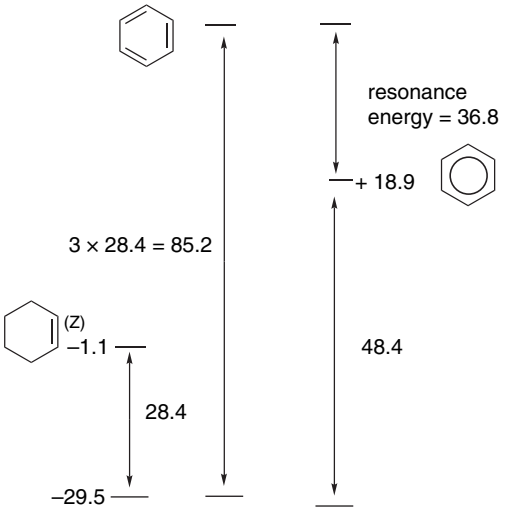

b. The enthalpy of oxidation can be obtained by a simple thermochemical calculation, since the ΔH_f for O_2, the element in its standard state, is 0.

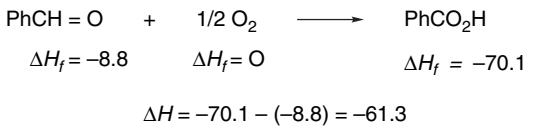

c. The difference in ΔH_f between 2-methyl-1-pentene and 2-methylpentane corresponds to the heat of hydrogenation.

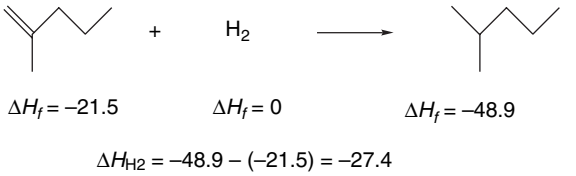

3.2. These conditions would lead to an isomeric mixture of 1,2-dimethylcyclohexanol that would be dehydrated to the three alkenes shown.

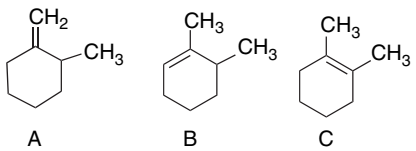

The formation of a stereoisomeric mixture of 1,2-dimethylcyclohexane from each is in accord with these assignments. The H^+-catalyzed equilibration would establish the thermodynamic equilibrium so that the structures can be assigned on the basis of relative stability. The relative stability of the alkenes should be C > B > A, based on the number of double-bond substituents.

3.3. A plot of ln K versus $1/T$ gives a good straight line with a slope of 2428. By use of Equation (3.1), this give $\Delta H = 4.80$ kcal/mol and $\Delta S = -12.2$ eu

Temp C	Temp K	1/Temp	K	Ln K	ΔG	ΔH	ΔS
−2.9	270.2	0.00370	16.9	2.827314	−1512.6	−4807.64	−12.1948
11.8	284.9	0.00351	11.0	2.397895	−1352.7	−4807.64	−12.1270
18.1	291.2	0.00343	8.4	2.128232	−1227.1	−4807.64	−12.2958
21.9	295.0	0.00340	7.9	2.066863	−1207.3	−4807.64	−12.2047
29.3	302.4	0.00331	6.5	1.871802	−1120.8	−4807.64	−12.1921
32	305.1	0.00328	6.1	1.808289	−1092.4	−4807.64	−12.1772
34.9	308.0	0.00325	5.7	1.740466	−1061.4	−4807.64	−12.1631
37.2	310.3	0.00322	5.3	1.667707	−1024.6	−4807.64	−12.1915
42.5	315.6	0.00317	4.6	1.526056	−953.61	−4807.64	−12.2117

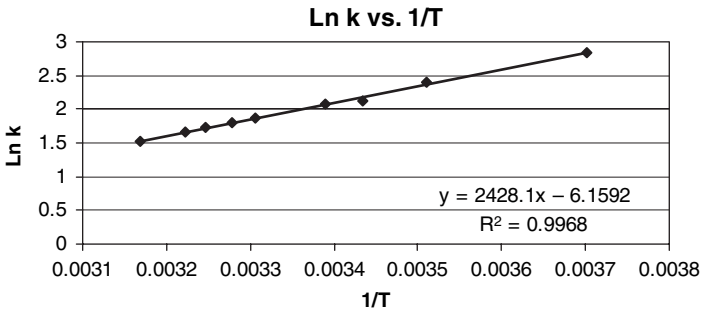

Fig. 3.P3. Plot of ln K versus $1/T$.

3.4. a.

A

Temp C	Temp K	1/T	k s^{-1}	ln k	Ea	$\Delta H^{\ddagger}$	$\Delta G^{\ddagger}$	$\Delta S^{\ddagger}$
25.0	298.1	0.003355	1.36E-07	−15.811	23008	22417	9332	43.9
40.0	313.1	0.003194	8.50E-07	−13.978	23008	22387	8665	43.8
50.1	323.2	0.003094	2.72E-06	−12.815	23008	22367	8200	43.8
58.8	331.9	0.003013	7.26E-06	−11.833	23008	22350	7776	43.9

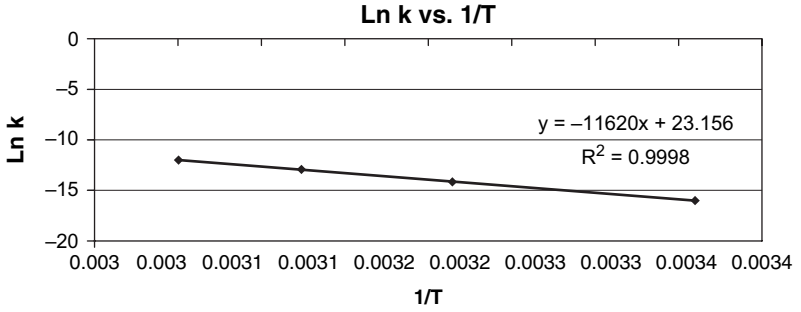

Fig. 3.P4a. Plot of ln k versus $1/T$ for acetolysis of 3-chlorobenzyl tosylate.

b.

B

Temp C	Temp K	1/T	k s^{-1}	ln k	Ea	$\Delta H^{\ddagger}$	$\Delta G^{\ddagger}$	$\Delta S^{\ddagger}$
60	333.1	0.003002	0.000030	−10.4143	27439	26780	6868	59.8
70	343.1	0.002915	0.000097	−9.2408	27439	26760	6277	59.7
75	348.1	0.002873	0.000179	−8.6281	27439	26750	5947	59.8
80	353.1	0.002832	0.000309	−8.0822	27439	26740	5651	59.7
90	363.1	0.002754	0.000892	−7.0220	27439	26720	5048	59.7
95	368.1	0.002717	0.001590	−6.4440	27439	26710	4697	59.8

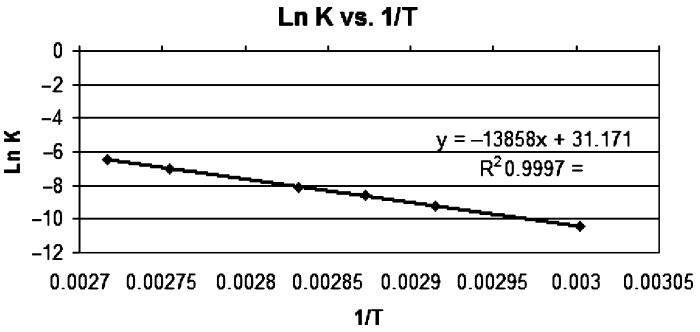

Fig. 3.P4b. Plot of ln k versus $1/T$ for thermolysis of 3-chloro-3-(3-chlorophenyl) diazirine.

3.5. a. The reaction profile would show a depression for the diradical intermediate for mechanism (a), but would show only a TS for mechanism (b).

b. An isotopic labeling study could determine if the exocyclic methylene carbon and the C(3) methylene had exchanged. Exchange would be expected for the diradical mechanism, but not for the concerted mechanism. Deuterium labeling showed that there was interchange of these carbons on the reaction path, indicating that the two-step mechanism is occurring.

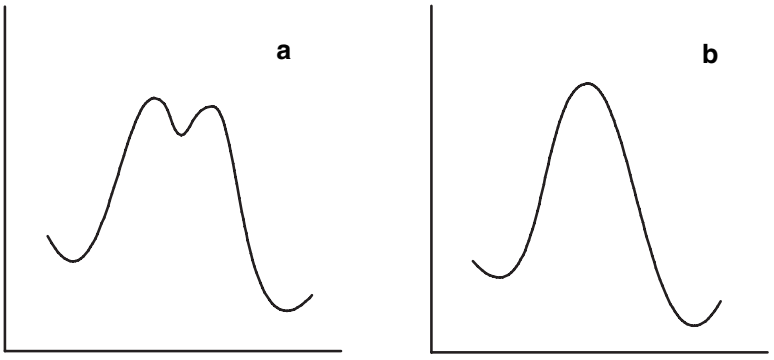

Fig. 3P.5. Reaction energy profiles for diradical and concerted mechanism.

3.6. The reaction can occur by migration of either of the bridgehead carbons, which are in sterically similar environments. The data show that polar EWGs favor migration of the more remote carbon. The same trend is evident, although with attenuated magnitude, in the substituted phenyl derivatives. Thus EWGs disfavor migration of the adjacent bridgehead carbon, whereas ERGs favor such migration. Migration is facilitated by the group's capacity to donate electrons to participate in the migration process. The cited authors favor hyperconjugation as the cause for the substituent effect, but it could also be formulated in terms of the effect of the bond dipole.

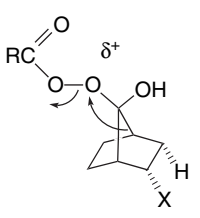

hyperconjugation-unsubstituted bond is better able to migrate

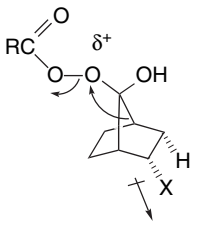

polar: opposing charges are more seperated

3.7. a. The data and plot show a somewhat higher correlation with σ than with σ^-. The ρ value is +1.23, indicating that EWGs favor the reaction. The magnitude of the ρ, which is modest, and the poorer of correlation with σ^- suggest a relatively early TS, occurring before full conjugation of the phenolate anion leaving group has developed.

Group	Rate	k/k_o	Log k/k_o	σ	σ^-
CH_3O	21.3	0.57	−0.244	−0.27	−0.26
CH_3	24	0.642	−0.192	−0.17	−0.17
H	37.4	1	0	0	0
Br	95.1	2.54	0.405	0.23	0.25
NO_2	1430	11.5	1.061	0.78	1.27

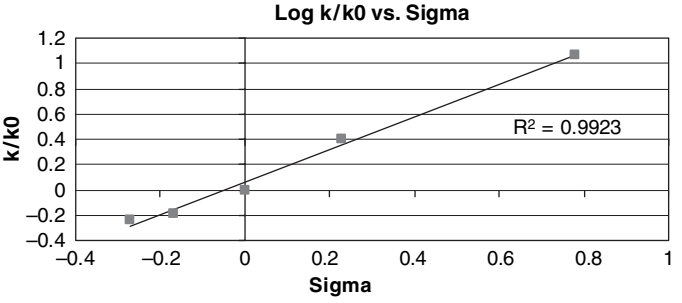

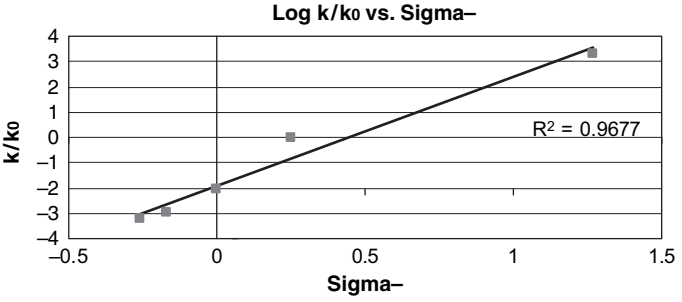

b. The correlation with σ^+ is considerably better and the fairly large negative ρ of −3.58 is consistent with substantial cationic character at the transition state.

Substituent	k	k/k_o	log k/k_o	σ	σ^+
4-CH_3O	4.88E − 03	6.02E + 02	2.779	−0.27	−0.78
4-CH_3	1.64E − 04	2.02E + 01	1.306	−0.17	−0.31
H	8.11E − 06	1.00E + 00	0	0	0
4-Cl	3.18E − 06	3.92E − 01	−0.407	0.23	0.11
4-NO_2	1.44E − 08	1.78E − 03	−2.751	0.78	0.79

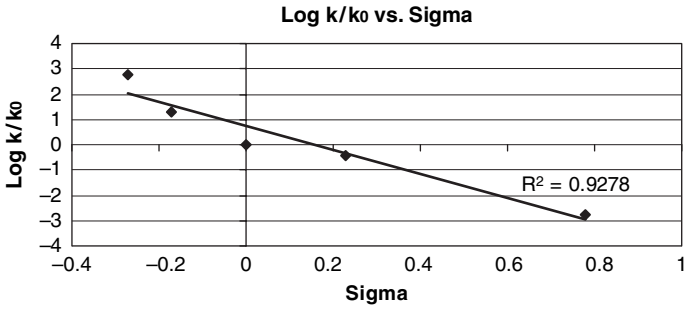

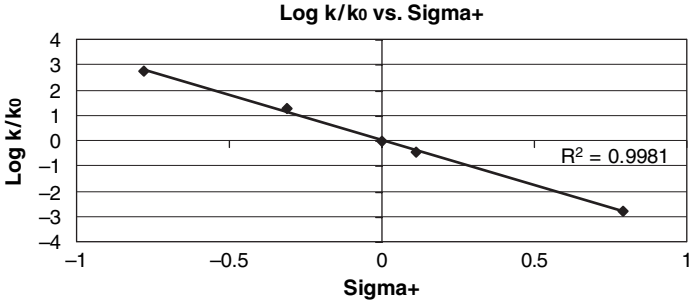

c. The correlation is much better with σ than with σ^+. The ρ is modestly negative (−1.14), consistent with the expected qualitative substituent effect. The modest value of ρ and the lack of correlation with σ^+ indicate that the substituent effect is primarily polar in nature.

Substituent	log K	log K/K_0	σ	σ^+
4-CH_3O	−9.32	−0.29	−0.27	−0.78
4-CH_3	−9.22	−0.19	−0.17	−0.31
3-CH_3O	−9.04	−0.01	0.12	0.12
H	−9.03	0.00	0.0	0.0
4-F	−8.94	0.09	0.06	−0.07
4-Cl	−8.83	0.20	0.23	0.11
3-Cl	−8.67	0.36	0.37	0.37
3-NO_2	−8.19	0.84	0.71	0.71
4-NO_2	−8.14	0.89	0.78	0.79

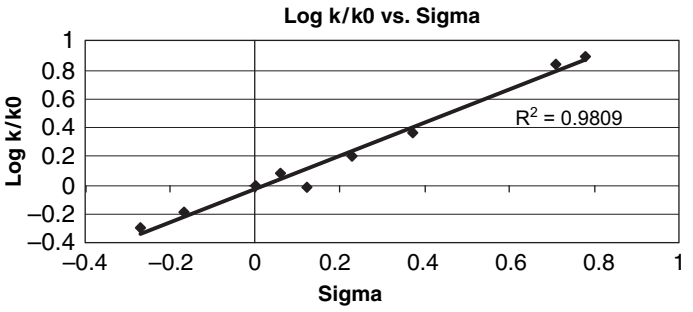

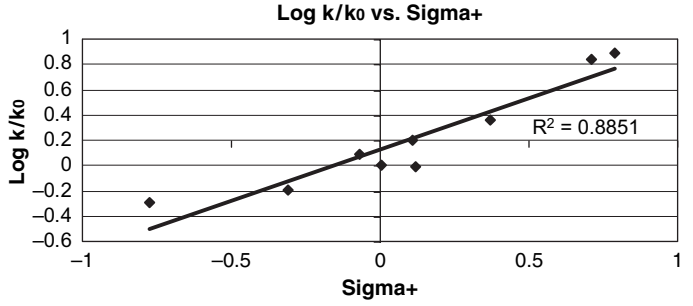

3.8. a. The first step can be treated as an equilibrium and the concentration of the anion expressed in terms of the reactants.

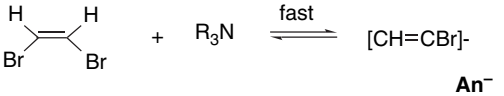

$$[\mathbf{An}^-] = K[BrCH{=}CHBr][R_3N]$$

$$\text{rate} = k_2[\mathbf{An}^-] = k_2K[BrCH{=}CHBr][R_3N]$$

$$\text{rate} = k_{obs}[BrCH{=}CHBr][R_3N]$$

b. This represents an example of the classical S_N1 reaction Rate $= k[\mathrm{R-X}]$. The ratio of products would be given by k_2/k_3.

c.

$$\mathrm{Ar-H + Br_2 \underset{k_{-2}}{\overset{k_2}{\rightleftharpoons}} [ArHBr^+] + Br^- \text{ is rate controlling.}}$$

Steady state approximation for $[\mathrm{ArHBr^+}]$ leads to

$$k_2[ArH][Br_2] = k_{-2}[ArHBr^+][Br^-] + k_3[ArHBr^+]$$

and

$$[ArHBr^+] = \frac{k_2[ArH][Br_2]}{k_{-2}[Br^-] + k_3}$$

The effective $[\mathrm{Br_2}]$ is determined by the tribromide equilibrium

$$K_4 = \frac{[Br_3^-]}{[Br_2][Br^-]}$$

Substituting gives

$$-\mathrm{d}\frac{[\mathrm{Br_2}]_{\mathrm{Stoich}}}{\mathrm{dt}} = \frac{1}{1+\mathrm{K_4}[\mathrm{Br^-}]} \times \frac{\mathrm{k_2 k_3}[\mathrm{ArH}][\mathrm{Br_2}]}{\mathrm{k_{-2}}[\mathrm{Br^-}]+\mathrm{k_3}}$$

When $\mathrm{k_3}[\mathrm{ArHBr^+}] >> \mathrm{k_{-2}}[\mathrm{ArHBr^+}]$, this simplifies to

$$-\mathrm{d}\frac{[\mathrm{Br_2}]_{\mathrm{Stoich}}}{\mathrm{dt}} = \frac{1}{1+\mathrm{K_4}[\mathrm{Br^-}]}\mathrm{k_2}[\mathrm{ArH}][\mathrm{Br_2}]$$

d. This can be formulated by using a steady state approximation for the enol [Enol]:

$$k_1[\mathrm{Keto}] = k_{-1}[\mathrm{Enol}] + k[\mathrm{Cr}][\mathrm{Enol}]$$

$$[\mathrm{Enol}] = \frac{\mathrm{k_1}[\mathrm{Keto}]}{\mathrm{k_{-1}}+\mathrm{k}[\mathrm{Cr}]}$$

The rate then is

$$\mathrm{Rate} = \mathrm{k}[\mathrm{Enol}][\mathrm{Cr}] = \mathrm{k}\frac{\mathrm{k_1}[\mathrm{Keto}][\mathrm{Cr}]}{\mathrm{k_{-1}}+\mathrm{k}[\mathrm{Cr}]}$$

3.9. The apparent stabilization is given by [ΔH_{H2} (cyclic system)] – [ΔH_{H2} (ref.)] The following are the apparent stabilizations:

System	Apparent stabilization
Cyclopropenyl cation	23.9
Cyclopropenyl anion	−64.3
Cyclobutadiene	−51.2
Cyclopentadienyl cation	−53.5
Cyclopentadienyl anion	−2.6
Benzene	27.2
Cycloheptatrienyl cation	7.5
Cycloheptatrienyl anion	−15.1

This computation seems to emphasize the antiaromatic character more than the aromatic character. Note, for example, that the cyclopentadiene anion is calculated to be slightly *destabilized* by conjugation, which runs counter to the observed relative acidity of the cyclopentadiene ring. The qualitative agreement with Hückel's rule is excellent but the agreement with the calculated β values is poor. This treatment makes no explicit separation of strain. For example in the C_3 system, the reference point is the allyl system, so the strain associated with closing a three-membered ring is subsumed into the calculated (de)stabilization. Inclusion of a separate term for strain would increase the apparent stabilization of the cyclopropenyl cation and decrease the destabilization of the anion by the amount of strain assigned.

3.10. a. The very large heat of hydrogenation of the cyclobutadiene reflects the antiaromatic destabilization present in this molecule. The more or less normal heat of hydrogenation of the second step indicates that there is not much change of strain in this step.

b. The larger exothermicity of the first ring cleavage is the result of the rehydridization that is possible in the dimethylcyclopropane product. The relief of strain is greater in the first step than in the second because of the adjustment in hybridization.

c. The successive steps reflect: (1) change from di- to tri-substituted double bond; (2) relief of strain resulting from reduction of sp^2 carbons in the ring from one to two; (3) further relief of strain by removal of the sp^2 carbon from the ring; (4) the final heat of hydrogenation is slightly lower than 1-butene, suggesting a small stabilization of the double bond by the cyclopropyl ring.

3.11. The mechanism is believed to involve rate-determining hydride donation from hydrated benzaldehyde. The lack of exchange with solvent protons indicates that it is the formyl hydrogen that is transferred. Reversible formation of the aldehyde hydrate and its conjugate base accounts for the appearance of ^{18}O in both products. The third-order rate expression is also consistent with involvement of the hydrate. The role of aromatic substituents could be complex. The extent of hydration and the reactivity of the aldehyde to hydride transfer would be favored by EWG substituents. On the other hand, the hydride transfer itself would be retarded by an EWG in the hydrate. The positive ρ indicates that some combination of the former two factors must be dominant. The inverse isotope effect rules out rate-limiting O–H bond-breaking and is consistent with the greater nucleophilicity of ^{-}OD compared to ^{-}OH. The observations are consistent with a mechanism in which the aldehyde hydrate acts as the hydride donor.

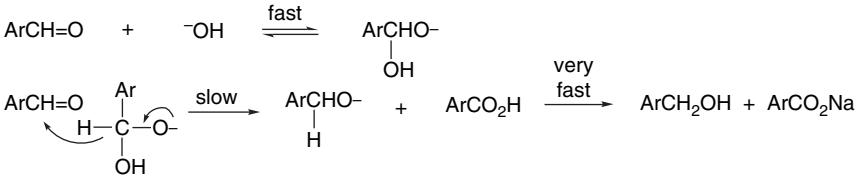

3.12. The first step must be rate determining, since the aromatic hydrogens exhibit a primary isotope effect, whereas there is no isotope effect for elimination of hydrogen from the styrene reactant, which occurs in Step 3. Step 2 would not be expected to exhibit a primary isotope effect because the aryl hydrogens are not directly involved in the reaction, but should exhibit a secondary isotope effect for styrene-β-d_2.

3.13. 1. The larger substituent effect in the gas phase is due to the "leveling effect" in solution. In the gas phase, the adjustments to changes in the electron distribution resulting from ionization must be accommodated internally, so substituent effects are large. In solution, much of the effect of the negative charge is stabilized by solvation, and this reduces the relative importance of the substituent effects.

2. The larger and more polarizable benzoic acid molecule is able to better accommodate the charge of the anion in the gas phase.

3. Stabilization of the anion in solution causes solvent organization, which appears as an entropy contribution. Substituent effects are translated into differences in solvation. Anions better stabilized by internal substituent effects result in somewhat looser solvation.

3.14. The correlation with σ^+ is marginally better than for σ and both are significantly better than with σ^-. This indicates that the chemical shifts result from a mixture of polar and resonance effects that weight resonance slightly higher than for

the standard ionization of benzoic acid. The data were used to assign "pure" resonance σ^R values by using a dual substituent parameter correlation.

Substituent	Δδ	σ	σ^+	σ^-
NH_2	−9.86	−0.66	−1.30	−0.15
CH_3O	−7.75	−0.27	−0.78	−0.26
F	−4.49	0.06	−0.07	−0.03
CH_3	−2.89	−0.17	−0.31	−0.17
Cl	−2.05	0.23	0.11	0.19
Br	−1.62	0.23	0.15	0.25
CF_3	3.29	0.54	0.61	0.65
CN	3.80	0.66	0.66	1.00
CH_3O_2C	4.12	0.45	0.49	0.74
CH_3CO	4.18	0.50	0.52	0.84
CH_3SO_2	4.64	0.72	0.74	1.13
NO_2	5.53	0.78	0.79	1.27

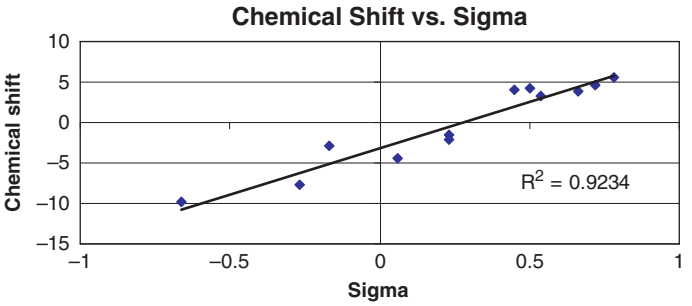

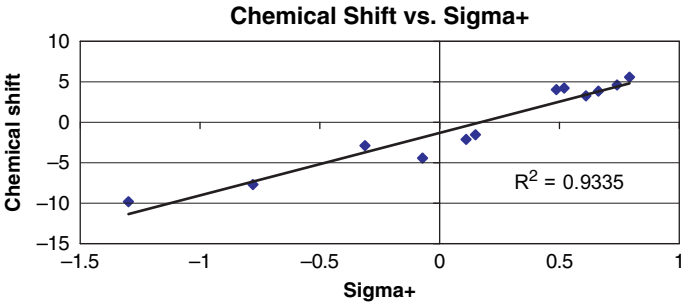

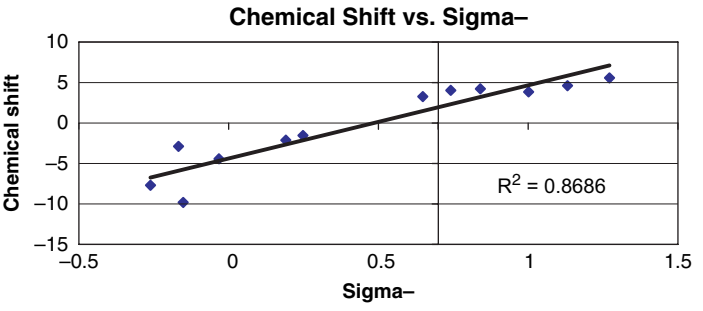

3.15. The correlation with σ is somewhat better than with σ^+, although a direct resonance interaction does exist. Both ΔH and ΔS show good linear correlations with ΔG, indicating that the substituent effect operates by both electronic stabilization and solvation.

Substituent	pK_a	K_a	ΔG	ΔH	ΔS	σ	σ^+
NH_2	9.12	7.6×10^{-10}	12.4	11.3	−3.7	−0.66	−1.30
CH_3O	6.58	2.6×10^{-7}	8.9	6.8	−7.0	−0.27	−0.78
CH_3	6.03	9.3×10^{-7}	8.2	6.1	−7.0	−0.17	−0.31
H	5.21	6.2×10^{-6}	7.1	4.8	−7.7	0.0	0.0
Cl	3.83	1.5×10^{-4}	5.2	3.6	−5.4	0.23	0.11
Br	3.75	1.8×10^{-4}	5.1	3.5	−5.4	0.23	0.15
CN	1.86	1.4×10^{-2}	2.5	1.3	−4.0	0.66	0.66

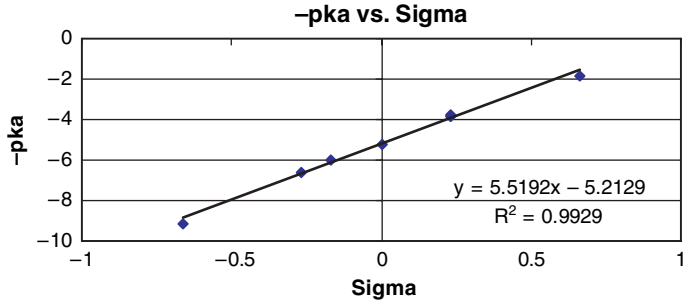

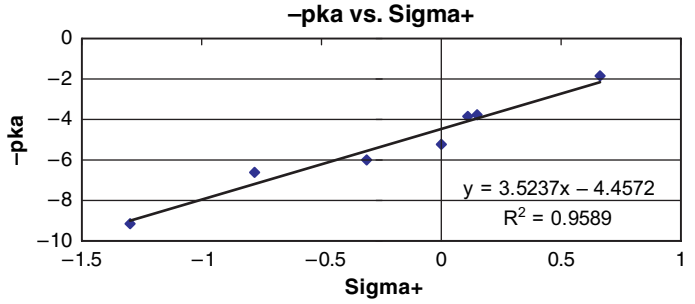

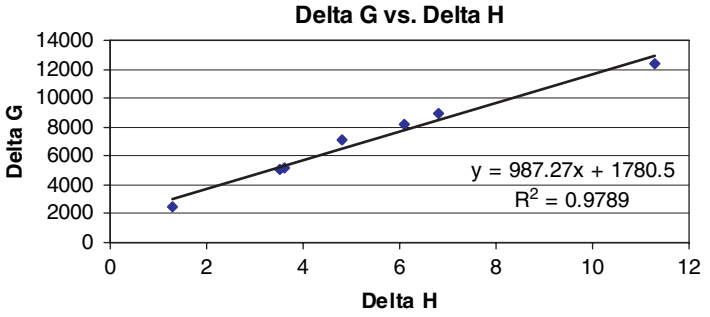

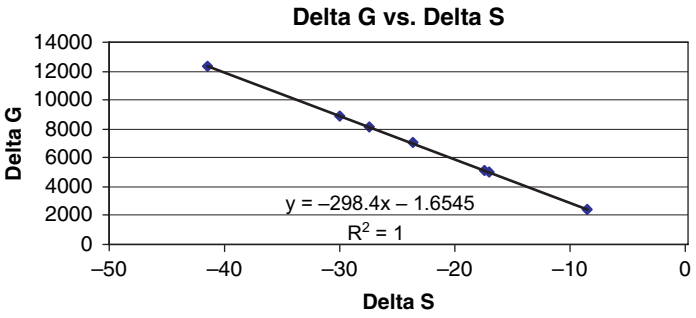

3.16. a. The absolute (unsigned) deviation for MM is quite small. PM3 gives slightly high values for all compounds, especially for nortricyclane and quadricyclane. AM1 is systematically high except for norbornane, and is especially high for nortricyclane and quadricyclane. MNDO is systematically high, except for norbornane and quadricyclane. Thus it appears PM3 gives the best results of the semiempirical methods, but all have some difficulty with the strained ring compounds.

b. The ab initio results are in quite good agreement with the experimental values, although norbornene and nortricyclane are consistently about 3–4 kcal/mol less than the experimental value. The B3LYP results are about 10 kcal/mol too high for the bicyclic compounds, but somewhat closer, although still high, for nortricyclane and quadricyclane.

c. The heats of hydrogenation results from the semiempirical calculations are similar to the ΔH_f calculations, with the AM1 results most seriously in error.

3.17. The order $(CH_3)_3N > (C_2H_5)_3N > (C_nH_{n+1})_3N$ presumably is mainly a steric effect. There is a small variation of the longer-chain compounds in the order 4 > 8 > 3 > 6, for which there is no obvious interpretation. Pyridine is comparable to the longer-chain trialkylamines because the sp^2 nitrogen is less nucleophilic than the sp^3 nitrogen. There is further reduction with quinoline, which is probably largely due to the steric effect of the C(8)–H. *N*,*N*-Dimethylaniline is still less reactive. The phenyl group would exert both a polar and resonance withdrawal of electron density from nitrogen and there is more steric hindrance than in pyridine.

Temp. (°C)	$(Me)_3N$	$(Et)_3N$	$(Pr)_3N$	$(Bu)_3N$	$(Hex)_3N$	$(Oct)_3N$	$PhNMe_2$	Pyridine	Quinoline
20	38.2								
24	50.2								
30	72.8								
40		1.67	0.354	0.471	0.290	0.336		0.168	
50		3.07	0.633	0.844	0.566	0.570		0.337	0.051
60		4.54	1.05	1.24	0.860	0.912	0.135	0.910	0.105
70		7.49	1.76	1.94	1.54	1.60	0.233	1.55	0.226
80			3.04	3.22	2.62	2.73	0.384	2.63	0.457
90							0.698		0.820

Temp K	1/T	Me_3N	k	ln(k)	ΔH	ΔG	ΔS
293.1	0.003412	38.2	0.000382	−7.87009	10780	21729	−37.4
297.1	0.003366	50.2	0.000502	−7.59691	10772	21873	−37.4
303.1	0.003299	72.8	0.000728	−7.22521	10760	22103	−37.4
			Intercept	11.64334			
			slope	−5718.24	ΔH	ΔG	ΔS
			Ea	11362	10770	21902	−37.4

Temp K	1/T	Et_3N	k	ln(k)	ΔH	ΔG	ΔS
313.1	0.003194	1.67	1.67E-05	−11.0001	10740	25201	−46.2
323.1	0.003095	3.07	3.07E-05	−10.3912	10720	25635	−46.2
333.1	0.003002	4.54	4.54E-05	−10	10700	26189	−46.5
343.1	0.002915	7.49	7.49E-05	−9.49936	10680	26654	−46.6
			Intercept	5.831199			
			slope	−5261.16	ΔH	ΔG	ΔS
			Ea	10453.92	10710	25920	−46.4

Temp K	1/T	Pr_3N	k	ln(k)	ΔH	ΔG	ΔS
313.1	0.003194	0.354	3.54E-06	−12.5514	10740	26166	−49.3
323.1	0.003095	0.633	6.33E-06	−11.9702	10720	26648	−49.3
333.1	0.003002	1.05	1.05E-05	−11.4641	10700	27158	−49.4
343.1	0.002915	1.76	1.76E-05	−10.9476	10680	27642	−49.4
353.1	0.002832	3.04	3.04E-05	−10.4011	10660	28084	−49.3
			Intercept	6.226278			
			slope	−5882.95	ΔH	ΔG	ΔS
			Ea	11689.43	10700	27140	−49.3

Temp K	1/T	Bu_3N	k	ln(k)	ΔH	ΔG	ΔS
313.1	0.003194	0.471	4.71E-06	−12.2658	10740	25988	−48.7
323.1	0.003095	0.844	8.44E-06	−11.6825	10720	26464	−48.7
333.1	0.003002	1.24	1.24E-05	−11.2978	10700	27048	−49.1
343.1	0.002915	1.94	1.94E-05	−10.8502	10680	27575	−49.2
353.1	0.002832	3.22	3.22E-05	−10.3435	10660	28044	−49.2
			Intercept	4.26121			
			slope	−5170.09	ΔH	ΔG	ΔS
			Ea	10272.97	10700	27024	−49.0

Temp K	1/T	Hex_3N	k	ln(k)	ΔH	ΔG	ΔS
313.1	0.003194	0.29	2.9E-06	−12.7508	10740	26290	−49.7
323.1	0.003095	0.566	5.66E-06	−12.0821	10720	26720	−49.5
333.1	0.003002	0.86	8.6E-06	−11.6637	10700	27290.	−49.8
343.1	0.002915	1.54	1.54E-05	−11.0811	10680	27733	−49.7
353.1	0.002832	2.62	2.62E-05	−10.5498	10660	28188	−49.6
			Intercept	6.338335			
			slope	−5972.96	ΔH	ΔG	ΔS
			Ea	11868.26	10700	27244	−49.6

Temp K	1/T	Oct_3N	k	ln(k)	ΔH	ΔG	ΔS
313.1	0.003194	0.336	3.36E-06	−12.6036	10740	26198	−49.4
323.1	0.003095	0.57	5.7E-06	−12.075	10720	26716	−49.5
333.1	0.003002	0.912	9.12E-06	−11.605	10700	27252	−49.7
343.1	0.002915	1.6	0.000016	−11.0429	10680	27707	−49.6
353.1	0.002832	2.73	2.73E-05	−10.5086	10660	28160	−49.6
			Intercept	5.773336			
			slope	−5765.65	ΔH	ΔG	ΔS
			Ea	11456.36	10700	27206	−49.5

Temp K	1/T	$PhNMe_2$	k	ln(k)	ΔH	ΔG	ΔS
333.1	0.003002	0.135	1.35E-06	−13.5154	10700	28516	−53.5
343.1	0.002915	0.233	2.33E-06	−12.9696	10680	29020	−53.5
353.1	0.002832	0.384	3.84E-06	−12.47	10660	29536	−53.5
363.1	0.002754	0.698	6.98E-06	−11.8725	10640	29961	−53.2
			Intercept	6.154445			
			slope	−6558.85	ΔH	ΔG	ΔS
			Ea	13032.44	10670	29258	−53.4

Temp K	1/T	pyridine	k	ln(k)	ΔH	ΔG	ΔS
313.1	0.003194	0.168	1.68E-06	−13.2967	10740	26629	−50.7
323.1	0.003095	0.337	3.37E-06	−12.6006	10720	27053	−50.6
333.1	0.003002	0.91	9.1E-06	−11.6072	10700	27253	−49.7
343.1	0.002915	1.55	1.55E-05	−11.0747	10680	27728	−49.7
353.1	0.002832	2.63	2.63E-05	−10.5459	10660	28186	−49.6
			Intercept	11.6027			
			slope	−7789.69	ΔH	ΔG	ΔS
			Ea	15478.12	10700	27367	−50.1

Temp K	1/T	quinoline	k	ln(k)	ΔH	ΔG	ΔS
323.1	0.003095	0.051	5.1E-07	−14.4889	10720	28265	−54.3
333.1	0.003002	0.105	1.05E-06	−13.7667	10700	28682	−54.0
343.1	0.002915	0.226	2.26E-06	−13.0001	10680	29041	−53.5
353.1	0.002832	0.457	4.57E-06	−12.296	10660	29414	−53.1
363.1	0.002754	0.82	8.2E-06	−11.7114	10640	29845	−52.9
			Intercept	11.02824			
			slope	−8248.09	ΔH	ΔG	ΔS
			Ea	16388.95	10680	29049.46	−53.6

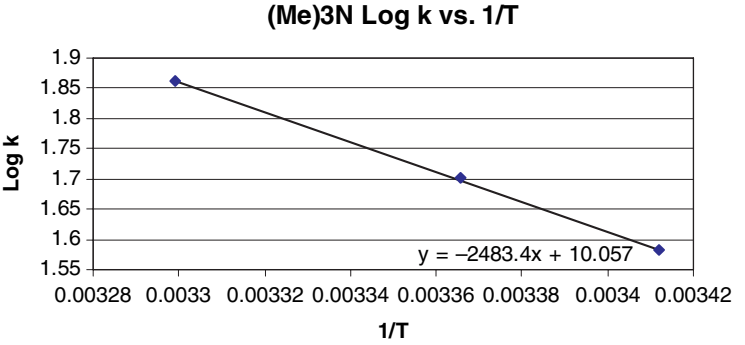

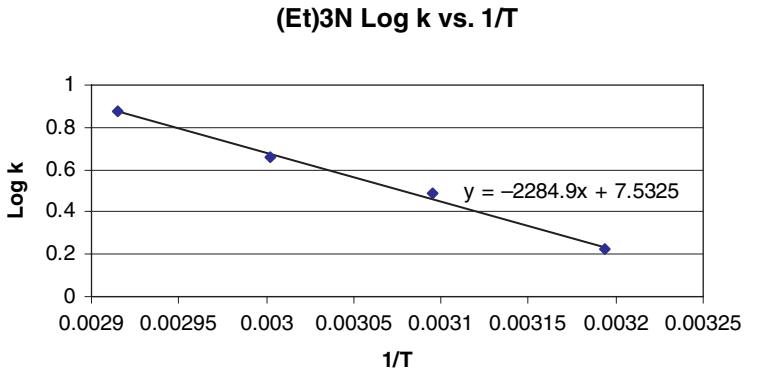
(Et)3N Log k vs. 1/T
Log k
1
0.8
0.6
0.4
0.2
0
y = –2284.9x + 7.5325
0.0029
0.00295
0.003
0.00305
0.0031
0.00315
0.0032
0.00325
1/T

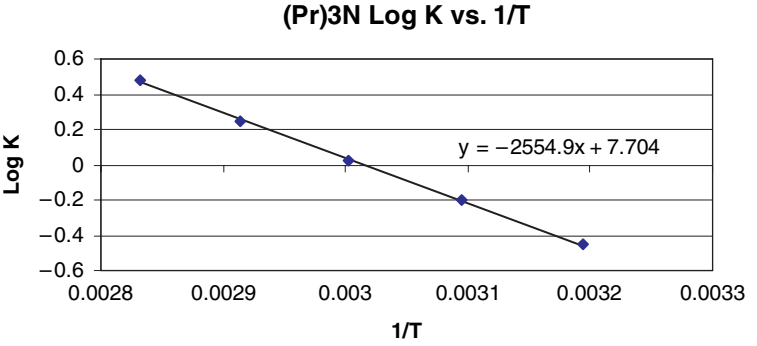
(Pr)3N Log K vs. 1/T
Log K
0.6
0.4
0.2
0
–0.2
–0.4
–0.6
y = –2554.9x + 7.704
0.0028
0.0029
0.003
0.0031
0.0032
0.0033
1/T

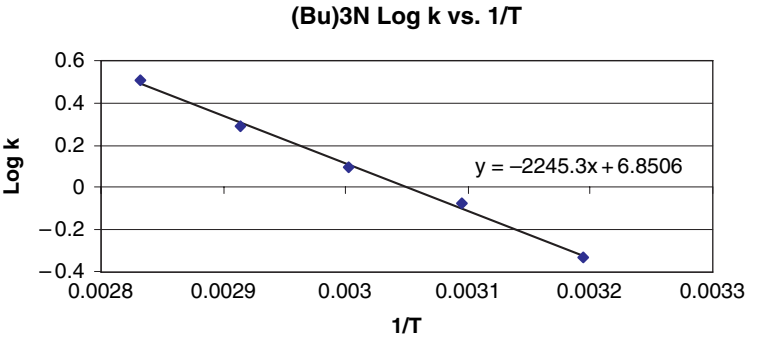
(Bu)3N Log k vs. 1/T
Log k
0.6
0.4
0.2
0
–0.2
–0.4
y = –2245.3x + 6.8506
0.0028
0.0029
0.003
0.0031
0.0032
0.0033
1/T

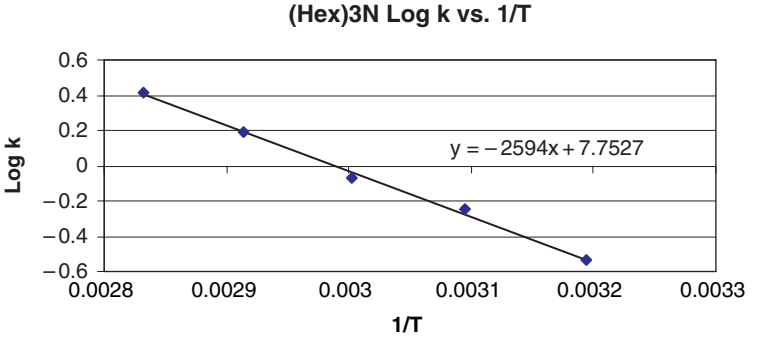
(Hex)3N Log k vs. 1/T
Log k
0.6
0.4
0.2
0
–0.2
–0.4
–0.6
y = –2594x + 7.7527
0.0028
0.0029
0.003
0.0031
0.0032
0.0033
1/T

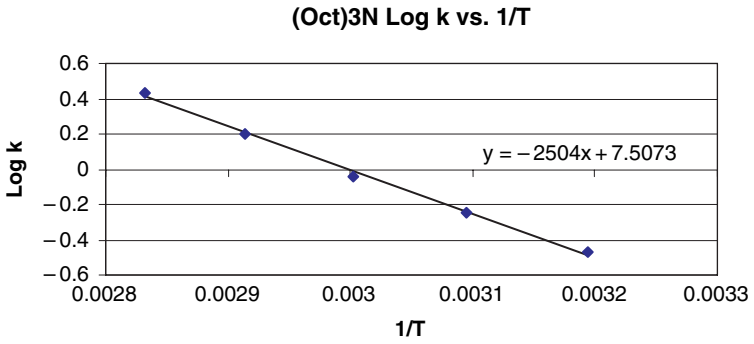

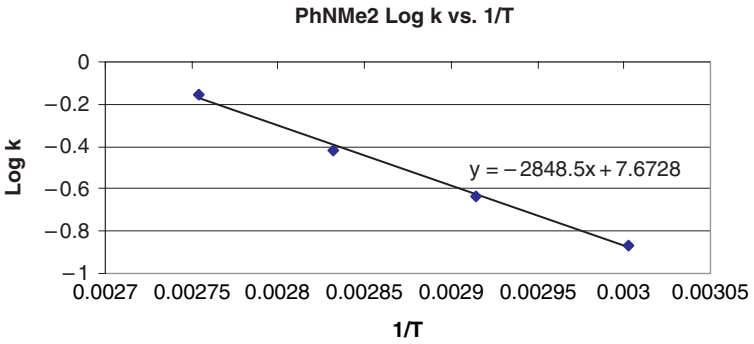

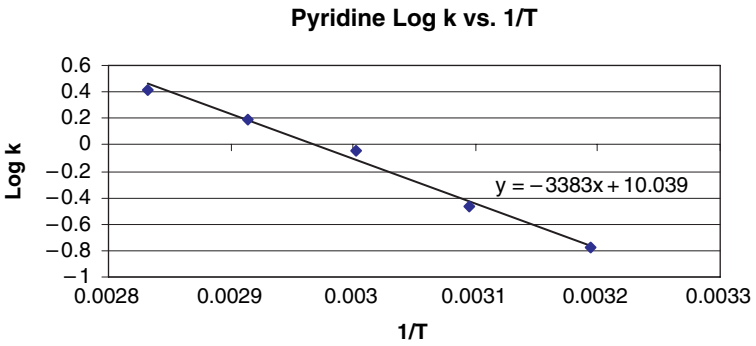

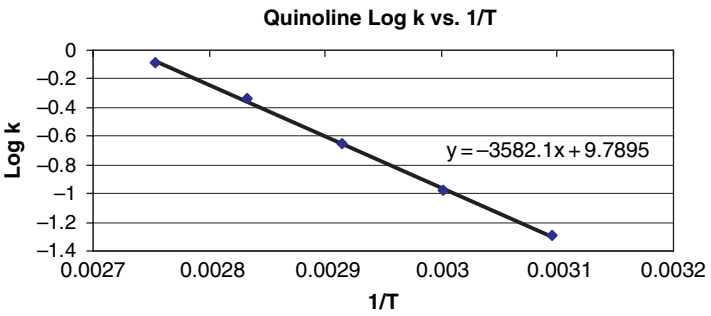

3.18. The slopes of the line *increase* with the number of cyano substituents. This indicates there is successively *more* solvent attenuation, with the increasing stabilization by cyano substituents. This may be because the charge is more localized on the benzylic carbon, permitting more effective solvation

Series 1 – Toluenes				Series 2 – Phenylacetonitriles				Series 3 – Phenylmalononitriles			
Group	sigma	ΔG	pK	Group	sigma	ΔG	pK	Group	sigma	ΔG	pK
H	0	373.7	43	H	0	344.1	21.9	H	0	314.3	4.24
4-NO_2	0.78	345.2	20.4	4-NO_2	0.78	323.3	12.3	4-NO_2	0.78	299.5	−1.8
3-NO_2	0.71	355.7	33.5	3-NO_2	0.71	330.9	18.1	3-NO_2	0.71	303	1.7
4-CN	0.66	353.6	30.7	4-CN	0.66	327.9	16				
				3-CN	0.56	332.3	18.7	3-CN	0.56	304.4	2.2
4-SO_2CF_3	0.96	340.7	24.1	4-CF_3	0.54	332.9	18.1	4-Cl	0.23	309	3.14
4-SO_2CH_3	0.72	359.3	29.8	3-CF_3	0.43	335.3	19.2	3-Cl	0.37	308.8	2.7
4-PhCO	0.43	353.5		4-Cl	0.23	338.5	20.5	4-CH_3O	−0.27	315.4	5.68
4-CH_3CO	0.5	354.9		3-Cl	0.37	337.5	19.5	4-CH_3	−0.17	315.7	4.85
4-CF_3CO	0.8	344.1	26.8	4-F	0.06	342.4	22.2				
4-CH_3O_2C	0.45	355.4		3-F	0.34	344	20				
4-$(CH_3)_2NCO$	0.36	367		4-CH_3O	−0.27	345	23.8				
				3-CH_3O	0.12	342.8					
				4-CH_3	−0.17	345	22.9				
				3-CH_3	−0.07	344.2					
				4-$(CH_3)_2N$	−0.83	346.6	24.6				

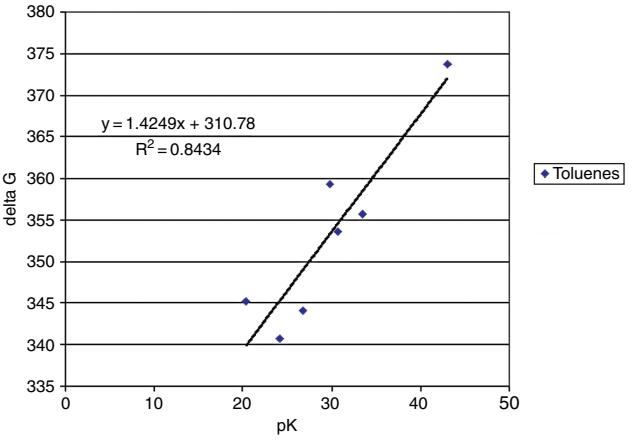
y = 1.4249x + 310.78
R2 = 0.8434
delta G
pK
Toluenes

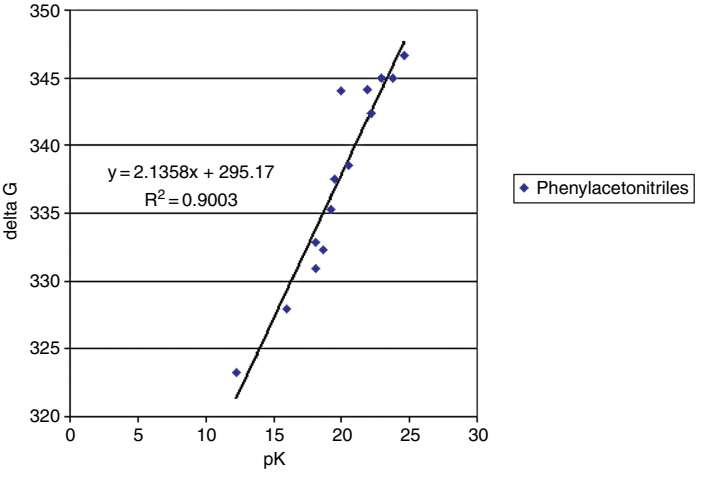
y = 2.1358x + 295.17
R2 = 0.9003
delta G
pK
Phenylacetonitriles

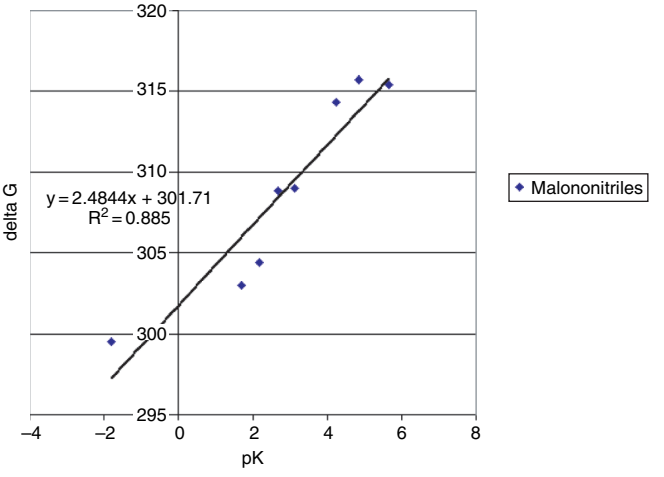
y = 2.4844x + 301.71
R2 = 0.885
delta G
pK
Malononitriles

3.19. There is no correlation with σ. The plot has a roughly parabolic shape with the greatest reactivity at the two extremes. The vinyl group, despite its low σ value, is among the strongest rate-enhancing substituents. The 4-phenyl and 4-methylthio substituents are also rate enhancing. The reaction is believed to proceed by rearrangement of an intermediate diradical, in which case the radical-stabilizing substituent effect should govern the relative reactivity. Indeed, this reaction was used to establish such a substituent scale.

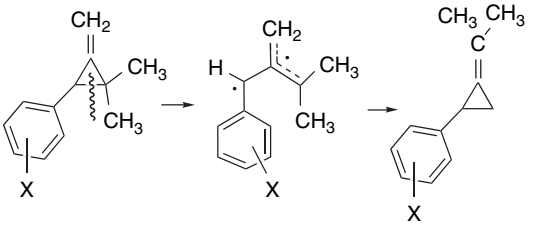

Substituent	σ	$10^4\ k\ s^{-1}$	k/k_0	log k/k_0
4-$(CH_3)_2N$	−0.83	28.2	7.88	0.896
4-CH_2=CH	0.04	16.7	4.66	0.669
4-NO_2	0.78	13.5	3.77	0.576
4-CN	0.66	10.28	2.87	0.458
4-Ph	0.01	10.3	2.88	0.459
4-CH_3S	0.00	9.53	2.66	0.425
4-CH_3O_2C	0.45	8.09	2.26	0.354
4-CH_3O	−0.27	6.16	1.72	0.236
4-$(CH_3)_3Si$	−0.07	5.24	1.46	0.165
4-Br	0.23	4.88	1.36	0.135
4-$(CH_3)_3C$	−0.20	4.78	1.34	0.125
4-Cl	0.23	4.75	1.33	0.123
4-CH_3	−0.17	4.65	1.30	0.114
4-CF_3	0.54	4.25	1.19	0.075
3-$(CH_3)_3Si$	−0.04	3.87	1.08	0.033
3-CH_3	−0.07	3.82	1.06	0.028
H	0.00	3.58	1.00	0.000
3-CH_3O	0.12	3.40	0.95	−0.022
3-Cl	0.37	3.30	0.92	−0.035
3-F	0.34	3.17	0.89	−0.053
3-CF_3	0.43	3.08		
4-F	0.06	2.98		
3-NO_2	0.71	2.76		
3-CN	0.56	2.69		

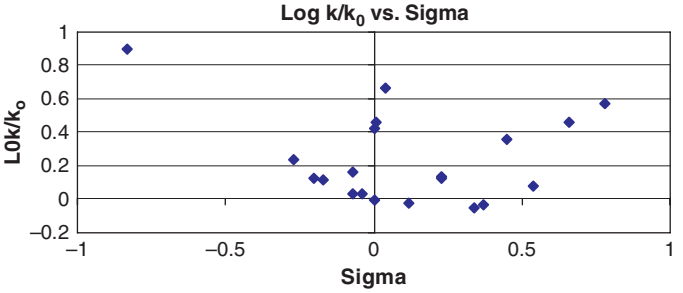

3.20. These data relate to the general acidifying effect of cyano groups, as manifested in the pK values of the "cyanocarbons." The referenced papers point to several properties of the cyano group, which is a strongly polar EWG, combining the electronegativity of *sp* carbon and nitrogen. The group is also rather undemanding sterically, allowing several groups to be accommodated without mutual steric repulsions. Richard, Williams, and Giao in the reference cited argue further that the effect is more polar than resonance and cite the relatively high energy of the ketimine resonance form as an explanation. Merrill, Dahlke, and Kass point to hyperconjugation as contributing to the β-stabilization, citing the lengthened C(β)-CN bond.

3.21. The two transition structures shown below are derived from reactant conformations **21-A** and **21-B**, respectively. As the attacking radical becomes larger, the steric repulsion with the methyl substituent becomes more significant and forces the TS to react through the less favorable reactant conformation **21-B.** The product ratios can be used to estimate the difference in the $\Delta G^{\ddagger}$ values, as shown in the figure.

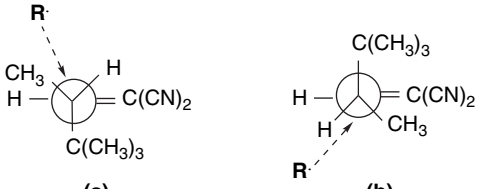

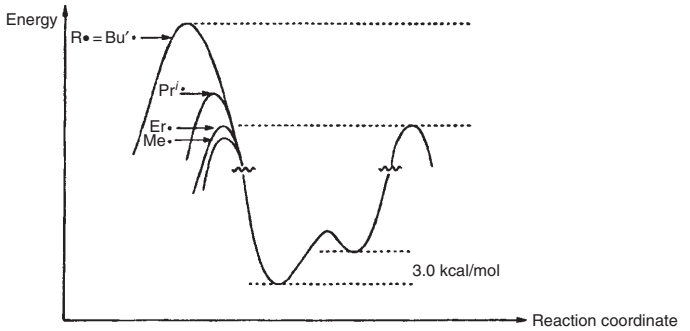

3.22. The $\delta\Delta H$ results show some of the characteristic features of aromatic substituents, reflecting the mixture of resonance and polar components. For example, 4-F is less acidic than 3-F and 4-OCH_3 is less acidic than 3-CH_3O, reflecting the π-donor effects of the 4-, but not the 3-substituents. The conjugated EWGs 4-CN and 4-NO_2 are more strongly acidifying than the corresponding 3-substituents, since they can enhance acidity by resonance. The charge differences that are computed are relatively small. The charge difference on H is a range of 0.007 units, about 3% of the charge in the unsubstituted compound. Similarly the ranges of charges on the CO_2H and CO_2^- groups are about 5 and 3%, respectively, of the charges on the unsubstituted compound. The HOMO energy of the anion might be expected to be a good indicator of acidity, since it reflects the ability of the structure to accommodate the negative charge. Here

the range is about 15% of the unsubstituted compound. The correlation between $\delta\Delta H$ and the HOMO energy is high. As might have been anticipated for gas phase data, *all* substituents lower the energy of the HOMO relative to hydrogen, but the effect of methyl groups is small. The broad general conclusion that can be drawn is that anion stability, as indicated by the HOMO energy, is the major factor. The rather poor correlation with σ, which is derived from aqueous ionization of benzoic acids, indicates that a considerably different combination of substituent effects operates in the gas phase.

Group	σ	$\delta\Delta H$	qH	qCO$_2$H	qCO$_2^-$	HOMO (eV)
H	0.0	0.0	0.229	−0.0503	−1.237	−4.4549
4-F	0.06	−3.68	0.231	−0.0436	−1.229	−4.6395
3-F	0.34	−4.02	0.231	−0.0415	−1.224	−4.6487
4-Cl	0.23	−3.11	0.230	−0.0460	−1.227	−4.6383
3-Cl	0.37	−3.10	0.230	−0.440	−1.226	−4.6323
4-CN	0.66	−7.95	0.232	−0.0385	−1.215	−4.8765
3-CN	0.56	−7.49	0.232	−0.0297	−1.217	−4.8451
4-NO$_2$	0.78	−12.98	0.234	−0.0297	−1.199	−5.1198
3-NO$_2$	0.71	−11.14	0.235	−0.0277	−1.207	−5.0247
4-CH$_3$	−0.17	0.44	0.228	−0.0519	−1.237	−4.4563
3-CH$_3$	−0.07	0.22	0.228	−0.0514	−1.237	−4.4585
4-CH$_3$O	−0.27	0.15	0.228	−0.0520	−1.237	−4.5000
3-CH$_3$O	0.12	−0.36	0.228	−0.0490	−1.230	−4.5047

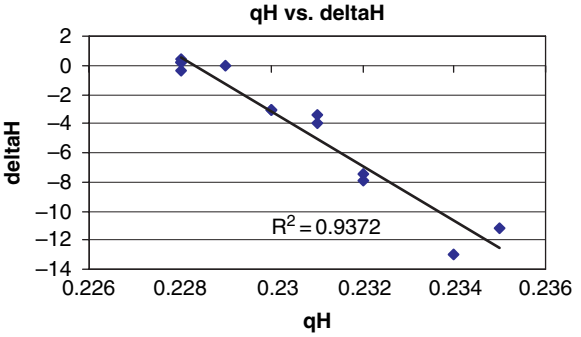

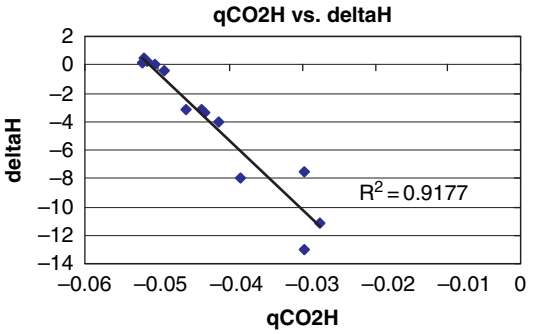

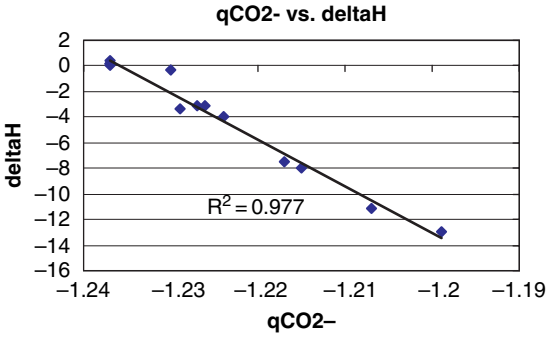

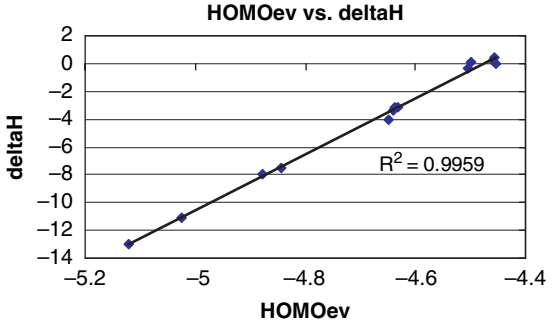

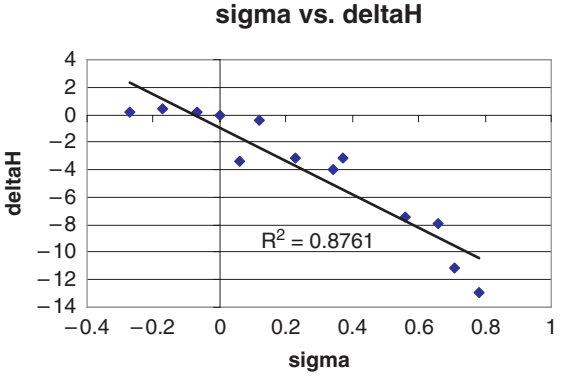

3.23. The reactions are all faster in DMSO than methanol, except for SCN^-. This can be the result of a combination of two factors—less solvation of the anion in DMSO and greater solvation of the transition structure in DMSO. The effect is greatest for Cl^- and least for I^- among the halides, which is consistent with stronger solvation of the harder chloride by methanol. The ΔS^* in DMSO becomes more negative in the order $Cl^- < Br^- < I^- < N_3^- < SCN^-$. A contribution to this order may come from the structure of the anions. The halides impose no orientational restriction, but N_3 (two orientations) and SCN^- (one orientation) have more restricted structural possibilities.

	Temp K	1/T		$k \times 10^{-4}$	ln k	Ea	ΔH	ΔG	ΔS		$k \times 10^{-4}$	ln k	Ea	ΔH	ΔG	ΔS
20	293.1	0.003412	Cl^-/DMSO	5.06	−7.58897	20958.65	20376.26	21565.73	−4.05825	Cl^-/MeOH	0.0055	−14.4133	24983.32	24400.93	25540.18	−3.88688
30	303.1	0.003299		16.7	−6.39493	20958.65	20356.39	21602.59	−4.11154		0.0226	−13.0001	24983.32	24381.06	25580.65	−3.95773
40	313.1	0.003194		50.4	−5.29035	20958.65	20336.52	21648.32	−4.18971		0.0852	−11.6731	24983.32	24361.19	25619.21	−4.01795
					average	**20958.65**	**20356.39**	**21605.55**	**−4.11984**			**average**	**24983.32**	**24381.06**	**25580.01**	**−3.95419**
				slope	−10547.9	intercept	28.40055				slope	−12573.4	intercept	28.48391		
			N_3^-/DMSO							N_3^-/MeOH						
20	293.1	0.003412		16.1	−6.43152	19387.62	18805.23	20891.64	−7.11843		0.152	−11.0942	21793.4	21211.01	23607.15	−8.17517
30	303.1	0.003299		48.3	−5.33291	19387.62	18785.36	20962.98	−7.18449		0.514	−9.87587	21793.4	21191.14	23699.02	−8.27413
40	313.1	0.003194		135	−4.30507	19387.62	18765.49	21035.34	−7.2496		1.66	−8.70352	21793.4	21171.27	23771.75	−8.30561
					average	**19387.62**	**18785.36**	**20963.32**	**−7.18417**			**average**	**21793.4**	**21191.14**	**23692.64**	**−8.25164**
				slope	−9757.23	intercept	26.85835				slope	−10968	intercept	26.32113		
			Br^-/DMSO							Br^-/MeOH						
20	293.1	0.003412		1.75	−8.65072	21144.56	20562.17	22184.08	−5.53365		0.0191	−13.1684	23447.67	22865.28	24815.14	−6.65254
30	303.1	0.003299		5.69	−7.47163	21144.56	20542.3	22251.05	−5.63756		0.0721	−11.84	23447.67	22845.41	24881.96	−6.71909
40	313.1	0.003194		17.8	−6.33114	21144.56	20522.43	22295.82	−5.66399		0.25	−10.5966	23447.67	22825.54	24949.51	−6.7837
					average	**21144.56**	**20542.3**	**22243.65**	**−5.61173**			**average**	**23447.67**	**22845.41**	**24882.21**	**−6.71844**
				slope	−10641.4	intercept	27.64972				slope	−11800.5	intercept	27.09274		
			SCN^-/DMSO							SCN^-/MeOH						
20	293.1	0.003412		0.115	−11.3732	20667.41	20085.02	23769.61	−12.5711		0.0512	−12.1824	20426.59	19844.2	24240.87	−15.0006
30	303.1	0.003299		0.365	−10.2182	20667.41	20065.15	23905.19	−12.6692		0.165	−11.0122	20426.59	19824.33	24383.36	−15.0413
40	313.1	0.003194		1.11	−9.10598	20667.41	20045.28	24022.13	−12.7016		0.481	−9.94223	20426.59	19804.46	24542.39	−15.1323
					average	**20667.41**	**20065.15**	**23898.98**	**−12.6473**			**average**	**20426.59**	**19824.33**	**24388.87**	**−15.0581**
				slope	−10401.3	intercept	24.10892				slope	−10280.1	intercept	22.89564		
			I^-/DMSO							I^-/MeOH						
20	293.1	0.003412									0.0767	−11.7782	22996.42	22414.03	24005.49	−5.42974
30	303.1	0.003299		1.75	−8.65072	21530.08	20927.82	22961.17	−6.70852		0.275	−10.5013	22996.42	22394.16	24075.71	−5.54783
40	313.1	0.003194		5.5	−7.50559	21530.08	20907.95	23026.49	−6.76634		0.956	−9.25534	22996.42	22374.29	24115.05	−5.55976
50	323.1	0.003095		16	−6.43775	21530.08	20888.08	23096.55	−6.83527			**average**	**22996.42**	**22394.16**	**24065.42**	**−5.51244**
					average	**21530.08**	**20907.95**	**23028.07**	**−6.77004**			slope	−11573.4	intercept	27.69969	
				slope	−10835.5	intercept	27.09919									

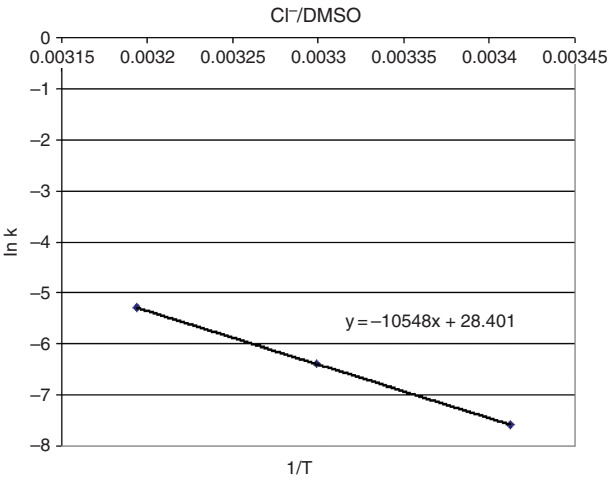
Cl⁻/DMSO
0
0.00315
0.0032
0.00325
0.0033
0.00335
0.0034
0.00345
–1
–2
–3
–4
–5
–6
–7
–8
ln k
y = –10548x + 28.401
1/T

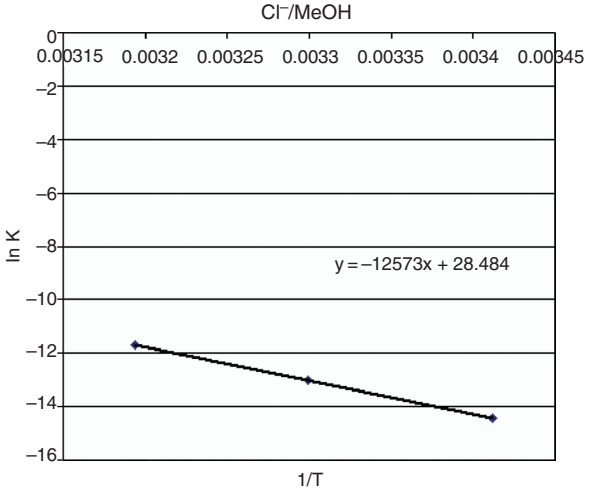
Cl⁻/MeOH
0
0.00315
0.0032
0.00325
0.0033
0.00335
0.0034
0.00345
–2
–4
–6
–8
–10
–12
–14
–16
ln K
y = –12573x + 28.484
1/T

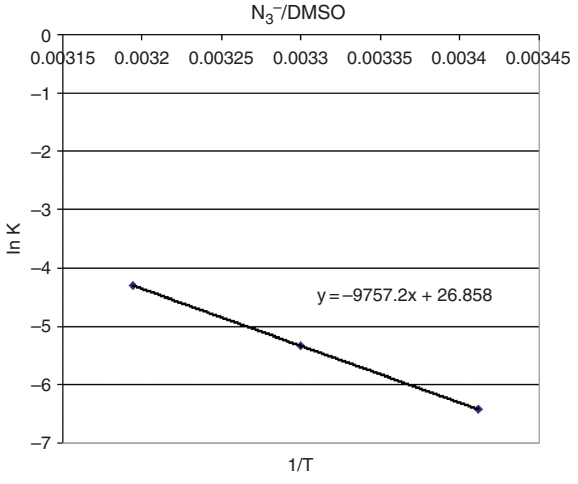
N3⁻/DMSO
0
0.00315
0.0032
0.00325
0.0033
0.00335
0.0034
0.00345
–1
–2
–3
–4
–5
–6
–7
ln K
y = –9757.2x + 26.858
1/T

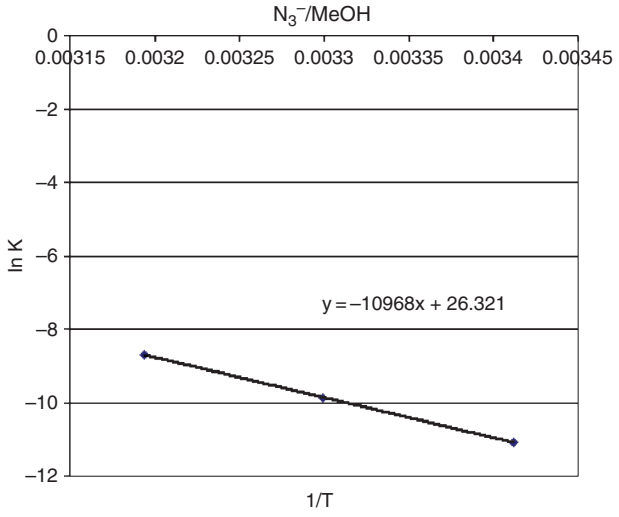
N_3^-/MeOH
0
0.00315 0.0032 0.00325 0.0033 0.00335 0.0034 0.00345
−2
−4
−6
−8
−10
−12
ln K
y = −10968x + 26.321
1/T

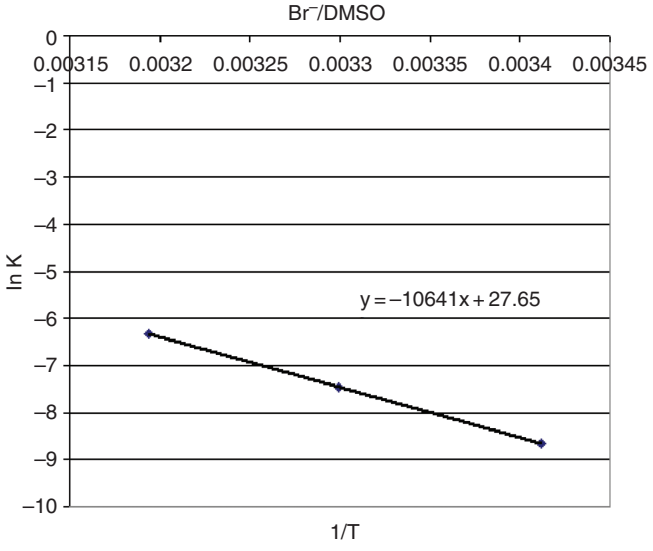
Br^-/DMSO
0
0.00315 0.0032 0.00325 0.0033 0.00335 0.0034 0.00345
−1
−2
−3
−4
−5
−6
−7
−8
−9
−10
ln K
y = −10641x + 27.65
1/T

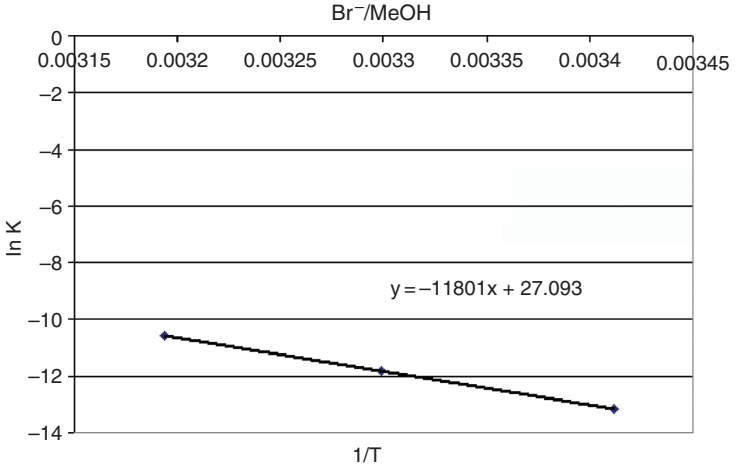
Br^-/MeOH
0
0.00315 0.0032 0.00325 0.0033 0.00335 0.0034 0.00345
−2
−4
−6
−8
−10
−12
−14
ln K
y = −11801x + 27.093
1/T

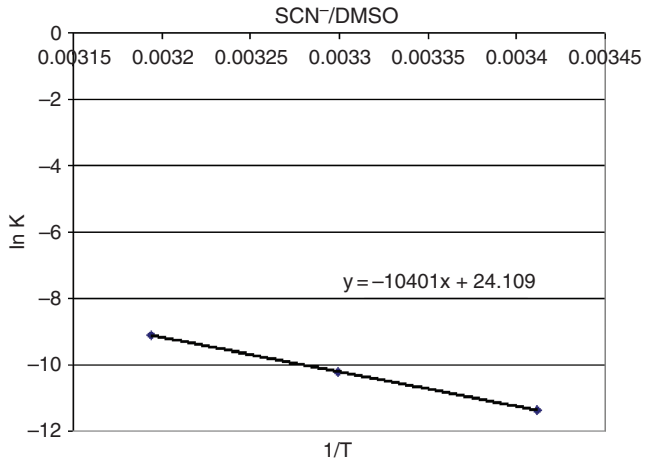
SCN⁻/DMSO
0
0.00315 0.0032 0.00325 0.0033 0.00335 0.0034 0.00345
–2
–4
–6
–8
–10
–12
ln K
y = –10401x + 24.109
1/T

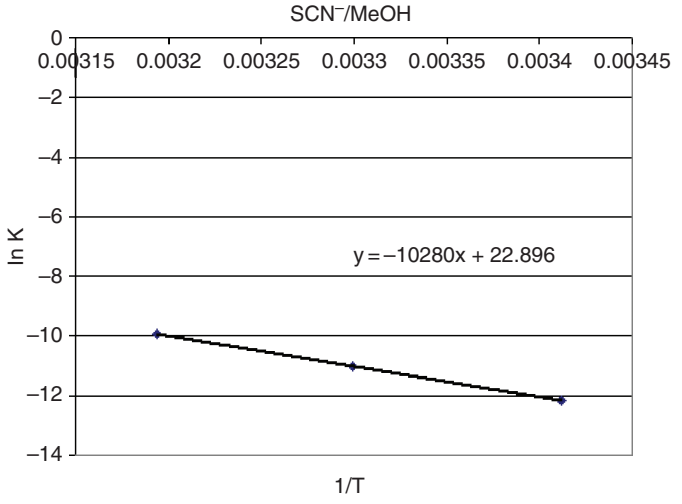
SCN⁻/MeOH
0
0.00315 0.0032 0.00325 0.0033 0.00335 0.0034 0.00345
–2
–4
–6
–8
–10
–12
–14
ln K
y = –10280x + 22.896
1/T

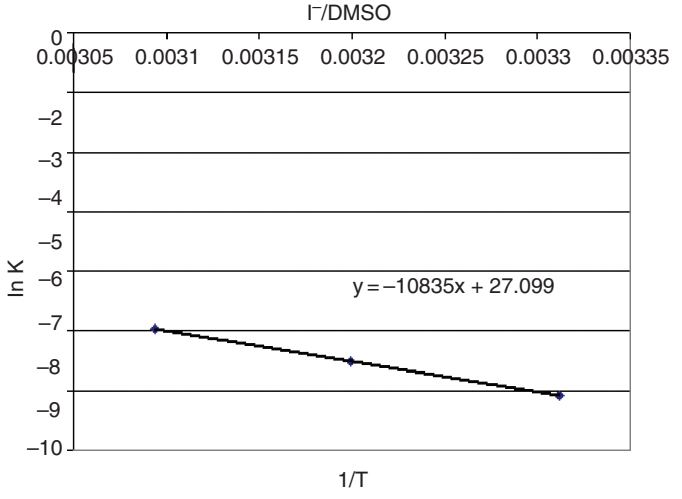
I⁻/DMSO
0
0.00305 0.0031 0.00315 0.0032 0.00325 0.0033 0.00335
–2
–3
–4
–5
–6
–7
–8
–9
–10
ln K
y = –10835x + 27.099
1/T

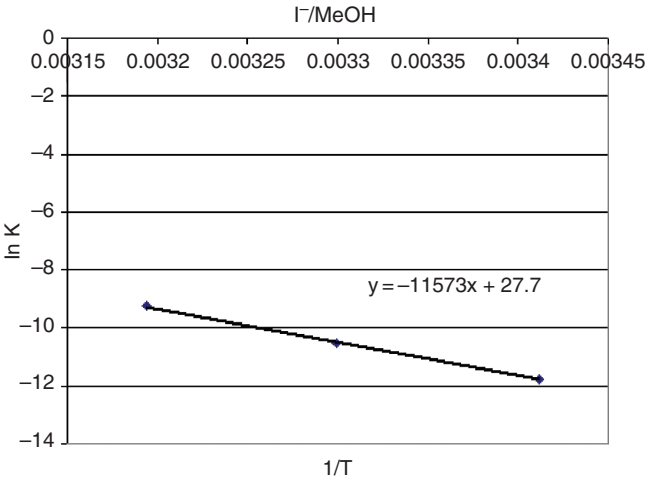

3.24. a. Cyclooctatetraene is strained by 14.5 kcal/mol, relative to butadiene.

+ 4 $CH_2{=}CH_2$ ⟶ 4 $CH_2{=}CH{-}CH{=}CH_2$

–308.96286 4 x –78.41192 = –313.64768 4 x –155.65855 = –622.63420

Σ = –0.02366 = 14. 5 kcal/mol

b. Bicyclo[1.1.0] is strained by 66.1 kcal/mol.

+ 5 CH_3CH_3 ⟶ 2 $CH_2CH_2CH_3$ + 2 $(CH_3)_3CH$

–155.62205 5 x –79.62641 = – 398.13205 2 x –118.85022 = –237.70044

2 x 158.07751 = –316.15502

Σ – 0. 10534 = –66.1 kcal/mol

c. Quadricyclane is strained by 71.3 kcal/mol.

+ 10 CH_3CH_3 ⟶ $CH_3CH_2CH_3$ + 6 $(CH_3)_3CH$

–270.93520 10 x –79.62641 = 796.26641 –118.85022 6 x –158.07751 = 948.46506

Σ = –71.3 kcal/mol = –0.11362

Chapter 4

4.1. a. The observed order reflects the relative carbocation-stabilizing effect of the substituent groups: cyclopropyl > phenyl > alkyl. The small differences

among the alkyl groups correspond to the electron donor capacity t-C_4H_9 > i-C_3H_7 > CH_3 and may also reflect steric acceleration.

b. The increasing magnitude of ρ reflects increasing electron demand in the TS in the order $CH_3 < CF_3 < CH_3SO_2$.

c. The modest increase in the series $CH_3 < C_2H_5 < i$-C_3H_7, followed by a sharp increase for t-C_4H_9 is reminiscent of the conformational $-\Delta G_c$ for these groups. A similar effect is operating and leads to ground state strain and destabilization and rate acceleration. The smaller groups can rotate to minimize van der Waals repulsion with 1,3-diaxial hydrogens, but no such rotation is possible for t-C_4H_9.

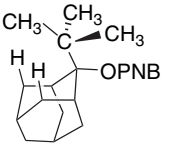

d. For $n = 1$, there is electronic stabilization resulting from electron delocalization of unshared sulfur electrons. For $n = 2$ to 5, neighboring-group participation similar to that by ether groups (Table 4.12) operates.

4.2. a. This is the Michaelis-Arbuzov reaction, which proceeds by formation and dealkylation of a tetravalent phosphonium ion.

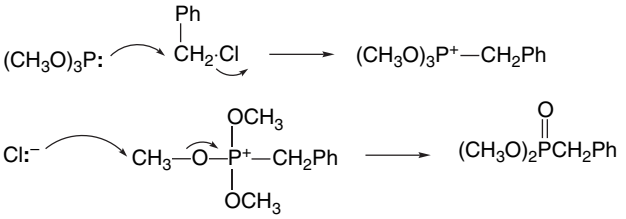

b. These stereospecific rearrangements occur by σ participation of the C−C bond *anti* the departing brosylate ion. The rearrangement is driven by relief of strain associated with the four-membered ring.

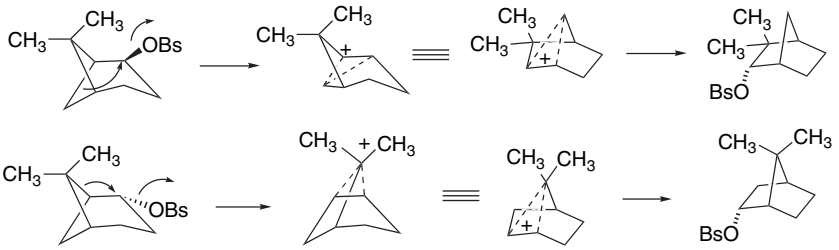

c. This reaction occurs by chorine participation resulting in an 5-*exo* cyclization, followed by ring opening of the chloronium ion at the sp^3 carbon in preference to the sp^2 carbon.

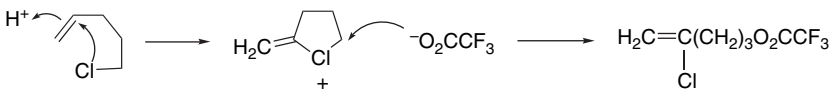

d. These contrasting rearrangements reflect the relative conformational preferences in the diazonium ion intermediates and imply participation in the migration process. The hydroxy groups favor the migration by carbonyl bond formation. In the conformationally biased *t*-butyl derivative, preferential migration of the *anti* hydrogen occurs.

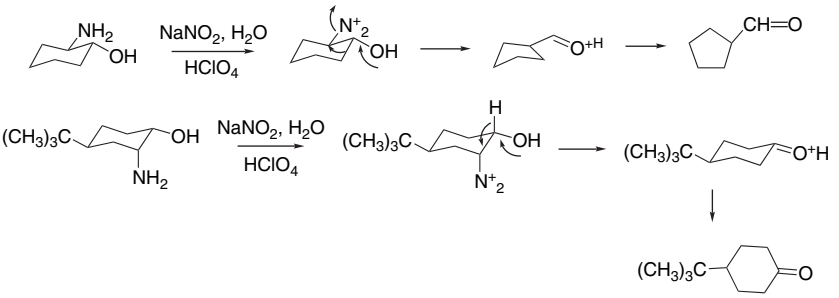

e. The bridging oxygen can assist a σ migration, leading to an oxonium ion, and then to hemiacetal that can open to the observed product.

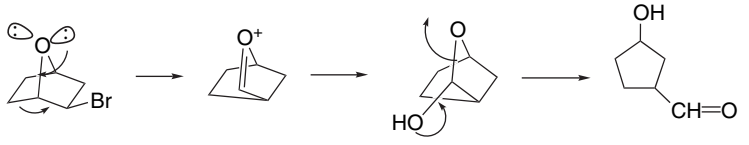

f. An achiral aziridinium ion can be formed from the *endo* isomer by back-side displacement, but this pathway is not open to the *exo* isomer. Alternatively, the racemization might involve acetoxy participation.

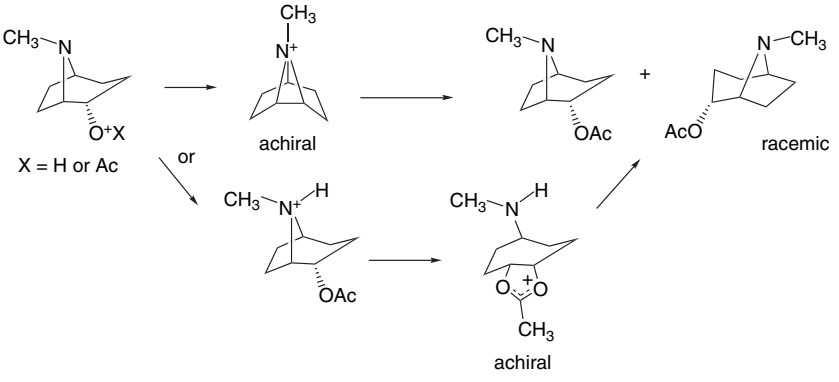

g. This rearrangement can occur by participation of one of the imide carbonyl groups.

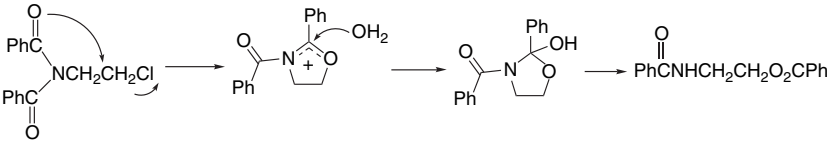

4.3. a. The 2,2,2-trifluoroethylsulfonate is a somewhat better leaving group and reacts about 175 times faster in the example cited.

b. The donor effect of the ERG CH_3 favors reaction, whereas the polar effect of the EWG group CF_3 retards the reaction. The difference is a factor of about 1000 in the example cited.

c. While there is some strain at the 7 position, the bridgehead position is very unreactive. The rate ratio is reported to be 16:1. According to one analysis (see the references), the strain associated with ionization of 1-, 7-, and 2-norbornyl derivatives are 30, 16.5, and 4 kcal/mol, respectively. Furthermore, nucleophilic solvent participation is precluded for the 1 isomer.

d. Reactant strain (B-strain) increases reactivity in the *t*-butyl case by a factor of 39,600 over the CH_3 compound.

e. The *exo* methylene derivative is 8.8×10^{-5} slower. The double bond is held perpendicular to the ionizing bond and cannot participate by electron delocalization in the TS. Additional strain and the unfavorable polar effect of the sp^2 carbons of the vinyl group also contribute to the diminished rate.

f. The α-sulfonyl chloride is less than one-twentieth as reactive as the β-sulfonyl halide. This is due to a steric effect of the branched sulfonyl, perhaps enhanced by the partial negative charge (repulsive to iodide) associated with the sulfonyl oxygens.

g. The cyclopropycarbinyl structure is about 100 times more reactive as a result of the cation-stabilizing effect of the cyclopropyl group.

h. The unsaturated compound is nearly 100 times more reactive and the products are norbornyl derivatives derived from 5,6-π participation.

i. The δ-phenylthio derivative is about 100 times more reactive because of the more favorable geometry for neighboring-group participation.

j. The *ortho* isomer is more than 150 times more reactive because of intramolecular neighboring-group participation.

4.4. This system would be expected to proceed through a stabilized phenonium ion by aryl participation, especially in view of the ERG methoxy substituent. The phenonium ion is achiral and its rate of formation governs the rate of decrease of optical rotation. The rate of exchange measures the rate of internal return of sulfonate with scrambling of the tosylate oxygens. The rate shows a slight preference for return of the original oxygen ($k_\alpha > k_{ex}$), which may be due to differential solvation of the oxygens. Conversion to the final racemic product by reaction of the cation with acetic acid occurs at about one-fifth the rate of its formation, that is, about four out of five of the phenonium ion pairs return to reactant.

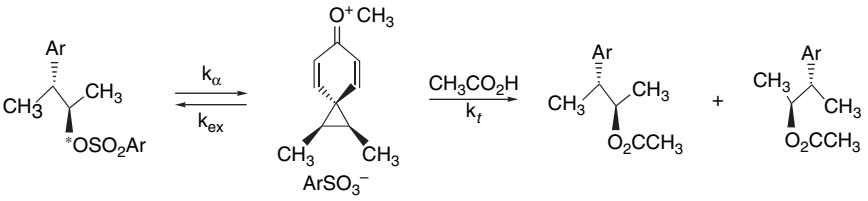

4.5. The nonpolar solvent and use of a soluble azide salt promote an S_N2 mechanism over ionization, as demonstrated by the inversion of configuration and the absence of any rearrangement. The reduced rate relative to cyclohexyl brosylate also implies that there is no kinetic enhancement from σ participation. All

of the *endo* and 80% of the *exo* isomer reacts via a back-side displacement. The nortricyclane must be formed by a bimolecular process as well, perhaps a concerted attack of azide on the *exo* C(6) hydrogen.

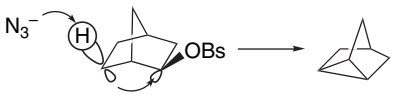

4.6.

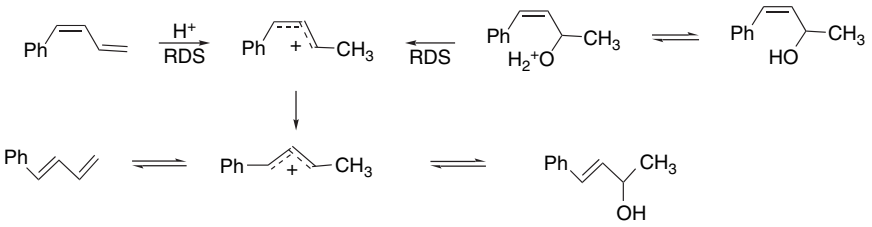

The results are consistent with the formation of a *Z*-allylic cation from both reactants, followed by isomerization to the *E*-cation and product formation. The normal deuterium isotope effect for the diene indicates rate-determining protonation, whereas the inverse isotope effect for the alcohol results from the higher extent of protonation in the deuterated solvent. The rate-determining step is the ionization of the protonated alcohol. The E_a values refer to the rate-determining step and indicate that the isomerization must occur with a lower energy requirement. The barrier to isomerization would be expected to be significantly reduced, as observed, by the presence of the phenyl group, which provides alternative (benzylic) stabilization of the carbocation. An approximate reaction energy profile is sketched in Figure 4.6P on page 54.

4.7.

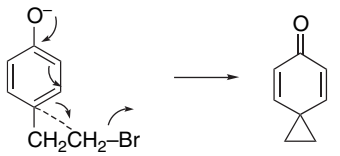

Deprotonation of the phenol group permits effective aryl participation and the resulting dienone has moderate stability.

Comment. The authors remark on the very surprising chemical shift equivalence of the α- and β-cyclohexadienone protons in the 60 MHz spectrum. So far as can be determined, this aspect of the properties of spiro[2.5]octa-4,7-dien-6-one has not been pursued.

4.8. The *syn* isomer can ionize with σ participation that leads to an allylic ion.

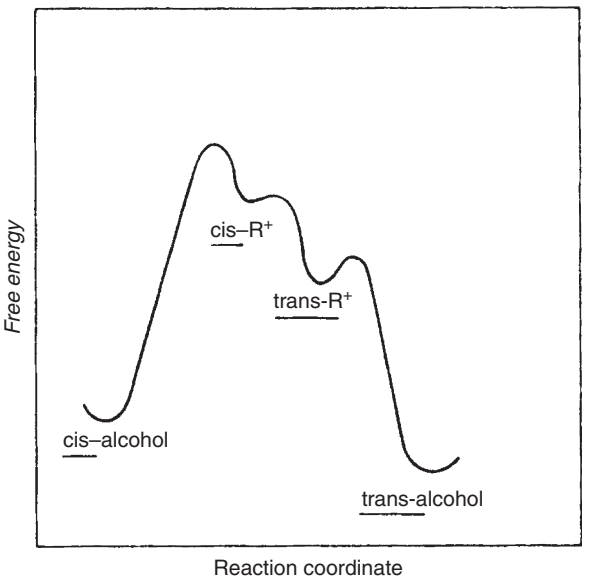

Fig. 4.6P. Approximate reaction energy profile for isomerization reactions. Reproduced from *J. Am. Chem. Soc*., 93, 691 (1971), by permission of the American Chemical Society.

4.9. The following ions are the most stable structures that are isomeric with the initial carbocation that would be formed. See pp. 436–438 for discussion of carbocation structures under stable ion conditions.

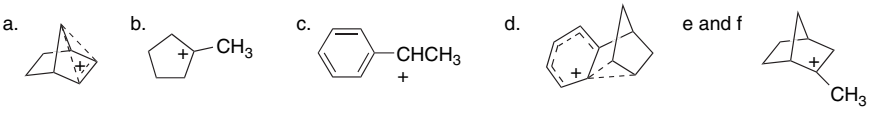

4.10. The ratios of solvolysis to exchange are 4.55, 4.47, 0.83, and very large, respectively. The relatively unhindered secondary systems represented by *i*-propyl and cyclopentyl indicate only about 20% internal ion return. This presumably results from major solvent participation. Note that the ratio is virtually unchanged, even though the absolute rates differ by a factor of 100. The extent of ion pair return becomes larger in the more hindered 2-adamantyl system, where nucleophilic solvent participation is decreased by steric factors. The 3,3-dimethyl-2-butyl system rearranges to a tertiary carbocation faster than internal return occurs. This suggests the possibility of concerted ionization and rearrangement.

4.11. The smaller ρ and *r* values in the Yukawa-Tsuno equation for the 1-arylpropenyl cation indicate a *reduced* electron demand, which must be due to the electron-releasing character of the methyl group.

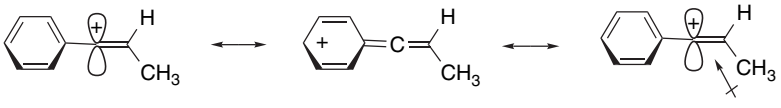

4.12. a. The dependence on $[N_3^-]$ with the EWGs reflects a shift from an uncoupled to coupled mechanism in response to lower carbocation stability.

b. This result is consistent with little direct nucleophilic participation in the reactions that proceed through discrete carbocations.
c. This result indicates greater selectivity for N_3^- by more stable (longer-lived) carbocations. Less stable carbocations may collapse so rapidly that solvent capture is more favorable in competition with the anionic nucleophile.
d. This result is as anticipated, since the N_3^- is acting directly as a nucleophilic participant.

4.13. a. The retention of configuration in both cases indicates π participation. The greater rate enhancement in **13-A** indicates that the isolated double bond is more effective at stabilizing the TS than an aryl ring. This can be explained in terms of the π-bond order of the participating bonds, which is 1.0 in **13-A** as opposed to 0.5 for **13-B**. This implies higher electron density to the back side of the bromine in **13-A**. The aromatic π electrons are also "harder."
b. The cyclopropylcarbinyl character of **13-D** reduces the electron demand.
c. The product array from reactant **13-E** is consistent with formation of the cyclopropylcarbinyl carbocation **13-G**.

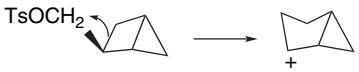

13-E **13-G**

Reactant **F** evidently has a more favorable pathway to the stabilized ion **13-H**, which can also account for the observed stereospecificity.

13-F **13-H**

It is suggested that the ring expansion preference is related to reactant conformation.

d. Reactants **13-I** and **13-J** have configurations that permit formation of cyclopropylcarbinyl cation **13-L**. On the other hand, the *syn* relationship of the leaving group to the double bond in reactant **13-K** precludes participation.

13-L

e. These results illustrate the effect of remote substituents on adamantyl solvolysis. The EWG fluoro substituent promotes retention in the *syn* isomer, whereas the ERG substituent $(CH_3)_3Sn$ leads to retention in the *anti* isomer. These results have been explained in terms of preferential σ bridging of the most electron-rich C−C bonds. The rate retardation for the *anti* fluoro derivative is consistent with this explanation. The nearly complete racemization for the *anti* isomer indicates nearly asymmetric solvation. Both stannyl derivatives are much more reactive, which is consistent with the ERG character of the stannyl group, but there is little rate difference between the two stereoisomers. The extensive inversion with the *syn* isomer must

presumably involve some nucleophilic solvent participation, since the expectation would be a very small barrier for the cation itself to attain the more favorable structure in each case. (See the related case of the methycyclohexyl cation in Section 4.4.)

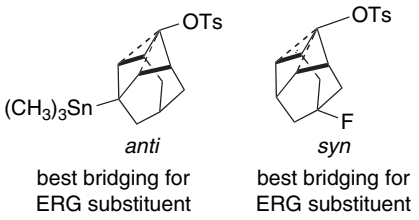

4.14. Ion **1** is an aromatic cyclopropenium ion. Ion **2** is allylic and can also be considered to be the homoaromatic analog of cyclopropenium ion. Ion **3** can be stabilized by conjugation with the adjacent double bond. Ions **4** and **5** are isomeric propargylic cations that benefit from resonance stabilization. Their relatively high energy is rather surprising. No conventional stabilization is evident for ion **6**, which is a vinyl cation.

4.15. The highly reactive *endo-anti* isomer benefits from optimal alignment of the cyclopropyl orbitals and can lead to a bridged ion **A**. This structure also accounts for the stereospecificity of the reaction. The *exo-syn* isomer can benefit from rearrangement to a cyclopropylcarbinyl cation **B**. The *exo-anti* and *eno-syn* isomers are not aligned well for cyclopropyl participation.

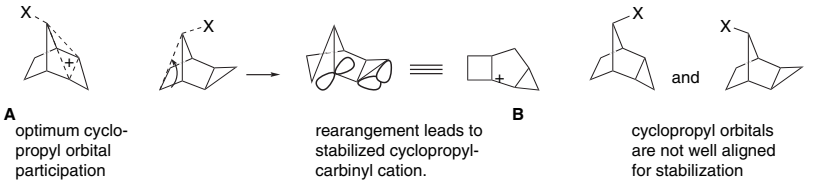

4.16. The first two cations benefit only from direct aromatic stabilization. This stabilization increases with the donor character of the substituent. On the other hand, in the third cation, the most effective stabilization is from the 2,3-double bond, as can be seen from the very large upfield shifts. This stabilization becomes relatively less important, as the aryl substituent becomes more stabilizing. This can be seen in the case of the 4-methoxy substituent, where the chemical shift is now similar to the other two cations. The strongly bridged carbocation might be formulated as π complexes, as for the norbornyl cation (see Section 4.4.5).

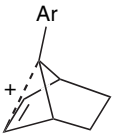

4.17. The 7-norbornyl system suffers angle strain on ionization and σ participation is minimized by the strain involved. The *endo*-2 isomer can be taken as the "normal" rate for the system. The *exo*-2-system benefits from C(5)−C(6) participation to give the bridged norbornyl cation. The *anti*-7-norborn-2-enyl

systems benefits from π participation. The two tricyclic systems benefit from cyclopropyl participation, with additional relief of strain in the case of the bicyclo[3.2.0.$0^{2,7}$]heptan-3-yl system.

4.18. The first-order reaction represents rate-limiting S_N1 ionization. As substituents become less electron donating, the first-order process becomes negligible in comparison with the second-order reaction. This is consistent with the need for carbocation stabilization in the ionization reaction. The curvature in the Yukawa-Tsuno plot for the second-order reaction suggests a continuous change in the "extra" resonance component. As the aryl group becomes less able to stabilize positive charge, the TS becomes more concerted and tighter, with less charge buildup and therefore less substituent sensitivity.

4.19. The r values suggest increasing "extra" resonance in the order $(CH_3, CH_3) < CH_3, H < H, H < CF_3, H$. This result would be anticipated from the electronic effect of the methyl and trifluoromethyl substituents. The CF_3 (EWG) enhances electron demand, whereas the CH_3 (ERG) attenuates it. The C(1)−C(2) bond orders increase in the same order. As electron demand increases, electron donation from the ring, which increases the C(1)−C(2) bond order, is enhanced.

4.20. The independence of $[N_3^-]$ implies an S_N1 (ionization) mechanism. The capture ratio of the carbocation is substituent dependent. The more stable ones (ERG) give the higher azide ratios, whereas the less stable carbocations (EWG) have rate ratios close to one. These results reflect the lifetime of the carbocations. Enhanced selectivity is associated with the more stable, longer-lived intermediates.

4.21. a. The chloride ion is more reactive than bromide in DMSO because it gains more in relative energy (6.6 versus 2.3) by the transfer to DMSO. It is more strongly solvated than bromide in methanol and thus less reactive.

b. The differential solvation of the thiocyanate is the smallest of those studied.

c. It is the nucleophile with the most stringent orientation requirement. Whereas Cl^-, Br^-, and I^- are spherical, the linear NCS^- can react only at one end. The linear N_3^- has two equivalent ends.

d. The softer ions are less affected by the transfer to DMSO, since they are relatively less solvated in methanol.

4.22. a. The first two reactions would be expected to proceed through a direct displacement mechanism with considerable cationic character at carbon in the TS. The CF_3 group will destabilize the carbocation and result in a later TS. The greater electron demand by the carbocation center leads to a larger "extra" resonance component.

b. The second set of reactions pertains to aryl-assisted processes. The resonance component is now somewhat smaller, but in the same direction, since the CF_3 group will again increase the need for resonance participation.

4.23. This is considered to be a case of opposing resonance and polar effects. While the cyano group is a strong polar EWG in both the α- and β-positions, the α-substituent can also provide resonance stabilization. This stabilization is qualitatively similar to propargyl resonance, but less favorable because of the more electronegative character of nitrogen.

4.24. The reaction in the unbranched system can be formulated as competition between direct S_N2 substitution and silyl participation leading to cyclopropane formation. The extent of silyl participation is dependent on the aryl substitution.

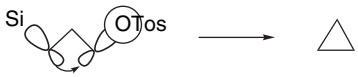

For the branched system, the potential for formation of a tertiary carbocation by rearrangement favors migration. The donor capacity of the silyl group favors migration of the silyl-substituted methylene in preference to the methyl groups.

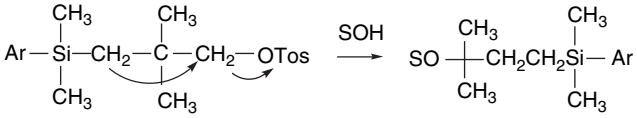

4.25. The conditions promote fragmentation and rearrangement reactions involving participation by the deprotonated hydroxy group. The compounds differ in the relative alignment of the orbitals, and therefore the effectiveness of the participation. Compound **25-A** is not aligned for orbital interaction and there is only transfer of tosyl groups. Compound **25-B** shows evidence of participation by formation of nortricyclane, but the alignment is poor and the yield is low.

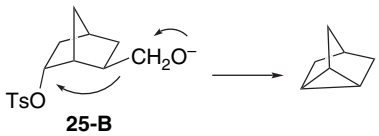

25-B

Compound **25-C** is well aligned for concerted participation and a high yield of nortricyclane is observed.

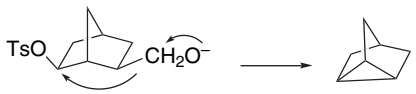

25-C

Compound **25-D** may react by an intramolecular elimination reaction.

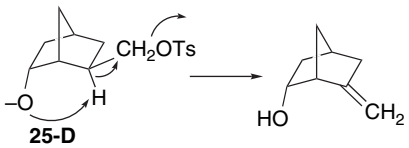

25-D

Compound **25-E** shows no evidence of participation and gives only a very low yield of apparent oxidation products. Evidently, the primary tosylate reacts only by direct displacement.

Compound **25-F** is favorably aligned for fragmentation of the "a" bond with cyclopropane formation.

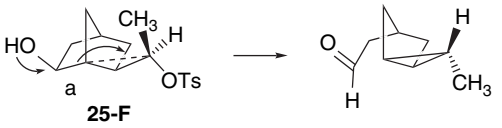

25-F

Compound **25-G**, although very similar, evidently does not have a favored alignment and three reaction modes compete. The difference between **25-F** and **25-G** probably lies in steric interactions between the ring and the methyl group, which is in an "inside" conformation in **25-G**. Note, however, that the participation does retain its stereospecificity.

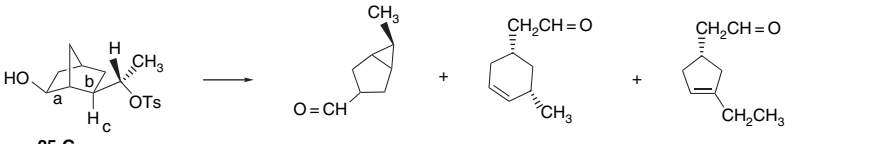

25-G

formed by fragmentation of bond a with stereospecific cyclopropane formation

formed by migration of bond b to give a ring-expansion product

formed by fragmentation with migration of hydride atom c

4.26. a. The vinyl cations are less stable than the ethyl and thus benefit more from electron donation by substituents.

b. The *sp* carbon in vinyl cations is more electronegative than the sp^2 carbon in ethyl cations. This results in a more unfavorable polar interaction with the more electronegative substituents, which partially cancels the stabilization by π donation.

c. The vinyl cations would be expected to be more electronegative than the ethyl cations and therefore would lose less electron density to polar EWG substituents, such as cyano and trifluoromethyl.

d. The order of stabilization is OH > Br > Cl > F > CF_3 > CN, which, except for OH, is in the order of the polarity of the substituents, indicating that a polar effect is dominant. All the CH_2-X groups except CH_2-CN remain stabilizing, although less so than methyl. This suggests that the dominant effect is alkyl group hyperconjugation, attenuated, but not dominated, by the polar effect of the substituent group.

e. These π-donor substituents are all strongly stabilizing in both ethyl and vinyl cations. The order is NH_2 > OH ~ SH for ethyl and NH_2 > SH > OH for vinyl. These substituents presumably have opposing resonance and polar compounds.

4.27.

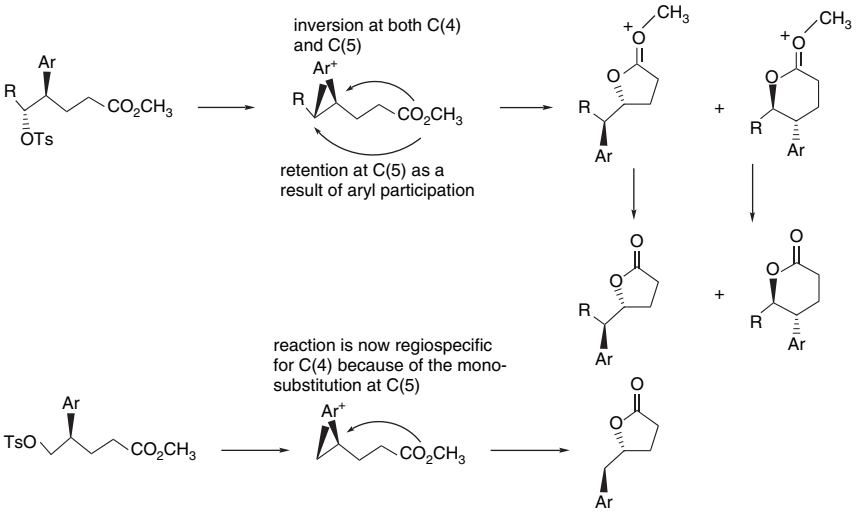

Chapter 5

5.1. a. The disubstituted alkene is about two times more reactive because of the cumulative effect of the electron-donating alkyl groups (see also the data in Table 5.2, which would suggest a somewhat larger difference).

b. The *cis* isomer, which has the CH_2Br in an axial position, is about nine times more reactive. At least two factors may contribute: (1) The ground state energy of this isomer is greater because of the axial orientation of the substituent. (2) The steric approach to the equatorial hydrogen in the *cis* isomer is less hindered.

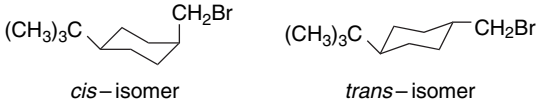

c. The EWG carboxy group destabilizes the carbocation intermediate and the unsubstituted compound is about 100 times more reactive in 20% H_2SO_4.

d. Both alkenes will give the same carbocation, which is tertiary and also benefits from cyclopropylcarbinyl stabilization. Under these circumstances, reactant energy should determine the relative E_a, and the less stable exocyclic compound is about 23 times more reactive.

e. The sulfonyl is a much poorer leaving group than the sulfonate and is substantially less reactive.

f. The EWG methyl stabilizes the β-chlorovinyl carbocation intermediate and is about 65 times more reactive.

g. The bridgehead structure prevents the oxygen from providing any stabilization to the carbocation intermediate. Under these circumstances, the polar EWG

character of the oxygen is dominant and the bridgehead compound is about 10^{-5} less reactive. Normally the strain associated with the bridgehead double bond would lead to enhanced reactivity, so the electronic factor is greater than the observed difference of 10^5.

5.2. a. This alkene would be expected to give an 5-*exo* cyclization product as a result of intramolecular nucleophilic participation. The preference between the two alternative cyclization TSs is small and a 2:1 mixture of products is formed.

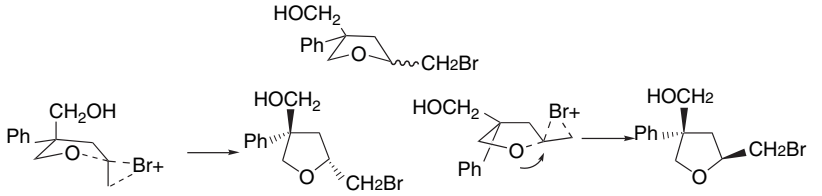

b. The regiochemistry is controlled by the stability of the cyclopropylcarbinyl cation. The addition is *syn*, reflecting involvement of a relatively stable carbocation. There is a modest preference for attack *anti* to the cyclopropylmethylene group, which can be attributed to a steric effect.

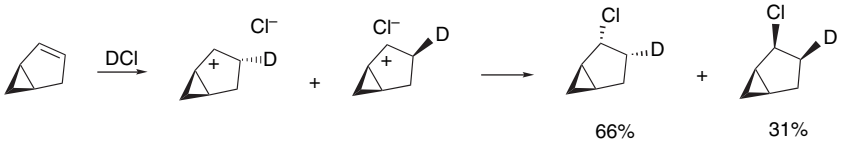

c. This reaction would be expected to proceed by removal of the acidic proton α to the carbonyl group. Elimination to the less sterically congested *E*-isomer is expected and observed.

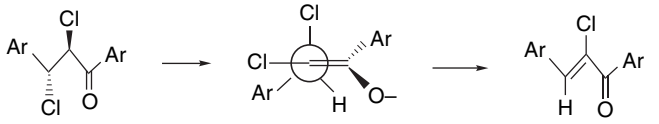

d. The regiochemical preference is for the less-substituted alkene (Hofmann rule).

e. The product composition corresponds to net substitution, suggesting a carbocation process. The observed product can be accounted for by terminal allene

chlorination, with the regiochemistry governed by the cyclopropyl group, followed by ring opening and deprotonation.

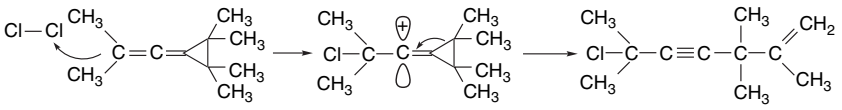

f. The highly hindered base leads to a 3:1 preference for the exocyclic alkene.

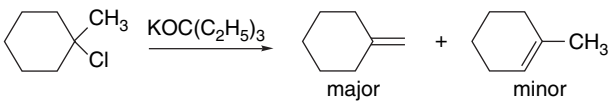

g. These reaction conditions lead to the isolation of the methoxymercuration product as the chloride. The methoxy group is located at the benzylic position.

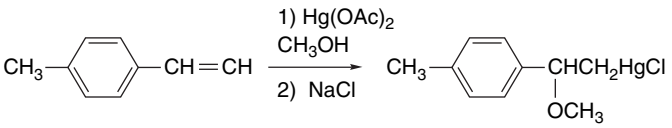

h. Because the reaction can proceed through a phenyl-stabilized vinyl cation, a mixture of *anti* and *syn* addition is expected. Both the dichloride and the solvent incorporation products are nearly a 1:1 mixture of *syn* and *anti* addition products. The solvent incorporation product regiochemistry is controlled by the phenyl substituent.

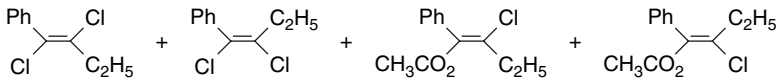

5.3. The *trans* isomer can attain *anti* alignment of a β-hydrogen only in a diaxial chair or nonchair conformation, thus disfavoring the elimination. Evidently the *syn* elimination mechanism is also strongly disfavored, because this would increase torsional strain.

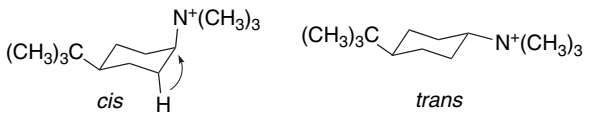

5.4. The relatively large positive ρ values are consistent with an E1cb-like TS for the quaternary ammonium salt. The relatively small isotope effect suggests a "late" TS with C−H bond breaking well beyond the midpoint. In relation to the ammonium salt, the better leaving groups show smaller ρ values and larger isotope effects, suggesting more synchronous TSs. None of the eliminations appear to be E1-like, since the ρ would be expected to be negative for an E1-like TS. The isotope effect near 7 for the bromide suggests an TS near the midpoint of C−H bond breaking. An interesting point is that the tosylate group, which is a better leaving group in S_N2 reactions than bromide, seems to be a somewhat poorer leaving group by these criteria.

5.5. In the *erythro* isomer, the deuterium is *anti* to the bromine in the conformation that gives rise to *E*-2-butene. The primary isotope effect should increase the amount of *Z*-2-butene and 1-butene at the expense of *E*-2-butene.

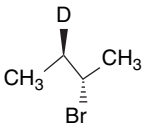

5.6. The order of reactivity is expected to be governed by carbocation stability and therefore is in the order shown. The reported second-order rate constants ($M^{-1}s^{-1}$) are given with the structures.

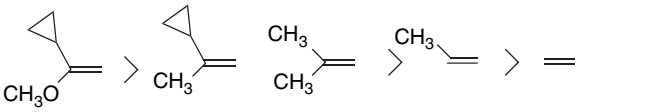

5.7. a. The observed regiochemistry is the result of phenyl stabilization of the carbocation intermediate. The *syn* addition is also consistent with the involvement of a stabilized carbocation with rapid nucleophilic capture. The protonation occurs from an axial direction to maximize the overlap with the π-electron density. The reactant conformation is controlled by the *t*-butyl substituent.

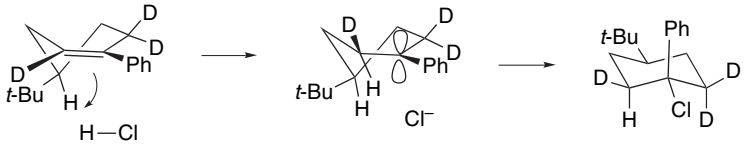

b. The regiochemistry is controlled by phenyl stabilization of the carbocation intermediate. The preferred *syn* addition is the result of phenyl stabilization of the ion pair, which collapses faster than dissociation or stereorandomization. There is a larger driving force for rotation to relieve strain in the *Z*-isomer, and this results in a higher degree of stereorandomization.

c. This reaction proceeds from the sterically preferred *exo* direction, with Markovnikov regioselectivity. There is no need to invoke a bridging carbocation, because *tert*-carbocations are of sufficient stability to avoid bridging.

d. The stereochemistry results from diaxial addition, with the *t*-butyl group controlling reactant and product conformation. Although regiochemistry is not an issue with the symmetrical reagent, the nucleophilic attack would be expected to occur at the more-substituted end of the bromonium ion.

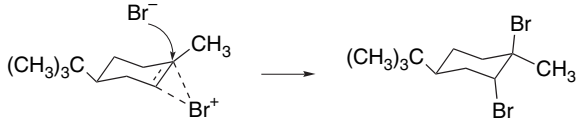

5.8. a. The ρ value is positive, which indicates a net negative charge buildup. The formation of **8-B** evidently involves an E2 mechanism with some E1cb character. A similar mechanism should occur in formation of **8-C**, but the aryl group is too remote from the site of charge buildup to influence the rate.

b. The regiochemistry is controlled by the influence of the methyl group, which leads to a 1,3-dimethylallyl cation (pent-3-en-2-ylium) [as opposed to a pent-2-en-1-ylium cation that would result from C(4) protonation.] The observed products are the result of 1,2- and 1,4-addition to the 1,3-dimethylallyl cation. The lack of equal distribution of the two products rules out a dissociated ion pair, where any distinction between C(2) and C(4) would be lost. Rather, the results indicate a tendency to capture the cation site closest to the site of protonation. This is consistent with formation and rapid collapse of an ion pair.

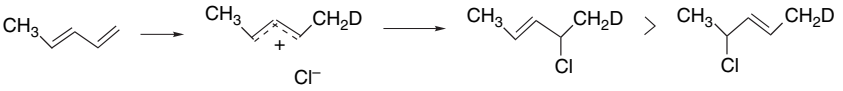

c. The EWG carbonyl destabilizes carbocation character at C(3), requiring the stereospecific *anti* addition mechanism. The regiochemistry of addition of Br−Cl, indicates that the benzylic site is the point of nucleophilic ring opening of the bromonium ion.

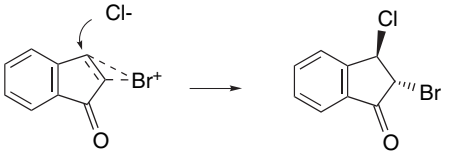

d. This is an example of the preferred terminal protonation of allene. Internal protonation does not lead to an allylic cation for stereoelectronic reasons (p. 545).

e. The results are consistent with the lesser stability of the cyclohexyl cation and the resulting involvement of an Ad_E3 mechanism. The rate acceleration is presumably due to chloride-assisted protonation (see p. 479). The more stable benzylic cation can be formed without any chloride participation.

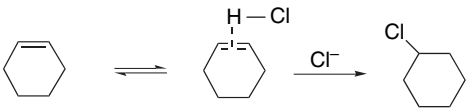

f. The increasing ρ values indicate that the reaction becomes more sensitive to substituents as the number of fluorines increases. This indicates greater E1cb character at the TS, and shows that the addition of each fluorine makes it more difficult to break a C−F bond.

5.9. a. The stereochemistry is consistent with *anti* addition followed by methoxide-induced *anti* elimination.

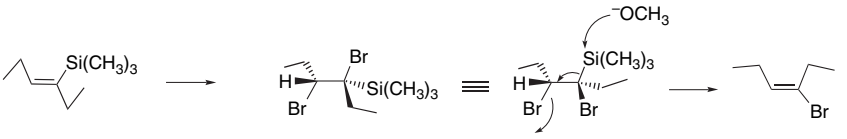

b. The stereochemistry indicates *syn* elimination, which is likely to occur via intramolecular formation of a oxasilacyclobutane intermediate.

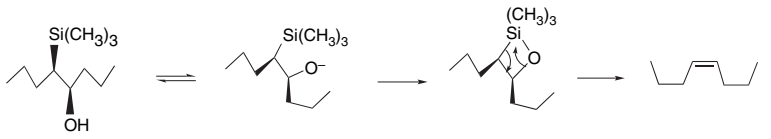

c. Reversible formation of the achiral bromonium ion can account for the racemization while retaining *anti* stereochemistry

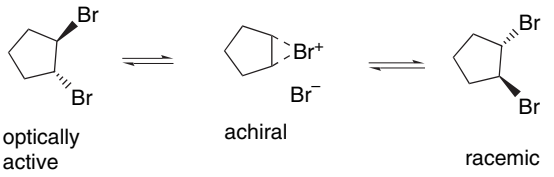

d. Double-bond participation in the bromine attack (or bromonium ion opening) can account for the formation of the product. The ring geometry favors this participation by shielding the back side of both double bonds.

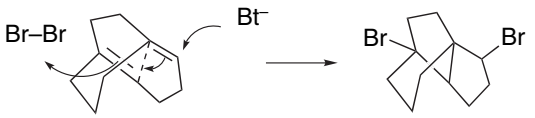

5.10. The bridged bromonium ion benefits from both substituents in the disubstituted derivative, whereas the more localized vinyl cation that is the intermediate in hydration is primarily stabilized by only one substituent.

5.11. The first two products are *anti* addition products that can be formed through bromonium ions. The major isomer is the diaxial addition product, with respect

to a pseudoequatorial aroyloxy substituent. The third and fourth products can be formed by intramolecular participation of the aroyloxy group.

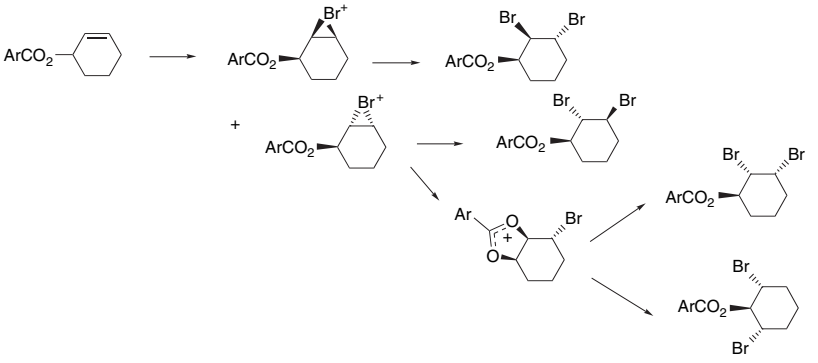

5.12. This correlation is consistent with a rate-determining formation of a benzyl cation having direct resonance interaction with the Ar ring. The effect of the second ring is not so strong, as indicated by the 0.23 factor and the normal σ substituent constant. In particular, these results are not consistent with direct formation of a phenonium ion by Ar′ participation in the ionization.

5.13. An Ad_E3 mechanism involving nucleophilic capture of an alkene-HCl complex would appear to be ruled out by the observed rate decrease in the presence of added chloride ion, since added chloride should accelerate the rate of capture of an alkene-HCl complex. Another mechanism that would exhibit third-order kinetics is HCl-assisted formation of the carbocation. Added chloride could inhibit the reaction by complexing with HCl. The lack of deuterium incorporation into the reactant indicates fast capture of the carbocation by chloride.

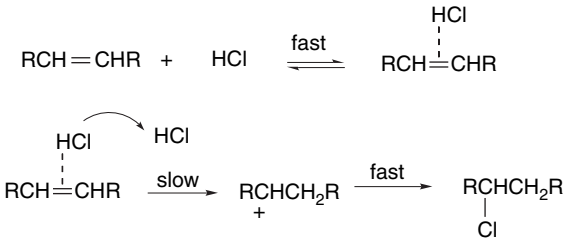

5.14. These results are consistent with a change of mechanism from a bridged bromonium ion for EWG substituents to an open carbocation for ERGs. The more negative ρ value is consistent with a more localized charge for the ERG reactants. The loss of stereospecificity is also consistent with a shift to an open carbocation.

5.15. Consistent with other alkene hydrations, the reaction is expected to proceed through a carbocation intermediate. The observation of both 1,2- and 1,4-addition products is consistent with this expectation. The normal value of k_H^+/k_D^+ is consistent with rate-determining protonation The substituent effects in the order ethoxy > cyclopropyl > methyl > chloro are also consistent with rate-determining formation of a carbocation intermediate.

5.16. The reactions of the weaker acids give no indication of reversible carbocation formation since there is no deuterium incorporation or reactant isomerization. These results are consistent with an Ad_E3 type mechanism.

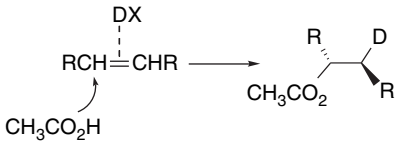

With the stronger acid, a carbocation can be formed and there is some reversal leading to both deuterium incorporation and reactant isomerization. The addition is also somewhat less stereoselective. This result indicates that CF_3SO_3H can effect protonation without solvent participation.

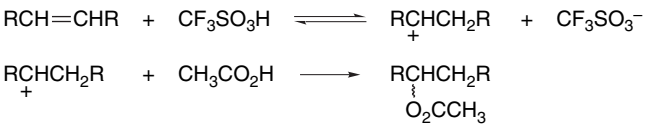

5.17. The following trends are apparent in the data: (1) The ratio of elimination to substitution increases with base concentration. The trend is gradual in methanol but quite sharp in the DMSO mixtures. (2) The reaction rate increases only slightly with [$^-$OMe] in methanol, but more rapidly in the DMSO mixtures. (3) In the absence of base, the rate decreases somewhat as the amount of DMSO increases and the extent of elimination increases. Since the reactant is a tertiary halide, the competition is expected to be among E1, S_N1, and E2 mechanisms. The very slight increase in rate with [$^-$OMe] in methanol suggests that little E2 reaction is occurring in this solvent. The change in product ratio results from increasing deprotonation of the carbocation intermediate with increasing [$^-$OMe]. The enhanced basicity of MeO^- in DMSO, along with the somewhat retarded ionization rate can account both for the increased total rate and the increased extent of elimination in the DMSO mixtures.

5.18. a. Each of these cations benefits from the delocalization by the aryl substituent. The order of the r^+ values suggests that this is of increasing importance in the order *tert* sp^2 < *sp* < *sec* sp^2.

b. The energy profile suggests that TS1 is close in structure and energy to the product cation-H_2O complex. There is more charge on the phenyl ring (+0.369) than in the case of the alkene protonation TS (+0.196). The alkene protonation TS is much closer to the reactants than to the product. By the Hammond postulate, it has an "early" transition state. This is consistent with the reduced extra resonance stabilization, as measured by the Yukawa-Tsuno r^+.

5.19. These catalysts are believed to function by complexation of the halogen, with release of halide, probably as trihalide anion. The enhanced nucleophilicity of the halide (or trihalide) and diminished electrophilicity are responsible for the improved steric control of regioselectivity. The thiourea derivative may be a favorable catalyst by enhancing the attraction for the polarizable halogens.

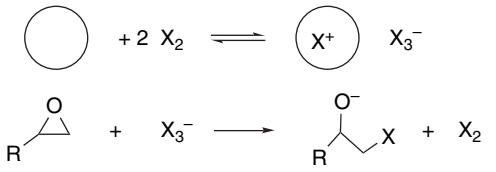

5.20. The mechanism of oxymercuration is believed to involve nucleophilic capture of a reversibly formed mercurinium ion or π complex. Markovnikov orientation is generally observed for unsymmetrical alkenes. In conformationally biased cyclohexane systems, ring opening is preferentially diaxial. The results are consistent with these generalizations. The three *t*-butyl systems all show a strong preference for the introduction of hydroxy in axial positions, consistent with the preference for axial ring opening. In 4-*t*-butylcyclohexene there is little selectivity between the two stereochemically distinct intermediates. In 3-*t*-butylcyclohexene, there is a strong preference for attack away from the *t*-butyl group, as a result of steric shielding of the position adjacent to the substituent. This effect is also seen in 3-methylcyclohexene, although the extent is reduced. About 10% of the product from 3-methylcyclohexene results in introduction of equatorial hydroxy, owing to the lower conformational bias, compared to the *t*-butyl system. In 1-methyl-4-*t*-butylcyclohexene, the regiochemistry is controlled by the methyl substituent, but the addition of hydroxy is entirely from the axial direction. Like 4-*t*-butylcyclohexene, 4-methylcyclohexene shows no regioselectivity, but the hydroxylation is axial at both ends of the double bond. These results are all compatible with reversible mercuration followed by product-determining nucleophilic capture.

5.21. a. The *cis* ring junction leads to a molecule with distinctive convex and concave faces. Direct epoxidation occurs from the less hindered convex face. The bromonium ion is formed from the same face but the nucleophile approaches from the concave face at the less hindered position. The subsequent inversion of configuration leads to the desired epoxide.

b. The stereochemistry and regiochemistry of the solvobromination are as expected, with the nucleophile attacking the more substituted (cationic) position of the bromination intermediate. Subsequent participation of the carbonyl group in displacement of the bromide and hydrolysis leads to the more hindered *cis*-diol.

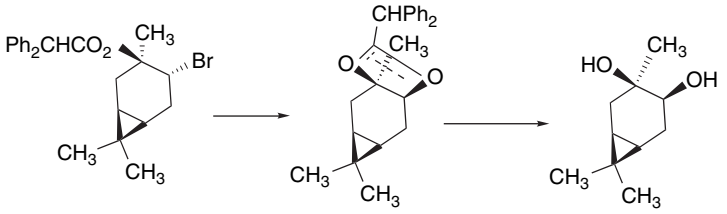

c. Various reagents have been used to achieve chemoselective functionalization of polyenes, based on differential reactivity. This example is reported to go in 99% yield. All the double bonds are trisubstituted, suggesting similar reactivity, although a small polar EWG effect may deactivate the allylic ether. The differentiation between the remaining terminal and internal trisubstituted double bonds may be the result of steric accessibility, perhaps accentuated by conformational effects.

6.1. a. cyclohexane < benzene < 1,4-cyclohexadiene < cyclopentadiene. The values of cyclohexane (49), benzene (~ 43), and cyclopentadiene (~ 16) are given in the text. 1,4-Cyclohexadiene benefits from pentadienyl conjugation and should be more acidic than cyclohexane, but is not aromatic and will thus be less acidic than cyclopentadiene. Given that allylic stabilization results in a pK of about 36–38 for propene, it is likely that 1,4-cyclohexadiene is more acidic than benzene.

b.

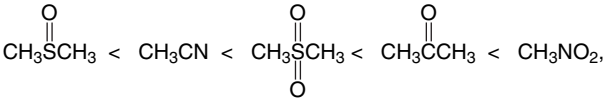

Most of this information is given in Table 6.6 in the text, although DMSO is not included. However, because it has only a single oxygen substituent, it should be less acidic than dimethyl sulfone. The pK value for DMSO is 35.

c.

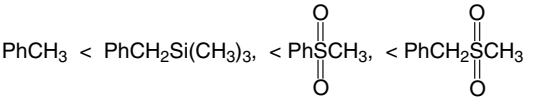

The order of stabilization will be H < $Si(CH_3)_3$ < SO_2Ph. The two sulfones differ in that the benzyl methyl sulfone benefits from conjugation with the phenyl group. The pK of $PhCH_2Si(CH_3)_3$ has been measured as 37.5 (Cs^+, THF)

d.

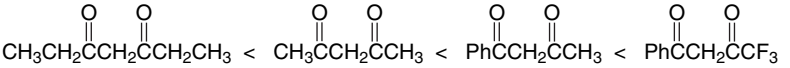

The additional methyl groups in heptan-3,5-dione should slightly destabilize the anion and decrease the acidity. The phenyl and CF_3 groups will be stabilizing in comparison to the parent pentan-2,4-dione as a result of their polar (electronegativity) effects. The pK of 5-phenyl-1,1,1-trifluoropentan-2,4-dione has been recorded as 6.5.

e. The order of increasing acidity is p-OCH_3 < p-CH_3 < H < m-OCH_3 < m-Cl. This series should follow the EWG capacity of the 9-phenyl substituent groups, as measured by σ substituent constants. The free-energy relationship found experimentally suggests that both polar and resonance effects are important.

6.2. The most acidic hydrogen is marked in bold.

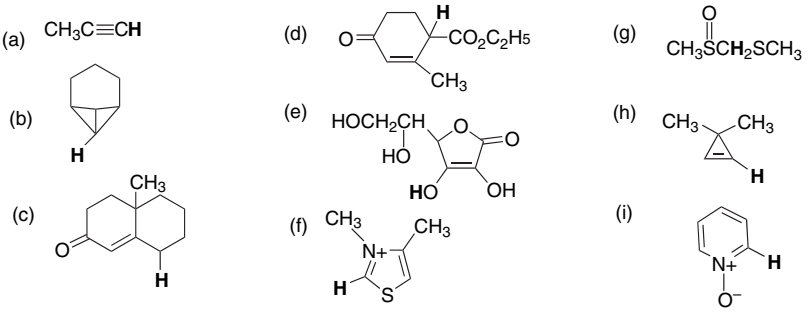

a. The terminal *sp* hybridization will have a stronger effect on the acidity of H(1) than the allylic delocalization on the C(3) hydrogens.
b. The C(6) hydrogens will be more acidic because of the enhanced *s* character and strain at this position.
c. α,β-Unsaturated enones such as the structure in (c) give the conjugated dien-1-olate as the thermodynamically stable enolate, although the kinetic deprotonation occurs at the α'-position.
d. The anion resulting from deprotonation at this position is conjugated with both the ketone and ester carbonyls.
e. This is an enolic hydrogen of a β-keto ester that benefits from delocalization.
f. The 2-position on the thiazolium ring benefits from the polar effect of the electronegative N^+ and S atoms. The relative acidity of this site was demonstrated by facile isotopic exchange and has both synthetic and biological consequences.
g. This position benefits from the anion-stabilizing effect of both sulfur substituents.
h. Early studies observed a high relative metalation rate and high *s* character, as judged by J ^{13}C–H. More recently, the gas phase acidity has been shown to be comparable to a terminal alkyne. The high acidity is due to hybridization effects.
i. The polar effect of the ring nitrogen facilitates C(2) deprotonation.

6.3. a. Because of its geometry, cubane has a high degree of *s* character in the C− H bond; one calculation gives 32% *s*, which is higher than for cyclopropane by the same calculation (28% *s*). The same analysis suggests that the *s* character *increases* in the anion. The relatively high acidity of cubane results from the cumulative strain of the ring system and the resulting hybridization change.
b. Any effect from the *s* character is negated by the increase in strain that results from enolate formation.

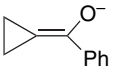

c. The gain in aromatic stabilization is maximum in the case of cyclopentadiene. In the benzo-fused analog, the per ring stabilization is smaller. There is also

a strong solvation effect. The smaller cyclopentadienide ion is more strongly stabilized in solution. In the gas phase, the size of the molecules slightly increase the acidity of the fused-ring systems.

d. The Cs^+ compound should be the most ionic and dissociated. The considerably lower rotational barrier for Li^+ indicates some participation in the rotation process. This might involve partial covalent bonding at the TS, which could stabilize the localized charge associated with the bent anion.

6.4. a. The additional ring strain imposed by rehybridization accounts for the slow reaction of bicyclo[2.1.1]hexan-2-one.

b. The formation of a normal enolate is precluded, because the only α-H is at a bridgehead position and the resulting enolate would be highly strained. The exchange and racemization can occur through a "homoenolate" formed by deprotonation of C(6). This structure has a plane of symmetry, which accounts for the concurrent racemization. Several repetitions of the deprotonation-deuteration cycle will cause exchange at all the positions that are part of the cyclopropyl ring in the homoenolate.

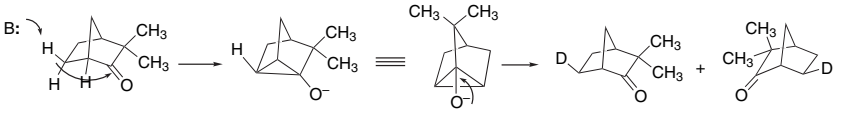

6.5.

$$pK_{R-H} = H_- + \log \frac{[RH]}{[R^-]}$$

a.

$$20.1 = 15 + \log \frac{[RH]}{[R^-]}$$

$$5.1 = \log \frac{[RH]}{[R^-]}$$

$$\frac{[RH]}{[R^-]} = 1.3 \times 10^5$$

b.

$$22.6 = 21 + \log \frac{[RH]}{[R^-]}$$

$$1.6 = \log \frac{[RH]}{[R^-]}$$

$$\frac{[RH]}{[R^-]} = 40$$

c.

$$30.6 = 19 + \log \frac{[RH]}{[R^-]}$$

$$11.6 = \log \frac{[RH]}{[R^-]}$$

$$\frac{[RH]}{[R^-]} = 4 \times 10^{11}$$

6.6. This result is in agreement with the importance of a stereoelectronic factor arising from better alignment of the axial C−H bond with the carbonyl π orbital.

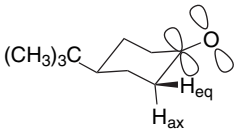

6.7. There is an excellent correlation between the pK and the rate of exchange.

Compound	log k	pK
9-Phenylfluorene	-1.762	18.5
Indene	-2.301	19.9
3,4-Benzofluorene	-2.044	19.8
1,2-Benzofluorene	-2.496	20.3
Fluorene	-3.403	23
2,3-Benzofluorene	-3.668	23.5

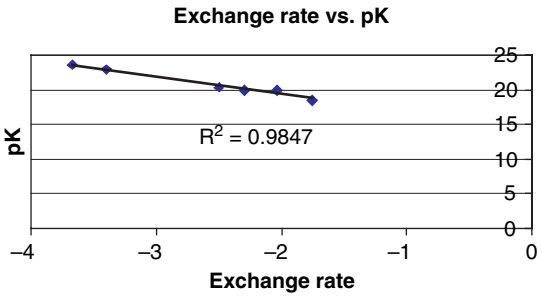

6.8. The correlation is best with σ. This is consistent with the absence of direct conjugation of the negative charge with a ring substituent. The σ^- correlation is the poorest. This confirms that lack of direct conjugation and enhanced resonance stabilization between the negative charge and the ring substituents.

Group	pK	pK/pKo	σ	σ^+	σ^-
4-$(CH_3)_2N$	27.48	1.126	−0.83	−1.7	−0.12
4-CH_3O	25.70	1.04	−0.27	−0.78	−0.26
3-$(CH_3)_2N$	25.32	1.025	−0.16		
4-CH_3O	25.19	1.02	−0.17	−0.31	−0.17
3-CH_3	24.95	1.01	−0.07		
H	24.70	1	0	0	0
4-C_6H_5	24.51	0.992	0.01	−0.18	0.02
4-F	24.45	0.99	0.06	−0.07	−0.03
3-CH_3O	24.52	0.993	0.1		
4-Br	23.81	0.964	0.23	0.15	0.25
4-Cl	23.78	0.963	0.23	0.11	0.19
3-F	23.45	0.949	0.34		
3-Br	23.19	0.939	0.37		
3-Cl	23.18	0.938	0.37		
3-CF_3	22.76	0.921	0.43		
4-CF_3	22.69	0.919	0.54	0.61	0.65
4-CN	22.04	0.892	0.66	0.66	1

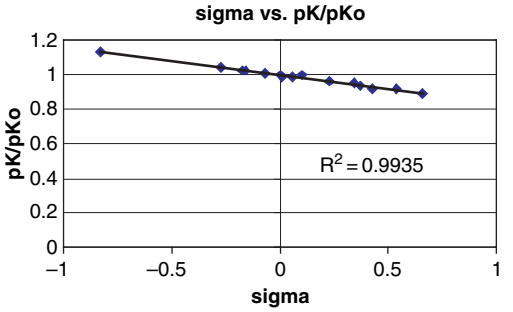

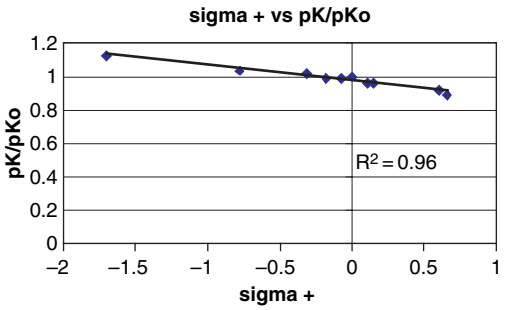

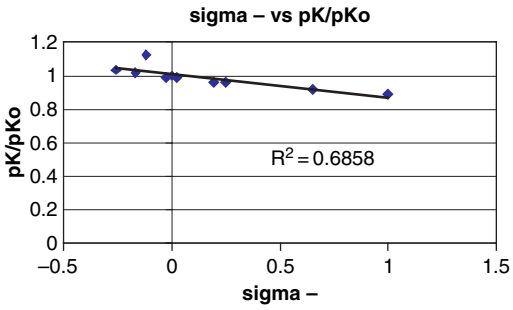

6.9. a.

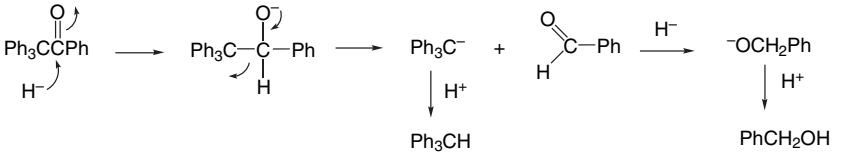

This unusual fragmentation of the ketone is due to the relative stability of the Ph_3C^- anion. It is suggested that the use of pyridine favors this process by coordination of Li^+ and Al^{3+} centers, which could otherwise stabilize the alkoxide.

b. This reaction is thought to proceed by hemiacetal ring opening, followed by enolization and elimination of an enediol. The latter species can account for the interchange of the carbonyl and alcohol oxidation levels in one of the products.

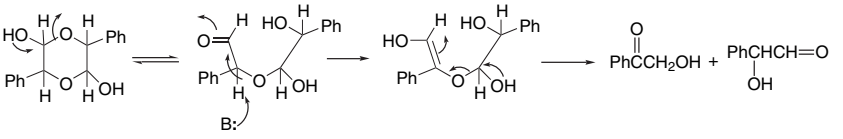

c. This stereoequilibration can occur via reversible ring opening, which is facilitated by the stabilization of the anion provided by the phenyl ring.

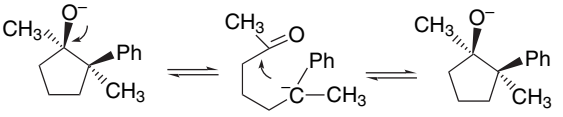

d. The opening of the cyclic hemiacetal generates an aldehyde with a single chiral center that can be racemized via the corresponding achiral enolate.

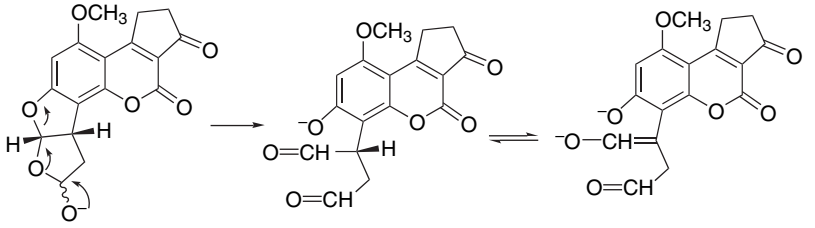

e. The enolates can equilibrate, perhaps through a 1,5-hydrogen shift. The more highly substituted one is more stable.

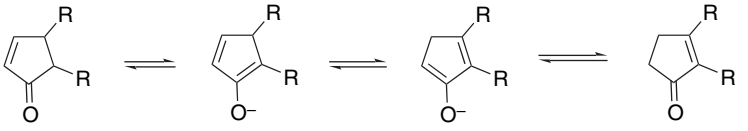

6.10. Part of the stabilization is likely due to the removal of steric constraints to planarity of the cyclic enolate. This would also account for the increased acidity of 5,5-dimethylcyclohexane-1,3-dione. The dependence on ring size suggests that the *E*-configuration imposed on the ester function by the ring, which is relaxed as the ring size increases, may *increase* the energy of the lactone and thus decrease the energy required for deprotonation. It is observed that the *s-trans* configurations of esters are about 3 kcal/mol less stable than the *s-cis* configurations, and this has been attributed to a stereoelectronic effect involving the sp^2 oxygen pair with the σ^* orbital of the carbonyl group.

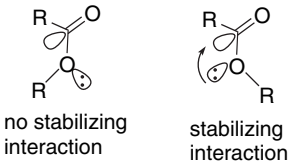

6.11. DMSO-alkoxide systems are characterized by a high degree of internal return. This may be due to the proximity of a relatively acidic coordinated alcohol molecule formed by the deprotonation. Such systems do not show a kinetic isotope effect, since dissociation of the complex rather than its formation is the rate-determining step in proton exchange. Under these conditions, there might not be a strong relationship between measured exchange rates and the acidity determined under equilibrium conditions.

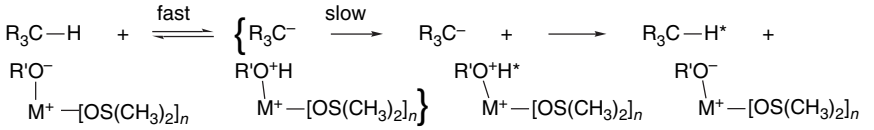

6.12. a. This is due to the somewhat greater stability of endocyclic double bonds in six-membered rings as compared to five-membered rings.

b. The keto forms of ethyl acetate and acetamide are stabilized by resonance involving the oxygen or nitrogen substituents, respectively, that is not available to acetone.

c. Structurally, this may be due to the extended conjugation in the enol of 2-indanone. The hydroxy group is conjugated with the aromatic ring. In the enol of 1-indanone, there is no such conjugation.

d. The ring favors coplanarity of the conjugated enolate and reduces nonbonded repulsions.

6.13. a. The enol of the 2-isomer is stabilized by an intramolecular hydrogen bond.

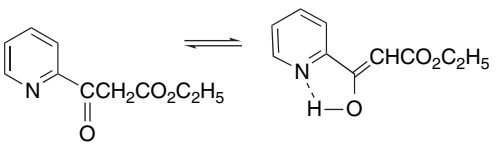

b. The acidity of both the keto and enol forms of 9-formylfluorene is enhanced by the aromaticity associated with the common enolate anion and this increases

the acidity of the carbonyl form by an especially large factor. The pK of the keto form is 6.2, whereas it is 7.4 for the enol form. The K for enolization can be calculated by using the relationship

$$pK_{enolization} = pK_{enol} - pK_{keto} = 7.4 - 6.2 = 1.2$$

c. The combined acidifying effect of the cyano and ester substituents, along with an intramolecular hydrogen bond, provides a stabilized enol.

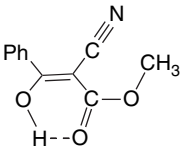

6.14. a. The enhanced acidity of 2-indanone can be attributed to greater stability of the enolate arising from increased planarity and reduction of nonbonded repulsions relative to the noncyclic model.

b. In addition to planarity and reduced steric repulsions, the enolate in this case benefits from aromaticity of the indole ring.

c. The cyclic enolate benefits from planarity and reduction of nonbonded repulsion relative to the acyclic model.

6.15. The two possible conformers of the enolate that are in equilibrium differ in nonbonded repulsions. Each of these enolates provides two faces for attack by the alkylating agent. In each enolate, however, one mode is characterized by eclipsed interactions, and on the basis of the discussion on p. 617 would be disfavored. The prediction can then be based on the relative steric encumbrances of each face of the staggered TS.

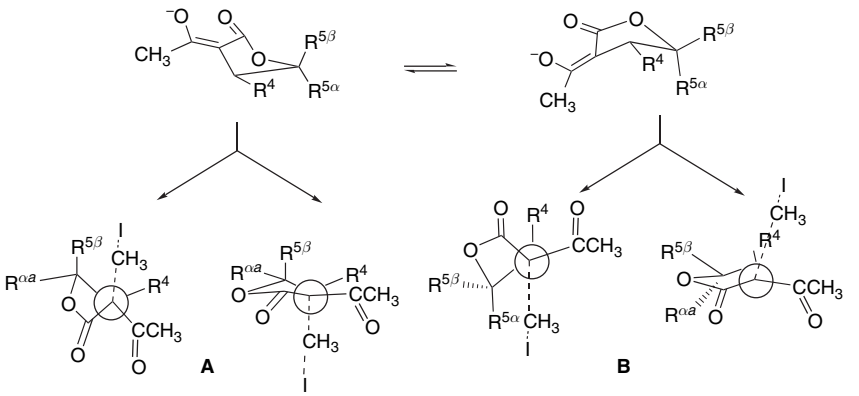

R^4	$R^{5\alpha}$	$R^{5\beta}$	**A:B**	explanation
CH_3	H	H	29:71	alkylation is *anti* to R^4 via TS **B**
CH_3	H	*n*-Pr	<3:>97	$R^{5\beta}$ Pr directs alkylation via TS **B**
CH_3	*n*-Pr	H	80:20	$R^{5\alpha}$ Pr directs alkylation via TS **A**
H	H	C_2H_5	25:75	$R^{5\beta}$ Et directs alkylation via TS **B**

6.16. Chelation by the metal ion increases the effective electronegativity of the carbonyl oxygen and promotes base-catalyzed deprotonation.

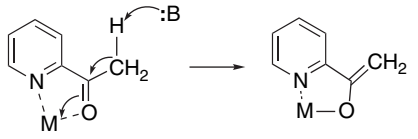

6.17. The stereoselectivity of the deprotonation and protonation implies a stereoelectronic effect that strongly favors an equatorial orientation of the carbanion. In MO terminology this can be attributed to a combination of destabilizing interaction with the sulfur unshared electrons in the axial carbanion and a stabilizing interaction with the C–S σ^* for the equatorial carbanion. The results also imply that the carbanion is pyramidal rather than planar.

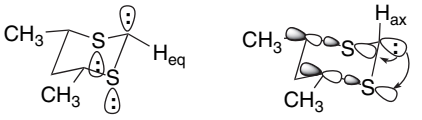

destabilizing stabilizing

6.18. a. The HOMO orbitals shown below for the butadiene dianion and the trimethylemethane dianion indicate that the latter would be more stable.

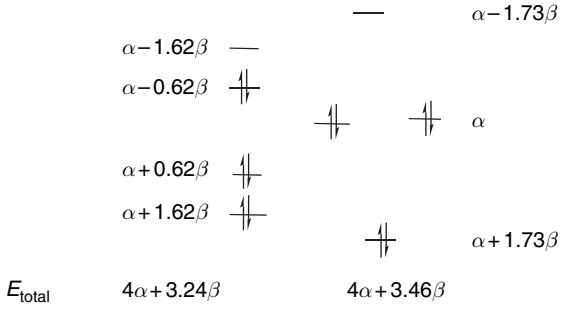

b. On the basis of the calculated total HOMO energies, the dianion **E** is the most stable. The authors of the referenced paper also calculated the REPA (resonance energy per atom) basis. On this basis, ion **F** was most stable. The experimental observation is that ion **F** increases at the expense of the other ions, implying that it is the most stable.

	C	**D**	**E**	**F**
	This is the equivalent of two isolated allyl anions	This is a trimethylene-methane dianion plus an isolated double bond	This is a hexatrienyl dianion	This is a branched methylenepentadienyl dianion
E_{total}	$8\alpha+5.6\beta$	$8\alpha+5.4\beta$	$8\alpha+6.4\beta$	$8\alpha+6.2\beta$

6.19. The second structure, which provides a relatively acidic enol moiety having delocalization of the negative charge over both oxygens, is much more consistent with the observed pK than the first, which provides only a single carbonyl group for anion stabilization.

6.20. a. Acid-catalyzed bromination occurs at the more substituted position.

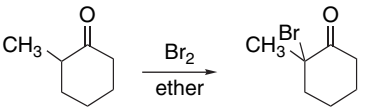

b. The more easily enolized C(2) position is preferentially brominated. The product can be easily decarboxylated to 2-bromo-6-methylcyclohexanone.

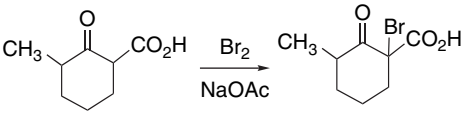

c. Base-catalyzed chlorination occurs at the more acidic chlorine-substituted position.

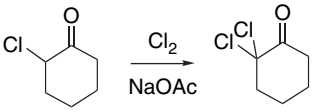

d. Base-catalyzed bromination occurs at the more acidic bromine-substituted position.

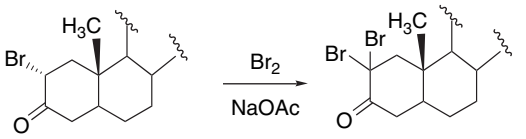

e. Acid-catalyzed chlorination proceeds at the more substituted position in a ratio of 10:1 under these conditions.

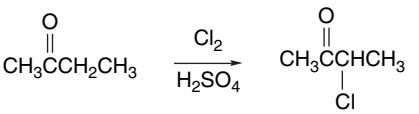

6.21. a. The less-substituted kinetic enolate will be formed. The stereoisomeric ratio of the products was not determined.

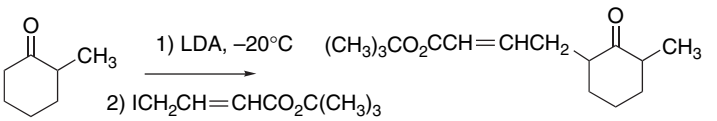

b. The less-substituted kinetic enolate will be formed. The axial methyl group provides a modest steric directive effect, but this is outweighed by the preference for an axial-type approach leading to chair product giving a roughly 2:1 ratio.

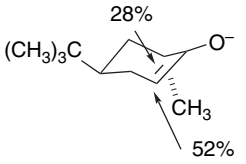

c. This is a case of axial versus equatorial attack in a conformationally biased system. There is a fairly significant preference for equatorial alkylation.

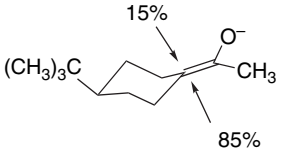

d. This is a case of intramolecular alkylation, where optimal alignment of the nucleophilic enolate and the leaving group determines the stereochemistry.

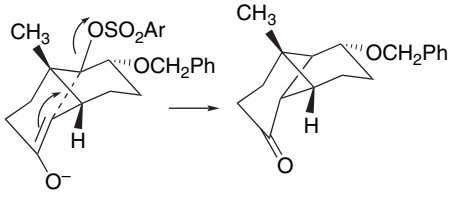

e. This is another example of an intramolecular enolate alkylation.

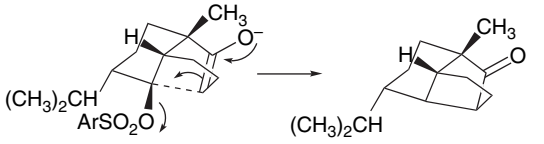

6.22. Two anions can be formed by deprotonation of 3-methylcyclohex-2-enone, which has electron density primarily at O, C(2), and C(4) or the exocyclic methylene. Each of the products has at least one new bond at C(2), indicating that this is the site of initial attack. The use of an excess of base in each case ensures the deprotonation of the initial product to a second enolate. With 1,2-dibromoethane ($n = 2$), dialkylation takes place at C(2) in preference to formation of a five-membered ring by O-alkylation. This is probably the result of a kinetic effect arising from the $3 > 5 > 6 > 7$ relationships for most ring closures involving nucleophilic substitution.

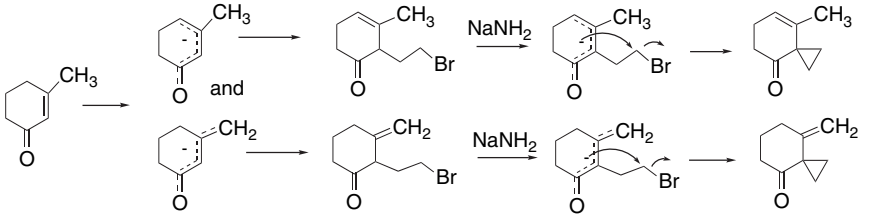

The dominant product from 1,3-dibromopropane is an O-alkylation product. This result can be explained in terms of ring size preference, in this case 6 > 4. The absence of product with the endocyclic double bond is attributed to equilibration of the endocyclic and exocyclic enolates with more rapid cyclization of the latter.

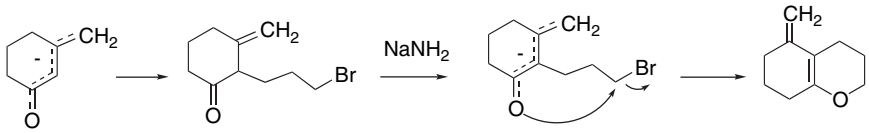

With 1,4-dibromobutane, the product is the result of a spiro dialkylation at C(2) because the formation of a five-membered ring is preferred to the seven-membered ring formed by O-alkylation. Again, only product from the exocyclic enolate is found and this result is attributed to equilibration of the exocyclic and endocyclic enolates prior to cyclization.

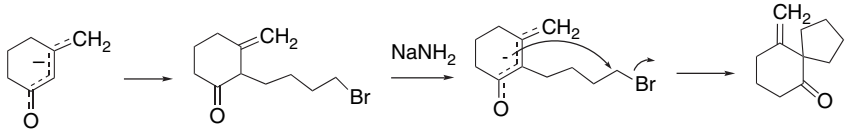

6.23. The retention observed with the cyano compound indicates that the proton exchange has occurred almost exclusively by internal return, whereas the ketone undergoes extensive dissociation. The ketone is somewhat more acidic and the role of delocalization in anion stabilization may be greater. Note that these are *vinyl* (sp^2) carbanions, which typically have significant inversion barriers.

6.24. Let the two product ratios be X/Y and X^1/Y, where Y is the unchanged rate of reaction at the methyl group. Then:

$$\frac{X}{Y} = {}^{94}/_{6} \quad \text{and} \quad \frac{X^1}{Y} = {}^{80}/_{20}$$

and

$$Y = \frac{6X}{94} \quad \text{and} \quad Y = \frac{20X^1}{80}$$

$$\frac{6X}{94} = \frac{20X^1}{80}$$

$$480X = 1880X^1$$

$$\frac{X}{X^1} = \frac{1880}{480} = 3.9$$

6.25. a. This result can be interpreted in terms of steric shielding by the *tert*-butyldiphenylsiloxy substituent.

b. The use of two equivalents of LDA means that the hydroxy group will be deprotonated and available to participate in coordination with Li^+. The preferred conformation of the enolate has the smallest group (H) eclipsed with the enolate oxygen. It has been suggested that the solvent molecules and amide ions associated with the Li^+ contribute the steric bulk that favors attack from the opposite face through a TS such as shown below.

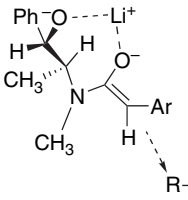

c. This reaction is an S_N2' alkylation. The observed stereoselectivity is consistent with a chairlike conformation for the TS for the intramolecular alkylation.

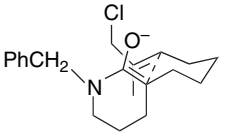

6.26. The computational structures reveal, as expected, that there is significant coordination of Li^+ to all the oxygens in the dianion. Also, as expected, the deprotonation is at the CH_2 group, not the CHO^- group. The structures also indicate that enolate **1** is less sterically encumbered that any of the enolates having *t*-butyl groups, because the *i*-propyl group assumes conformations with the hydrogen oriented toward the enolate. In the *t*-butyl esters, a methyl is placed over or under the enolate. Comparing **4** to **1**, there is an enhanced preference for the *si* face because of the added CH_3 group. In enolate **3**, the extra CH_3 is on the *si* face and the preference is reduced from 19:1 to 4.5:1. With the *bis*-*t*-butyl ester, the R^1 ester group is more effective at blocking approach than the R^2 ester substituent. The origin of the inherent *si* preference in the unhindered esters is not entirely evident. It may be related to the unsymmetrical location of the second Li^+ ion, which is on the *si* face.

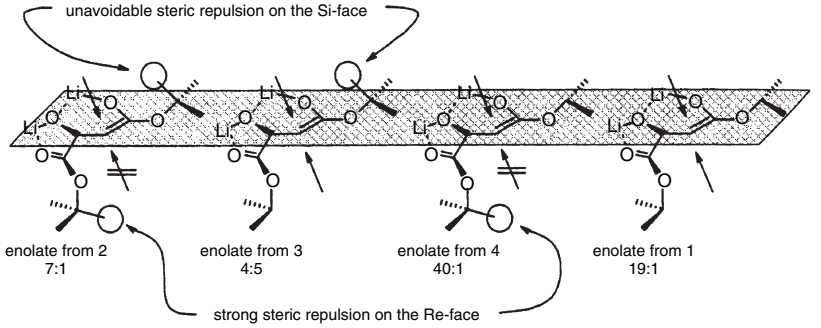

Reproduced from *Helv. Chim. Acta*, **85**, 4216 (2002) by permission of Wiley-VCH.

Chapter 7

7.1. The enhanced acidity is due to the polar effect of the additional hydroxy group. This presumably has both a polar (electrostatic) and a hyperconjugation (anomeric effect) component. The order for the substituents shows that acidity is further enhanced by electron-withdrawing substituents.

7.2. a. The more favorable K for addition, despite the adjacent *t*-butyl substituent, reflects the stabilization of the carbonyl form of acetophenone resulting from conjugation with the benzene ring.

b. The hydrate of the aldehyde group can react by intramolecular nucleophilic catalysis.

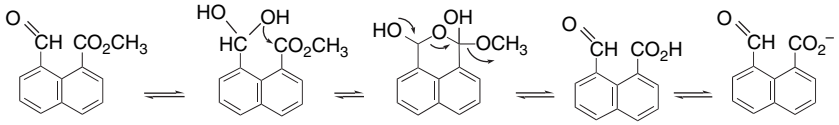

c. This result reflects the greater stabilization of the TS for elimination from the tetrasubstituted carbon in the former case. The stability of the elimination TSs should be in the same order as the products.

d. These ketones have aromatic character, whereas the tetrahedral addition intermediates for exchange do not. This loss of aromaticity contributes to a higher E_a for addition and results in a slower exchange rate.

7.3. a. The order is $CH_3CH{=}CHCH(OC_2H_5)_2 > CH_3CH(OC_2H_5)_2 > ClCH_2CH(OC_2H_5)_2$.

This order can be predicted on the basis of the rate-determining cleavage of an O-protonated acetal. Cleavage will be accelerated by the conjugated double bond in the but-2-enal acetal. The polar effect of the chloro substituent will both decrease the basicity of the acetal toward protonation and destabilize the oxonium ion intermediate.

b. The order is $(CH_3)_2C(OC_2H_5)_2 > CH_3CH(OC_2H_5)_2 > CH_2(OC_2H_5)_2$. This order reflects the stabilizing effect of the methyl group on the oxonium ion intermediate and also parallels the position of the equilibrium constant for hydration, which is less favorable for the more-substituted acetals.

c. The order is camphor $\sim$ cyclopentanone $>$ cyclohexanone. The order reflects a preference for $sp^3 \rightarrow sp^2$ hybridization change for five-membered rings. The rate of camphor, which also involves a five-membered ring, is slightly greater than for cyclopentanone.

d. The order is 3,3-dimethyl-2-butanone $>$ 4,4-dimethyl-2-pentanone $>$ acetone. This order is the result of the successively less steric congestion at the acetal carbon and results from steric destabilization of the acetal relative to the ketone.

e. The order is 4-methoxybenzaldehyde $>$ benzaldehyde $>$ butanal. This order is the result of conjugative stabilization of the oxonium ion intermediate by the aryl groups, with the ERG 4-methoxy adding an increment to the stabilization.

7.4. This result suggests more complete proton transfer for the more basic alkoxy groups. The general acid catalysis is consistent with concerted proton transfer and elimination. In terms of a two-dimensional reaction coordinate, the TS moves closer to a stepwise reaction as the alcohol becomes more basic and a poorer leaving group. The fact that the α values are relatively large suggests that proton transfer is advanced.

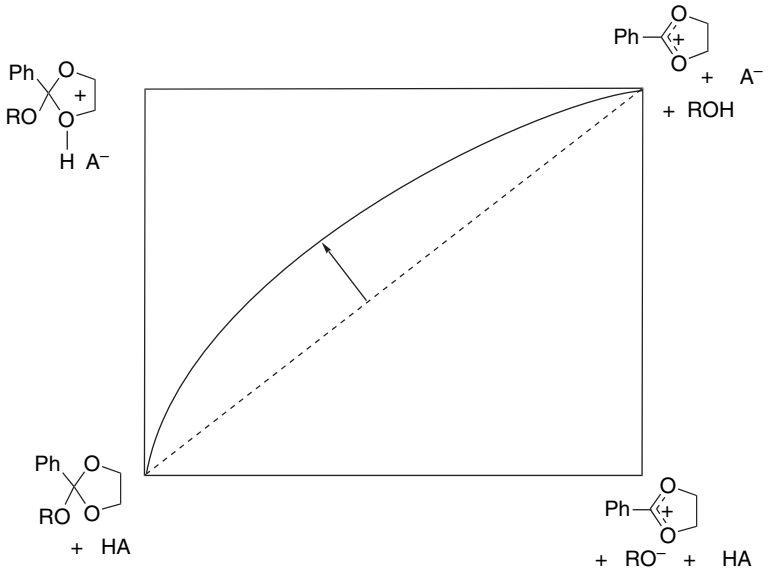

7.5. a. Intramolecular general base catalysis of water attack is the most likely possibility. Intramolecular nucleophilic catalysis is less likely because of strain. Intramolecular general base catalysis is evident as the upward bend in the pH profile corresponding to deprotonation of the quinoline nitrogen in the region pH = 2–4. This pH-independent mechanism is dominant in the pH range 4–8, after which unassisted hydroxide ion attack is the principal reaction.

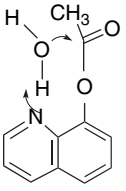

intramolelcular general
base catalysis of water attack

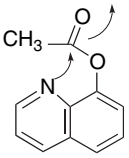

intramolecular
nucleophilic catalysis

b. Direct nucleophilic catalysis, general base catalysis of water attack, or intramolecular O-protonation all might be feasible. Either the carboxylate or the phenolic groups may be involved. The observed pH-rate profile suggests carboxylate nucleophilic attack in the pH region when the phenol group is protonated and intramolecular general base catalysis of water attack when the phenol is deprotonated. The increasing rate between pH = 1 and 5 corresponds to ionization of the carboxy group with a p$K \sim 3$. This mechanism is dominant in the pH range 6–8. The second upward bend between pH 8 and 9 is consistent with engagement of the phenol anion.

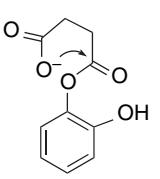

Intramolecular nucleophilic catalysis by carboxylate group

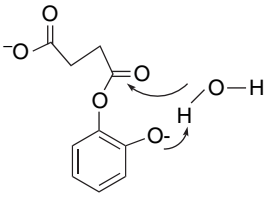

Intramolecular general base catalyst of water attack by phenolate group

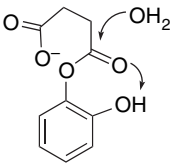

intramolecular general acid catalysis

c. Between pH 2 and pH 4 the protonated imidazolium ion can provide general acid-assisted water addition. The upward bend at pH 4 is consistent with general base catalysis of water attack by the deprotonated imidazole ring, which is pH independent and dominates for pH 6–8. At more basic pH, intramolecular nucleophilic catalysis by the imidazole anion is possible, although this was not observed for the unsubstituted compound.

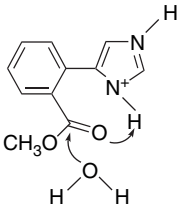

General acid assistance of water attack

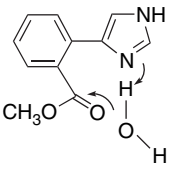

Intramolecular general base assistance of water attack

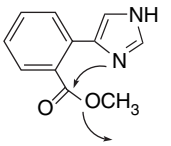

Intramolecular nucleophilic catalysis

d. Intramolecular general base catalysis by the amino group is possible. The pH-rate profile shows an upward bend corresponding to deprotonation of the amino group with a p$K \sim 10$.

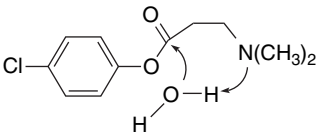

7.6. The rate depends on the concentration of the monoanion (HA^-), which is much more reactive than the neutral species H_2A or the dianion A^{2-}. These concentrations are related by the two acid dissociation constants K_{a1} and K_{a2}.

$$K_{a1} = \frac{(HA^-)(H^+)}{(H_2A)} \text{ and } K_{a2} = \frac{(A^{2-})(H^+)}{(HA^-)}$$

$$\text{Rate} = k_1\ (HA^-) + k_2(H_2A)$$

The (HA^-) and (H_2A) terms can be expressed on the basis of K_{a1} and K_{a2}

$$(H_2A_{tot}) = (H_2A) + \frac{(H_2A)K_{a1}}{(H^+)} + (H_2A) \bullet \frac{K_{a1}}{(H^+)} \bullet \frac{K_{a2}}{(H^+)}$$

$$= (H_2A)\left[(H^+)\frac{K_{a1}}{(H^+)} + \frac{K_{a1}K_{a2}}{(H^+)^2}\right]$$

$$= (H_2A)\frac{[(H^+)^2 + (H^+)K_{a1} + K_{a1}K_{a2}]}{(H^+)^2}$$

So $(H_2A_{tot}) = (HA^-)\left[\frac{(H^+)}{K_{a1}} + 1 + \frac{K_{a2}}{(H^+)}\right] = (HA^-)\frac{[(H^+)^2+(H^+)K_{a1}+K_{a1}K_{a2}]}{(H^+)K_{a1}}$

Substituting into the equation for the rate yields

$$-\frac{d(H_2A_{tot})}{dt} = k_{obs}(H_2A_{tot})$$

$$k_{obs} = \frac{k_2(H^+)^2 + K_1(H^+)K_{a1}}{(H^+)^2 + (H^+)K_{a1} + K_{a1}K_{a2}}$$

The most reactive species HA^- is at a maximum concentration near the average of the two pK_a values.

7.7. Treatment of 4-nitrophenyl esters with base can lead to cyclization to an oxazolinone. These are in equilibrium with an anion that racemizes the stereocenter. Subsequent coupling by the oxazolinone with ethyl glycinate gives racemic product.

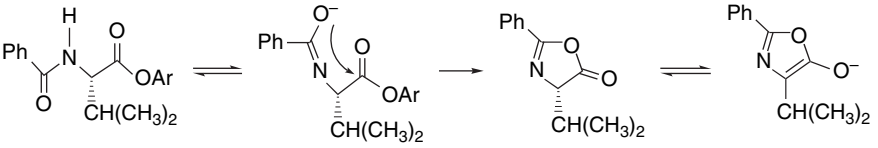

7.8. a. The bridgehead nature of the amide in structure **8-A** precludes a normal amide-type resonance. This means that addition to the carbonyl group to form the tetrahedral intermediate is more facile.

b. The geometry of structure **8-C** precludes participation of an oxygen unshared electron pair in breaking the C−X bond or stabilizing the resulting bridgehead carbocation. The *trans*-diaxial arrangement in structure **8-D** is ideal for participation.

7.9. a. The alkyl group is added entirely *trans* to the fused cyclopropane ring. This appears to be due primarily to the steric effect of the axial methyl substituent.

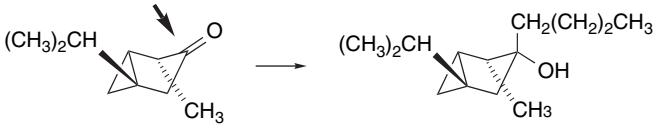

b. The phenyl group is added entirely *syn* to the fused benzo ring. On the basis of steric considerations, the flat benzene ring provides a somewhat more open trajectory.

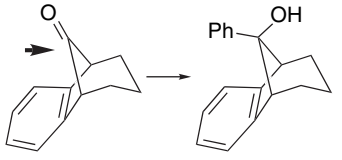

c. The stereoisomer predicted by the Felkin transition structure model accounts for 95–96% of the product.

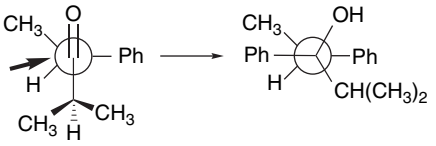

7.10. Because this is entirely a thermodynamic relationship, neither the structure of the TS nor the mechanism of hydrolysis is relevant. In making these comparisons, which are relative to methyl acetate, one has to consider two structural factors: (1) the (de)stabilization by resonance or polar effects of the carbonyl groups, and (2) the stability of the displaced group, which should correlate with its leaving group ability and basicity.

a. The methylthio ester is more negative (-7.7 kcal/mol) than the methyl ester (-5.1 kcal/mol) because of both diminished resonance stabilization of the reactant and the weaker basicity of the CH_3S^- leaving group.
b. The EWG character of the phosphate results in reduced resonance stabilization and a much more stable leaving group. The reported values of ΔG are -10.5 kcal/mol for the phosphate and -5.1 kcal/mol for the methyl ester.
c. The amino group is protonated at this pH and introduces a polar destabilization of the substituted reactant. The ΔG is -8.4 kcal/mol, compared to -5.1 kcal/mol for methyl acetate.
d. The acetyl group introduces a polar destabilization of the reactant, resulting in an increase of ΔG to -10.5 kcal/mol compared to -5.1 kcal/mol for the reference methyl acetate.
e. The imidazole ring, lacking conjugative stabilization because of its aromatic nature, together with the relative weakly basic imidazole ring as a leaving group ($pK = 7$), results in a considerably more favorable hydrolysis ($\Delta G = -13.3$ kcal/mol versus 5.1 kcal/mol for methyl acetate.)
f. The conjugation of the amide results in reactant stabilization and the secondary amine is more basic than an alcohol. Both factors make the hydrolysis of the amide less favorable than that of the ester.

7.11. This result can be ascribed to electrostatic stabilization of the anionic transition structure leading to the tetrahedral intermediate.

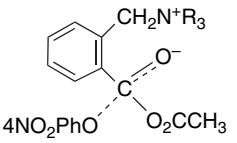

7.12. The second amino group can provide intramolecular general base catalysis.
7.13. There is a good correlation of the log/log plot with a slope of about 0.5. The results are consistent with general acid catalysis.

7.14. This reaction depends on the Lewis acid character of the Hg^{2+} to generate a thionium ion that can capture F^-. NaF would not have a similar effect. The dissociation is an S_N1 process of the Hg^{2+} complex. The F substituent does not provide sufficient stabilization to promote ionization of the second thiophenyl group.

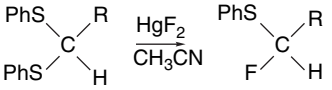

7.15. At the lower range of the acid concentration the neutral tetrahedral intermediate gives phenylacetanilide by elimination of H_2S. As the extent of protonation of the tetrahedral intermediate increases with acid concentration, the reaction is dominated by elimination of aniline from the N-protonated tetrahedral intermediate.

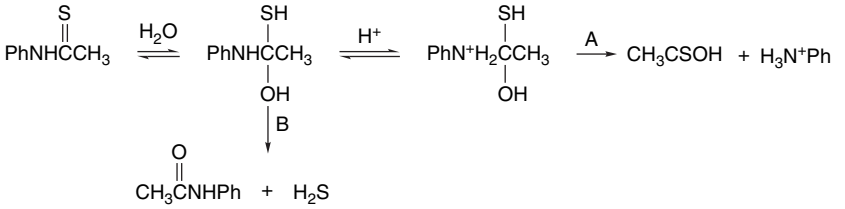

7.16. The less basic trifluoroethylamine is the poorer leaving group because it is less protonated in alkaline solution. The rate-determining breakdown of the tetrahedral intermediate is therefore more favorable for the more basic amine. The activation barrier for formation of the tetrahedral intermediate is slightly reduced by the trifluoroethyl substituent by a polar effect. The activation barrier for expulsion of the amine is increased by the trifluoromethyl group because of the decreased basicity.

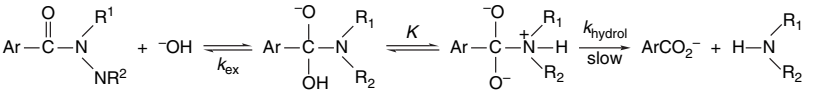

The rate of this step, which leads to exchange, is about 70 times slower for the pyrrolidine amide than for the trifluoro-substituted amine. There is about a 12-fold difference in k_{hydrol}. As a result, the extent of exchange is ~900 greater for the trifluoroethylamine.

The observed rate of hydrolysis is determined by the magnitude of k_{hydrol} and the protonation equilibrium governed by K. The substantial reduction in the rate of hydrolys is relative to the rate of exchange is due to the reduced basicity of the tetrahedral intermediate for the trifluoroethyl-substituted amine.

7.17. The Brønsted parameter α decreases for ERG in the benzaldehyde ring. This implies less proton transfer at the transition state, which would be consistent with the increasing stabilization of the carbocationic character by an ERG. For

the phenoxy substituents, the trend is in the other direction, with α increasing for ERG, because as the leaving group becomes poorer, the extent of proton transfer increases.

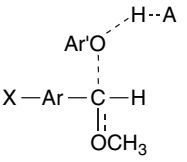

Extent of protonation decreases with extent of ERG electron donation because of increased carbocation stability.

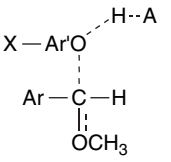

Extent of protonation increases with extent of ERG electron donation because of poorer leaving group ability.

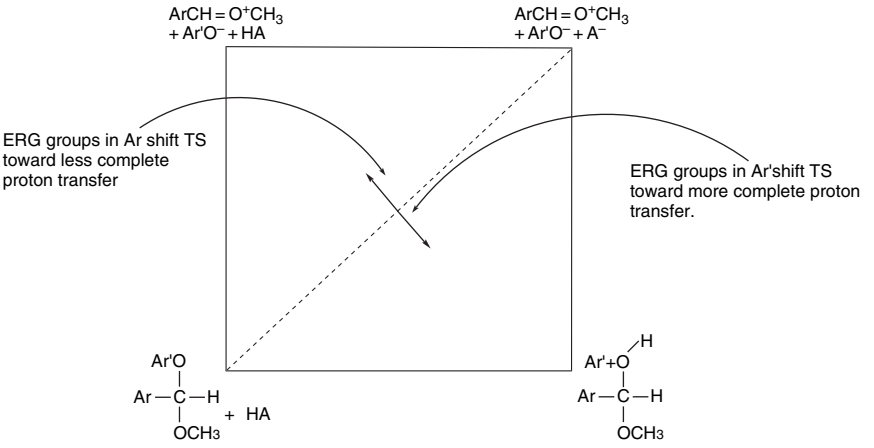

7.18. The maximum in the pH-rate profile near 3.8 suggests that the monoanion is the most reactive species, as was the case for aspirin (see p. 670). The observation of 3-hydroxyphthalic anhydride as an intermediate indicates intramolecular nucleophilic attack, followed by participation of the second carboxy group.

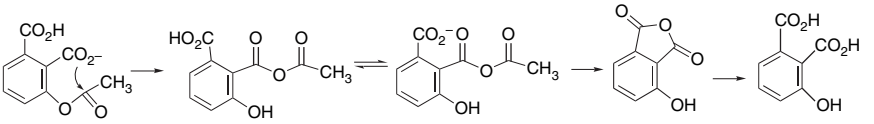

7.19. The kinetic results are consistent with an acetate-assisted attack by water. The mechanism at the acidic and basic extremes are presumably specific acid-catalyzed and specific base-catalyzed hydrolysis, respectively. At acidic pH, this can occur by initial protonation of the methoxy group and its elimination, whereas the hydroxide reaction presumably occurs by $^{-}$OH attack on the lactone carbonyl, followed by concerted breakdown of the adduct.

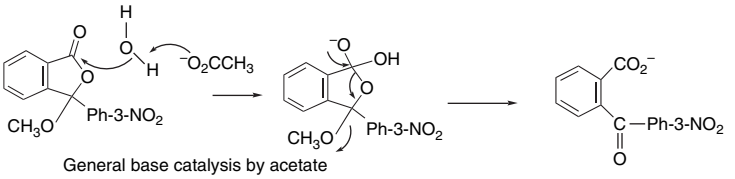

General base catalysis by acetate

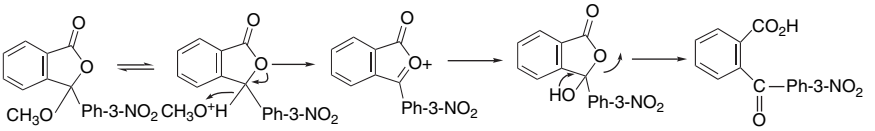

Specific hydronium ion catalysis

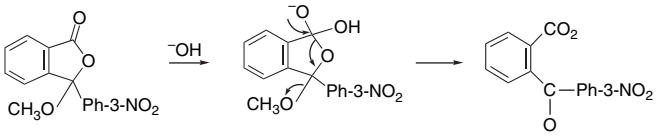

Specific hydroxide hydrolysis mechanism.

7.20. Separate plots of the rates versus σ for CH_3OH and CH_3OD both show curvature, with a larger ρ value for EWG substituents. The isotope effect is inverse, for *m*-NO_2, but gradually becomes normal for more ERG substituents, with an isotope effect of 1.75 for *p*-CH_3O. The curved Hammett plot and the change in the isotope effect suggest a change in mechanism. Assuming the normal addition-elimination mechanism proceeding through a tetrahedral intermediate, it would be expected that breakdown of the tetrahedral intermediate should be rate determining, since the methoxide ion is a better leaving group than an aniline anion in basic solution. The data are consistent with a rate-determining proton transfer for ERG substituents. For EWG substituents the proton transfer may be less important, with the nature of the leaving group becoming the dominant factor and the substituent effect becoming stronger (as reflected by the upward curvature of the Hammett plot).

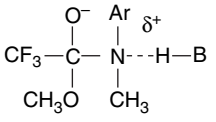

Proton transfer is rate-determining for X = ERG. Isotope effect is normal. There is relatively little C-N cleavage at the transition state

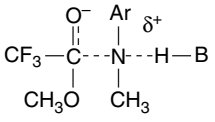

Leaving group ability is more important for X = EWG. There is more C-N cleavage at the transition state and higher sensitivity to the substituent.

7.21. The relative reactivity of these acetals can be explained on the basis of stereoelectronic effects involving the orientation of unshared electrons on the adjacent ring oxygen (anomeric effect). The antiperiplanar alignment in **21-C** is optimal. In **21-B**, the aryl-substituted O is poorly aligned with respect to the alkyl oxygen. In **21-A**, the bridgehead structure essentially precludes participation of the alkyl oxygen.

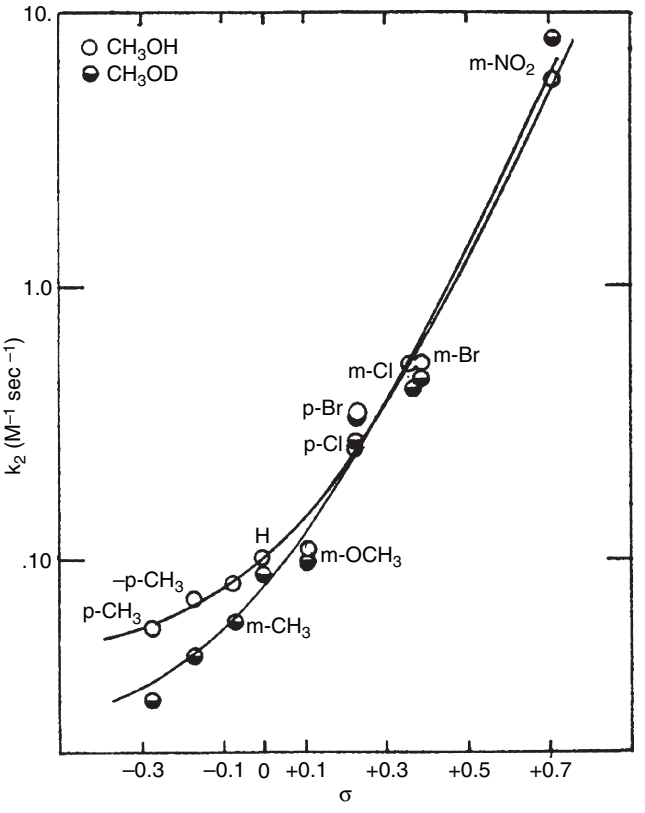

Fig. 7.P20. Hammett plots for methoxide-catalyzed methanolysis of trifluoroacetanilides in normal and deuterated methanol. Reproduced from *J. Am. Chem. Soc.*, **94**, 3095 (1972), by permission of the American Chemical Society.

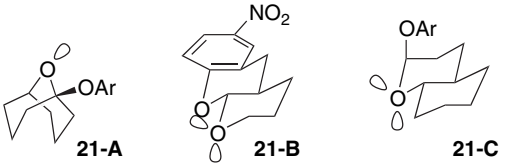

21-A **21-B** **21-C**

7.22. a. The specific [H^+] and [$^-$OH] mechanisms dominate below pH 5 and above pH 12, respectively, as indicated by the linear dependence on [H^+] and [$^-$OH]. There is an [$^-$OH]-dependent region from pH 6–8 that corresponds to the ionization of the phenol group and a pH-independent region from pH 8–10. In the pH-independent region reaction might occur through $^-$OH attack on an internal hydrogen bond structure, as depicted in TS **22-A** or the kinetically equivalent phenolate-promoted water attack as shown in TS **22-B**.

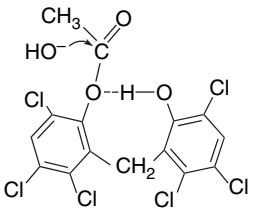

22-A

intramolecular
H-bonding assitance

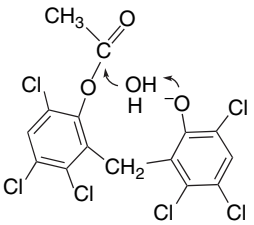

22-B

intramolecular general
base catalysis

b. There are $[H^+]$-dependent regions at pH < 1 and 3–4. Above pH 5, the reaction is pH independent. The reaction in the strongly acidic region is presumably H^+-catalyzed cyclization (Region A). The inflection near pH 2 corresponds to neutral water-assisted rate-determining cyclization (Region B). In the pH region 2–4, acid-catalyzed breakdown of the intermediate is rate determining (Region C). Above pH 4 the rate-determining step is water-assisted breakdown of the tetrahedral intermediate (Region D).

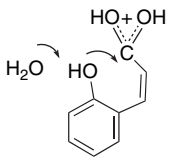

pH Region A

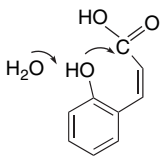

pH Region B

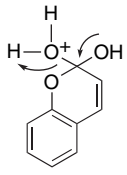

pH Region C

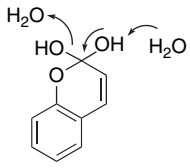

pH Region D

c. In the pH range 1–4, the reaction is water attack on the neutral reactant, presumably assisted by intramolecular hydrogen bonding. In the pH range 4–6, phenol ionization results in a change of mechanism to intramolecular assisted water attack (or conceivably the kinetically equivalent ^-OH attack on a hydrogen-bonded complex), which is dominant in the pH range 6–10. Intramolecular nucleophilic attack by phenoxide would also be consistent with the pH profile, although disfavored by the somewhat strained nature of the intermediate. Above pH 10, hydroxide ion attack becomes dominant.

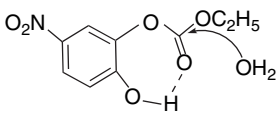

pH 0 – 4

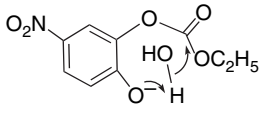

pH 6 – 10

d. An intramolecular general acid catalysis can account for the plateau from pH 2–5, which is in the region corresponding to ionization of the carboxy

group. Consistent with the base stability of acetals, there is no evidence for base-catalyzed hydrolysis.

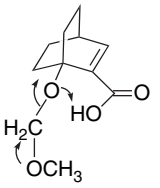

7.23. Both the 2- and 4-carboxy derivatives show a linear dependence on $[H^+]$ at the acid end of the pH range, but the 4-isomer is somewhat more rapidly hydrolyzed in this range. This results from the formation of the isolated phthalide intermediate, which undergoes hydrolysis somewhat more slowly than the starting acetal in the acidic pH range. The hydrolysis rate of the 2-isomer shows a plateau from pH 3 to 6, and becomes faster than the 4-isomer in this range. This is due to intramolecular general acid catalysis by the carboxy group. For the 2-isomer, the mechanism changes to ^-OH attack on the oxonium ion intermediate in the pH range 7–8. Above pH 8, the rate is $[H^+]$ dependent. In this pH range, the rate-determining step is protonation of the anion of the reactant.

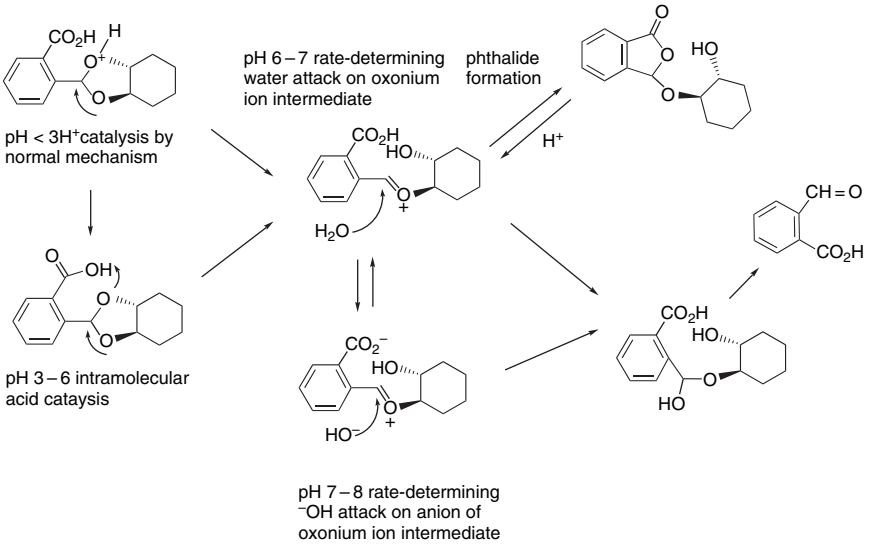

7.24. There are two opposing factors in the rate of addition. Because, as indicated in Section 7.2, the reaction is acid catalyzed, the basicity of the carbonyl group influences the extent of protonation. ERGs should favor protonation. On the other hand, ERG substituents will stabilize the C=O, which works in the opposite direction. For the reverse hydrolysis reaction, decomposition of the protonated acetal should be favored by ERG by the stabilization of the cationic intermediate. The overall K should be favored by EWGs, because they cannot effectively stabilize the aldehyde. The observed rates of hydrolysis, as measured by $\Delta G^{\ddagger}$, are favored by ERGs, as shown by the data below. The rates of formation are in the same direction, although somewhat less sensitive to the substituents, presumably

owing to the competing basicity/reactivity trends. The overall K's are somewhat more favorable for EWGs, as expected.

X	$\Delta G^{\ddagger}_{form}$	$\Delta G^{\ddagger}_{hydrol}$	K
p-CH_3O	20.0	16.2	2.0×10^3
p-CH_3	20.4	17.3	7.1×10^3
H	20.9	18.4	18.8×10^3
p-Br	21.5	19.3	34.5×10^3
p-Cl	21.5	19.2	35.0×10^3

7.25. The decrease in rate above pH 3 indicates that the neutral form of the reactant is much more reactive than the anionic form resulting from ionization of the carboxylate group. A likely mechanism is intramolecular general acid catalysis of attack by water. The formation of the anhydride suggests formation of a carbinolamine intermediate. The alkyl group effect appears to be of steric origin, because of the large increase on going to t-butyl. It is probably related to rotational aspects of the TS. It is interesting that the effects are observed despite the presumably planar double bond.

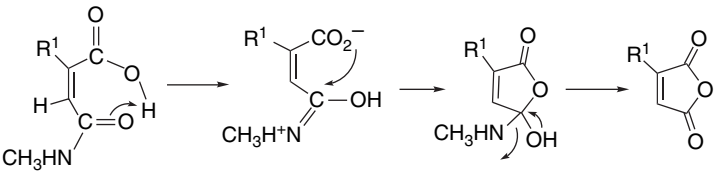

7.26. The mechanism given on p. 647 indicates that both water and hydroxide ion attack on the protonated imine contribute to the observed rate.

$$(\mathrm{ImH^+}) + \mathrm{H_2O} \underset{k_{-1}}{\overset{k_1}{\rightleftharpoons}} (\mathrm{Int}) + \mathrm{H^+}$$

and

$$(\mathrm{ImH^+}) + {}^{-}\mathrm{OH} \underset{k_{-2}}{\overset{k_2}{\rightleftharpoons}} (\mathrm{Int})$$

$$(\mathrm{Int}) \xrightarrow{k_3} \text{products}$$

$$\text{Rate} = \frac{d(\mathrm{P})}{dt} = k_3(\mathrm{Int}) = -\frac{d(\mathrm{Im}_{tot})}{dt}$$

where $(\mathrm{Im_{tot}})$ is the sum of neutral and protonated forms of the imine. The steady state approximation can be applied to (Int).

$$k_1(\mathrm{ImH^+}) + k_2(\mathrm{ImH^+})(^-\mathrm{OH}) = (\mathrm{Int})[\mathrm{k}_{-1}(\mathrm{H^+}) + k_2 + k_3]$$

$$(\mathrm{Int}) = \frac{k_1 + k_2(^-\mathrm{OH})(\mathrm{Im}_{tot})(\mathrm{H^+})}{[K_a = (\mathrm{H^+})][k_{-1}(\mathrm{H^+}) + k_{-2} + k_3]}$$

$$\mathrm{Rate} = k_{obs}(\mathrm{Im_{tot}}) = k_3(\mathrm{Int}) = \frac{k_3[k_1(\mathrm{H^+}) + k_2K_w]}{[K_a + (\mathrm{H^+})][k_{-1}(\mathrm{H^+}) + k_{-2} + k_3]}$$

At pH < 5 the hydroxide term becomes negligible and the k_2 and k_{-2} terms drop out and k_{obs} simplifies to

$$k'_{obs} = \frac{k_1k_3(\mathrm{H^+})}{[K_a + (\mathrm{H^+})][k_{-1}(\mathrm{H^+}) + k_3]}$$

Because the various imines have different pK values, the relative magnitude of the terms change with pH. For the most acidic region at pH < 2, k_{obs} becomes $k_1k_3/k_{-1}(\mathrm{H^+})$ and is pH dependent. In the plateau region at pH 4–5, k_{obs} reduces to k_1. In the strongly basic region at pH > 8, k_{obs} is given by k_2K_w/K_a and is pH independent.

7.27. a. The product composition indicates that aldol condensation has occurred, which would be consistent with the relatively high temperature. Although not determined, the major stereoisomer is probably E to maximize conjugation with the formyl group.

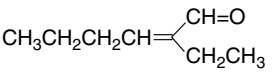

b. This reactant can undergo intramolecular aldol condensation.

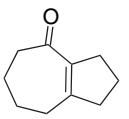

c. This reaction should give the kinetically controlled adduct. As discussed on p. 689, the main enolate is Z (98:2) and the major product is the *syn* stereoisomer (~ 9:1).

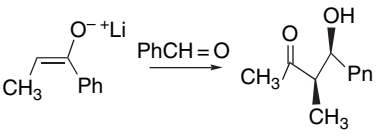

d. The composition of the product under alkaline conditions indicates aldol addition. These conditions are not expected to result in high stereoselectivity. The composition under acidic conditions indicates that dehydration has occurred. Because of the acidic conditions, the branched-chain product would be formed. It would be expected to have the E configuration of the double bond.

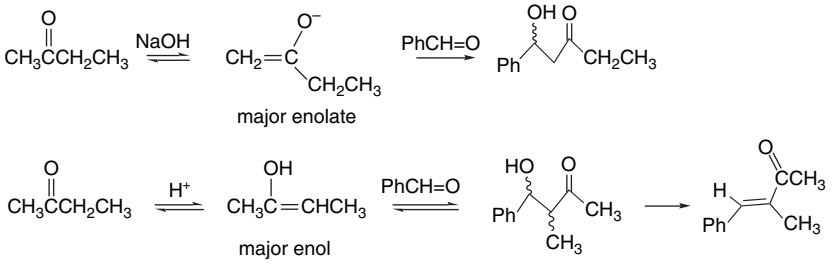

7.28. Thioester **28-A** shows a linear dependence on hydroxide ion, indicating a normal $B_{AC}2$ mechanism. Thio ester **28-D** also shows linear dependence on hydroxide, with a slight rate acceleration relative to **28-A**. This indicates a $B_{AC}2$ mechanism, with possible electrostatic stabilization of the anionic tetrahedral intermediate. Thio esters **28-B** and **28-C** show pH-independent regions corresponding to the ionization of the carboxylate and tertiary amino groups, respectively. This result is consistent with an intramolecular general base catalysis for these two compounds.

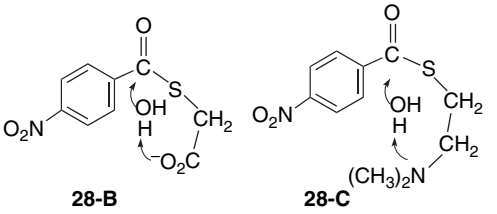

28-B **28-C**

7.29. In the [$^{-}$OH]-dependent range at pH > 10, the nitro compound is more reactive, consistent with the EWG effect making the amide carbonyl more reactive to hydroxide ion attack. In the plateau region, the nitro compound is less reactive than the unsubstituted compound. This favors mechanism **A** over mechanism **B**, since the nitro group would decrease basicity but should enhance hydrogen-bonding ability.

7.30. The reaction can proceed by participation of the hydrate of the aldehyde. The rapid exchange with water would incorporate ^{18}O, which would be transferred to the carboxy group.

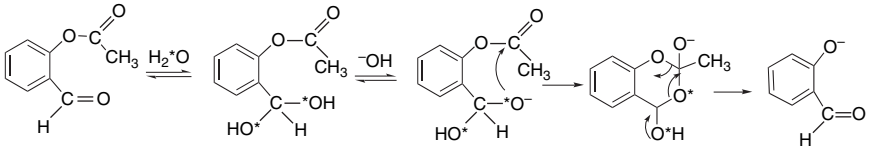

7.31. The rate remains constant between pH 4 and 9, at which point it increases with [$^{-}$OH]. The most likely mechanism for a pH-independent mechanism would be intramolecular general base catalysis. The direct involvement of a water molecule is consistent with the observed solvent isotope effect.

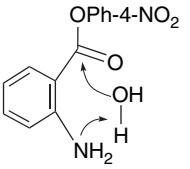

The rate expression is

$$\text{Rate} = k_{\text{obs}}\ (\text{Am}_{\text{tot}})$$

where (Am_{tot}) is the total concentration of all amine species—(Am) and (AmH^{+}), the neutral and protonated forms.

$$\frac{d(\text{Am}_{\text{tot}})}{dt} = k_{obs}(\text{Am}_{\text{tot}})$$

The term k_{obs} consists of two contributions, one involving intramolecular catalysis and the other the ($^{-}$OH) reaction:

$$k_{\text{obs}} = [k_0 + k_{\text{OH}}(^{-}\text{OH})](\text{Am})$$

The term [Am] is a function of the pH and can be obtained from the acid dissociation constant K_a:

$$K_a = \frac{(\text{Am})(\text{H}^{+})}{(\text{AmH}^{+})}$$

$$(\text{Am}_{\text{tot}}) = (\text{AmH}^{+}) + (\text{Am}) = \frac{(\text{H}^{+}) + K_a}{K_a}(\text{Am})$$

$$(\text{Am}) = \frac{(\text{Am}_{tot})K_a}{(\text{H}^{+}) + K_a}$$

Thus,

$$k_{\text{obs}} = \left[k_o + \frac{k_{^{-}\text{OH}}K_w}{(\text{H}^{+})}\right]\left[\frac{K_a}{(\text{H}^{+}) + K_a}\right]$$

8.1. A rectangular structure for the cyclobutadiene ring implies that there would be two isomeric 1,2-diphenyl isomers, and if the barrier to bond migration is low, they would be in equilibrium.

1-D **1-E**

For steric reasons, isomer **1-D** should be more reactive as a dienophile. One possible explanation for the results is that the reaction of *p*-benzoquinone (and maleimide) are slow relative to this equilibrium, and, as a result, all of the reaction proceeds through **1-D** to give product of structure **1-A**. On the other hand, if the Diels-Alder reaction of tetracyanoethylene and dicyanomaleimide are faster than the equilibrium, the product ratio of 1:7 favoring **1-C** would correspond to the **1-D**:**1-E** ratio. The reactions with the less reactive dienophiles are examples of the Curtin-Hammett principle, with the bond shift as the rapid interconversion mechanism.

8.2. a. A dipolar resonance structure having benzenoid character for the pyridinium ring and an aromatic cyclopentadienide ring would stabilize this structure.

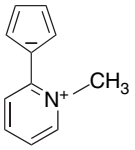

b. The aromatic cyclopentadienide character of the following resonance structure would stabilize this diazo compound.

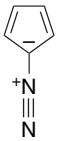

c. There is a resonance structure having charged aromatic rings that would be stabilizing.

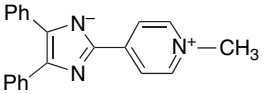

d. Among many dipolar resonance structures are several that depict the five-membered ring as cyclopentadienide and the seven-membered ring as cycloheptatrienylium. These structures should stabilize this compound, although one of the rings must have quinoid character. So far, the compound has not been synthesized and its physical properties are unknown.

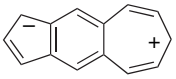

8.3. a.

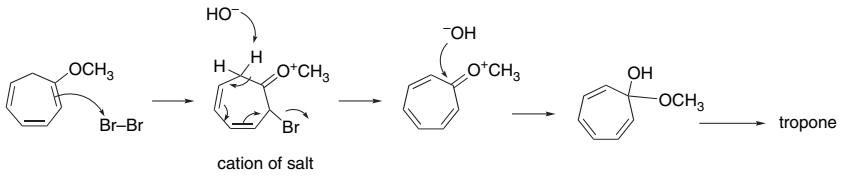

b. If the enol were an intermediate, the reaction would incorporate deuterium in deuterated solvent. That is not observed, ruling out an enol intermediate.

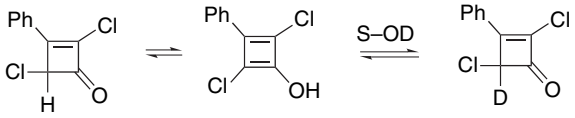

8.4. a. This is a $4n\pi$-electron system analogous to the cyclopentadienylium cation and should be antiaromatic.

b. The π-electron system perpendicular to the ring contains 14 electrons (two for each triple bond) and should be aromatic. There are no serious geometric or steric constraints to planarity.

c. This is a 10π-electron system has the potential to be homoaromatic. However, in view of the lack of evidence of strong stabilization of anions by homoaromaticity, coupled with the fact that it is a dianion, suggests that this structure would be nonaromatic.

d. This six-electron system has the potential to be *bis*-homoaromatic.

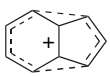

e. This compound is isoelectronic with the phenalenyl anion and according to the phenalenyl MO pattern (p. 757), it should be aromatic.

f. If the S is considered to be a C=C replacement, this is an azulene analog. As such it should have aromatic stabilization, and the NMR spectrum is consistent with a diamagnetic ring current.

g. This structure is isoelectronic with the tropylium ion. Although the more electronegative nitrogen would be expected to somewhat destabilize the structure, it should be aromatic. CAS-SCF calculations indicate a planar, delocalized structure.

h. This structure is isoelectronic with the acepentalene dianion, which is calculated to have aromatic properties, including a negative NICS (see Problem 8.17).

i. This structure is isoelectronic with the phenalenyl anion and should be aromatic (p. 757).

8.5. a. The structure shows a cyclobutadiene ring. Attaining an aromatic number in both rings would require the transfer of two electrons from the four-membered to the eight-membered ring or vice versa. Such a large charge transfer would be destabilizing.

b. An alternative resonance structure might be construed as a peripheral 10 π-electron system, provided that the structure maintained planarity.

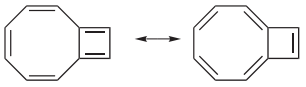

c. The major criteria of aromaticity would apply: (a) stabilization or destabilization energy determined by experiment (e.g., heat of hydrogenation) or computation; (b) bond length alternation as determined by experiment or computation; and (c) magnetic criteria such as evidence from NMR for a diamagnetic ring current or calculation of the NICS. The experimental and theoretical evidence currently available suggests only weak stabilization (see p. 753).

8.6. The HMO and calculated energies are as follows:
HMO energy – Hess-Schaad reference energy = Stabilization

a. HMO energy $= 8\alpha + 10.3812\beta - 10.562\beta = -0.181\beta$ (destabilized).

Hess-Schaad reference energy:	(HC=CH) $= 3 \times 2.070$	$= 6.210$
	1 (C=C) = 2.172	$= 2.172$
	5 (HC−C) $= 5 \times 0.436$	$= 2.180$
		10.562

b. HMO energy $= 10\alpha + 13.3635\beta - 13.132\beta = +0.231\beta$ (stabilized).

Hess-Schaad reference energy:	3 (HC=CH) $= 3 \times 2.070$	$= 6.210$
	2 (HC=C) = 2 3 2.108	$= 4.216$
	3 (HC=CH) $= 3 \times 0.466$	$= 1.398$
	2 (HC−C) $= 2 \times 0.436$	$= 0.872$
	1 (C−C) = 0.436	$= 0.436$
		13.132

c. HMO energy $= 10\alpha + 12.7993\beta - 13.1228\ \beta = -0.329\beta$ (destabilized).
d. HMO energy = 10α + 13.6832β – 13.128 β = +0.555 (stabilized).
e. HMO energy = 12α + 16.2313β – 16.120 = +0.111 (stabilized).

These results are in good accord with the properties of these hydrocarbons. Benzocyclobutadiene and fulvene are distinctly destabilized. Naphthalene and, to a lesser extent, azulene exhibit aromatic stabilization. *s*-Indacene has at most small stabilization.

8.7. a. There is a substantial difference in basicity in the order cyclopropenone > cycloheptatrienone > cyclopentadienone. This suggests that the dipolar resonance form, which puts a positive charge on the polyene ring, is of decreasing importance for 3 > 7 > 5. A positively charged ring should be stabilizing for three- and seven-membered rings, but destabilizing for the five-membered ring.

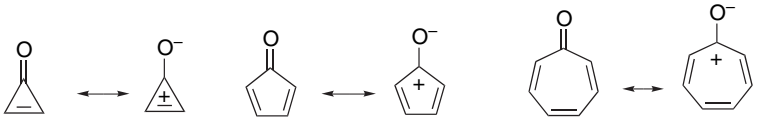

b. These results indicate that the dipolar stabilizing structure is more important for the cyclopropene system than for the tropone system. This, at least in part, may be a reflection of the ability of tropone to adopt a nonplanar structure.

8.8. The calculations are as follows:

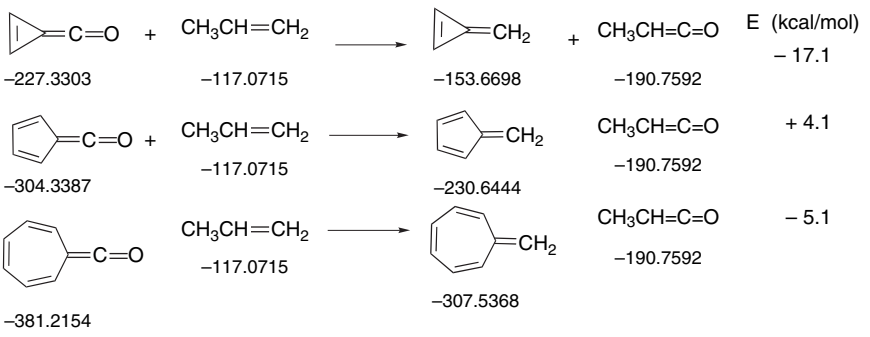

These results indicate that in contrast to the cyclopolyenes, the ketenes are stabilized for the five-membered ring and destabilized for the three- and seven-membered rings. This has been attributed to the polarization of the ketene function, which places a negative charge on the β-carbon, and would provide destabilizing negative charges to the three- and seven-membered rings, whereas the negative charge would be favorable in a five-membered ring.

8.9. The isomer shown on the left appears to be "more" aromatic, since there is a considerably larger difference in the chemical shifts. The HMOs would be identical for the two compounds, since HMO theory considers only the connectivity and not the shape of the conjugated system. It is possible that the structure of the two isomers might differ substantially in terms of planarity, which would affect the diamagnetic anisotropy.

8.10. a. The anion of **10-A** has an identical resonance structure, and both are cyclopentadienide-like, suggesting good stabilization of the anion. The fused structure in each case is a [10]annulene. On the other hand, delocalized structures of the anion of **10-B** do not indicate as complete a delocalization of charge. The fused structures are of the heptafulvene type.

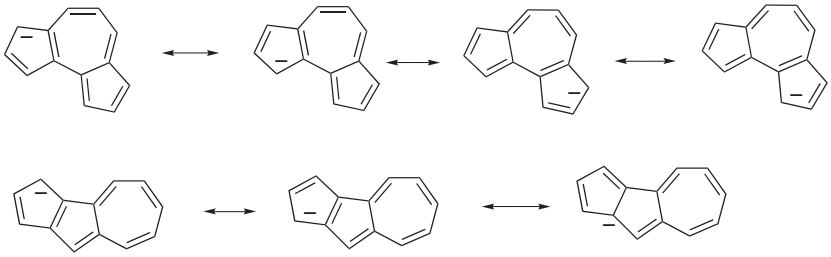

b. Both the dication and dianion correspond to phenalenyl structures. The monocations and monoanions correspond to phenalenyl structures in one of the rings and can be delocalized over both rings.

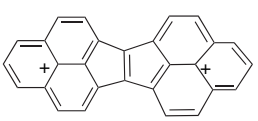
bis-phenalenyl dication

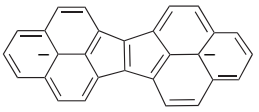
bis-phenalenyl dianion

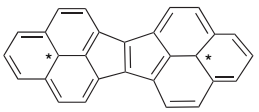
monocation or monoanion can be delocalized over two phenalenyl ring systems

c. A dipolar structure having both phenolate and tropylium conjugation decreases the bond order of the inter-ring bond.

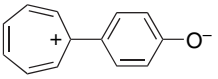

d. A peripheral 14π-electron system with an isolated charge on the center carbon would correspond to an aromatic system. A downfield shift of the ring hydrogens would then indicate a diamagnetic ring current. The large upfield shift of the central carbon would be the result of increased electron density because of the negative charge on the center carbon.

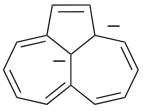

8.11. a. The bond lengths and alternation in the six-membered rings of acenaphthene are quite similar to those of naphthalene. The C(2)−C(2a) bonds are longer than aromatic bonds, suggesting that acenaphthene can be regarded as a naphthalene, with a fused cyclopentene ring having minimal delocalization.

b. In the anion, the bonds of the five-membered ring become more uniform. The naphthalene ring bond lengths change quite substantially, with the C(3)−C(4) bond being particularly short. The uniformity of the bond lengths in the five-membered ring suggests that it might have cyclopentadienide character. If so, the remaining system could be considered to be a delocalized heptatrienyl radical.

c. The ^{1}H positions are shifted substantially upfield, consistent with increased electron density associated with the two negative charges. Positions C(4) and C(7) are shifted somewhat less than the others. The ^{13}C shifts are also less at C(4) and C(7), and C(5a) and C(8b) shift downfield. These shifts are in reasonably good correlation with the HOMO coefficients for the anion, which show zero coefficients at C(5a) and C(8b). A representation of the dianions that is in good accord with these data suggests two delocalized anions. A cyclopentadienide anion in the five-membered ring and a noncyclic heptatrienyl anion encompassing C(3)−C(8). In particular this would explain the shortening of the C(3)−C(4) bond.

8.12. The ^{1}H-NMR spectrum shows the expected relative downfield positions in the cation and upfield in the anion. There is also a strong downfield shift for C(1) in the cation and an upfield shift for the anion. This is in accord with the HMO levels in that the orbital that formally bears the cationic and anionic charge has density only at C(1) and the corresponding positions. The downfield shift of the C(3a) and C(9b) carbons indicates an aromatic ring current.

8.13. The delocalized structure **13-A** implies planarity and would have only four different kinds of carbon. Structure **13-B** would be expected to be tub-shaped, similar to cyclooctatetraene. This structure would be expected to be symmetrical with respect to a plane bisecting the molecule and to have a maximum of four signals, since the two rings are structurally equivalent. The two rings in structure **13-C** are different and have seven different kinds of carbon. The most likely conformation of **13-C** is nonplanar, in which case all 14 carbons are different. They can be equilibrated by a conformational process, which leads to the seven-line spectrum at intermediate temperatures. The four-line spectrum would be expected to arise through a bond shift process that interchanges the character of the two rings. The delocalized structure **13-A** would be a likely transition state for this process.

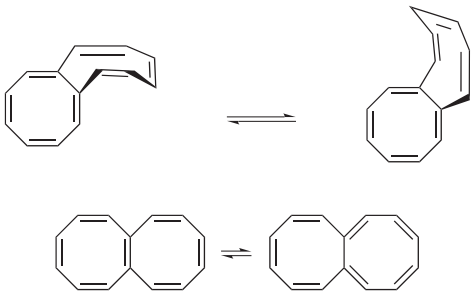

13-B **13-C**

8.14. The cation might have cyclopropylcarbinyl (**14-B**), *bis*-cyclopropylcarbinyl, *bis*-homoaromatic, (**14-D**), or allylic (**14-E**) character. The $-\nabla^2\rho(\mathbf{r})$ shows no maximum between C(2) and C(9) indicating the absence of a formal bond as in the *bis*-cyclopropylcarbinyl structure **14-C**. The bond length alternation in the six-membered ring is less than might be expected for structure **14-E**. The bond orders are consistent with structure **14-D**, showing close to 1.5 bond order for the homoaromatic bonds, and a bond order slightly less than 0.5 for the C(2)−C(9) and C(5)−C(7) interactions. The $-\nabla^2\rho(\mathbf{r})$ shows no maximum, indicating that there is not a formal bond path, but the calculated bond order indicates a strong interaction. (See p. 744 for examples of electron density profiles in homoconjugated cations).

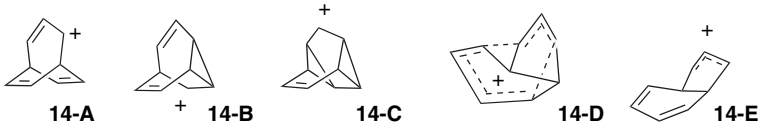

14-A classical carbocation

14-B cyclopropylcarbinyl carbocation

14-C *bis*-cyclopropylcarbinyl carbocation

14-D *bis*-homoaromatic carbocation

14-E allylic carbocation

8.15. a. The stabilization can be calculated by comparing the ΔH_c on a per CH basis.

Benzene: $781 + 36 = 817 = 136.2$ /CH
Cyclooctatetraene: $1086 + 4 = 1090 = 136.2$/CH
[16]annulene: $2182 + \text{SE} = 16(136.2)$; SE = 3 kcal/mol

b. The thermodynamic cycle is

	$[C_8H_8]$	$[C_{16}H_{16}]$
$C_nH_{n+2} + 2\ NaOH_{(aq)} \rightarrow 2Na^+(C_nH_n)^{2-} + 2H_2O_{(l)}$	+33.3	+10.9
$[C_nH_n] + H_2 \rightarrow C_nH_{n+2}$	−25.6	−28.0
$2Na_{(s)} + 2H_2O_{(l)} \rightarrow 2NaOH_{(aq)} + H_2$	−88.2	−88.2
$2Na_{(s)} + [C_nH_n] \rightarrow 2Na^+(C_nH_n)^{2-}$	−80.5	−105.3

The lower heat of reaction of $[C_{16}H_{16}]^{2-}$ with water indicates that the anion is somewhat less reactive toward protonation, which may be due to a somewhat lower energy because of the larger size of the dianion in the case of [16]annulene. The two-electron reduction is also somewhat more exothermic than for cyclooctatetraene.

8.16. The double-annulene structure would imply similar bond lengths along the inner and outer perimeters. It would also suggest similar properties for all the rings. The phenanthrene-like structure implies significant differences between the alkenelike (angular fusion) and benzenoid (linear fusion) rings. The ^{1}H-NMR chemical shift values are somewhat more downfield than observed for phenanthrene, particularly the inner hydrogen, which would be in the deshielding region of the benzenoid-like rings in the phenanthrene-like structure. The bond lengths show a phenanthrene-like pattern. The rings depicted with delocalized electrons are all close to 1.39 Å. In the other rings, the double bond is distinctly shorter than the adjacent single bonds. These structural features are in good accord with the phenanthrene-like structure. The substantial NICS difference is also in accord with this structure, since the double-annulene structure would not account for large differences between the two rings.

8.17. a. The dianion and, to a somewhat lesser degree, the dication exhibit magnetic properties suggestive of aromaticity. The bond length pattern for the dianion indicates a symmetrical structure with shortened (aromatic) bond lengths particularly for the C(1)−C(2) and the bonds to the central carbon. On the other hand, the neutral molecule has strong bond alternation, consistent with a localized structure. The pyramidal structure is presumably the result of angle strain at the central carbon, which is reduced by pyramidalization.

b. The HMO pattern, while strictly applicable only to the planar structure, offers a rationale for the observed aromaticity of the dianion and the dication. Both the anion and cation would have a fully paired electronic configuration, with all electrons in bonding orbitals. On the other hand, the diagram shows degenerate orbitals that would be half-filled in the neutral molecule.

8.18. The reduced rate might reflect arene oxide stabilization and/or instability in the TS for ring opening. B3LYP/6-311+G** calculations suggest about 6.6 kcal/mol of stabilization attributable to a homoaromatic stabilization.

8.19. The data permit comparison of chloride transfer reactions that should be indicative of relative carbocation stability.

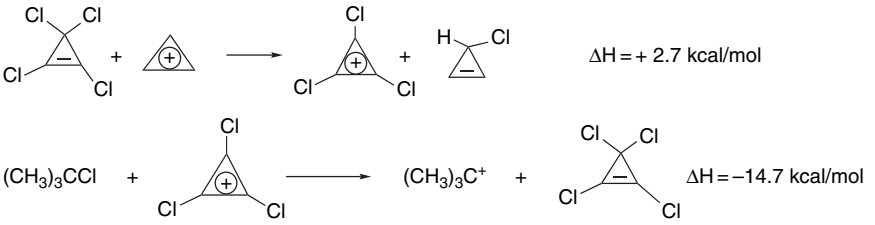

According to this comparison, the chlorines are weakly destabilizing, but nevertheless the trichlorocyclopropenium ion is more stable than the *t*-butyl carbocation.

8.20. The fact that the three successive ΔH_{H2} are very similar indicates there is little homoaromatic stabilization. Any stabilization would be lost in the first hydrogenation and it should be less exothermic than the other steps. Furthermore, the isodesmic reaction indicates that three isolated double bonds in cyclopentene are slightly more stable than triquinacene.

Chapter 9

9.1. a. The polar effect of the single fluorine decreases the *o,p* preference of the alkyl group, but the *o,p* products remain dominant. The reported product ratio is 28% *ortho*, 18% *meta*, and 54% *para.*

b. The trifluoromethyl group is strongly *meta* directing. According to the data in Table 9.3, 91% of the product is *meta*.

c. The single methoxy group is not sufficiently electron withdrawing to overcome the normal *o,p*-directing effect of an alkyl substituent. According to the data in Table 9.3, 93 % of the product is *ortho* and *para*.

d. The quaternary nitrogen is strongly *meta* directing. According to the data in Table 9.3, 89% of the product is *meta.*

e. As indicated on p. 780, fluorine is an *o,p*-directing group, with a preference for the *para* isomer.

f. The sulfonyl group is an EWG substituent. The reported product is 89% *meta*.

9.2. *Ortho*-alkyl substituents force the rotation of the dimethylamino group by a steric effect and diminishes the conjugation of the donor substituent with the ring.

9.3. Application of the method for calculation of partial rate factors given on p. 787, leads to the following results: toluene: o = 51.8; m = 2.5; p = 58.5; isopropylbenzene: o = 18.1; m = 2.1; p = 43.7. The largest difference is at the *ortho* position, where the *i*-propyl group leads to a reduced reactivity relative to methyl because of a steric effect. The methyl group is slightly more activating at the *meta* and *para* positions. The overall reduction in rate for isopropylbenzene is largely attributable to a steric factor that decreases the reactivity of the *ortho* position.

9.4. The plot shows considerably better correlation with σ^+ than with σ. The ρ for the σ^+ plot is -7.8, indicative of a very strong substituent effect. This is consistent with the mechanisms for electrophilic bromination via a cyclohexadienyl cation intermediate, which permits direct conjugation with substituent groups.

Group	log rate	log k/ko	σ	σ^+
H	−5.57	1	0	0
CH_3	−1.82	3.75	−0.14	−0.31
CH_3O	3.99	9.56	−0.12	−0.78
OH	4.6	10.17	−0.38	−0.92
$(CH_3)_2N$	8.34	13.91	−0.83	−1.7

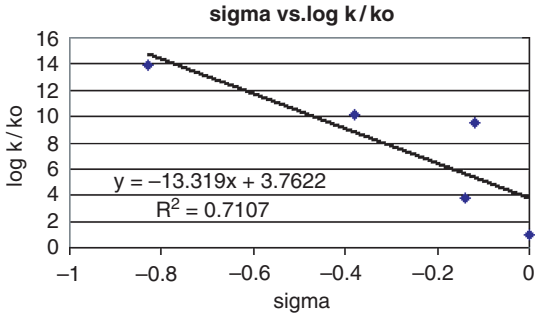

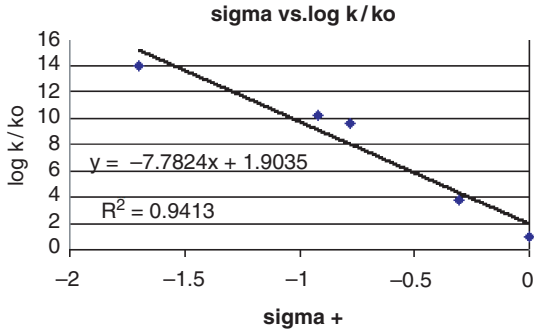

9.5. The appearance of the 1,3,5-substituted product **5-C** at 50°C indicates that equilibration by alkyl migration is occurring. This may be somewhat faster for the *i*-propyl than for the *n*-propyl substituent because of more steric interference in the case of the branched *i*-propyl group. Equilibrium has not been reached, however, because at equilibrium, the product composition should be the same from both precursors. The formation of 1,2,4-substituted product with *i*-propyl groups from the *n*-propyl reactant indicates that rearrangement of the alkylating agent is occurring at a rate that is competitive with ring alkylation. Several mechanisms can be proposed, but the simplest is $AlCl_3$-mediated ionization and competing isomerization. Equilibration with the 1,3,5-Isomer may occur by dealkylation.

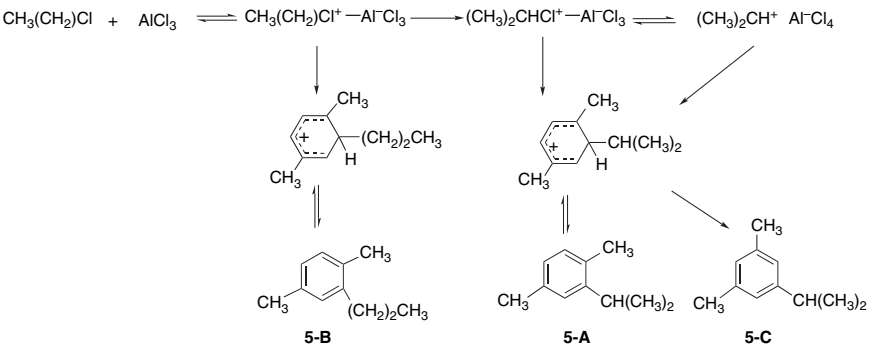

9.6. The calculation of the partial rate factor can be done as described on p. 787.

X	Rel rate	f_o	f_m	f_p
Br	0.56	0.35	0.050	2.5
CH_3	19.8	19.0	1.8	77.2
CH_3O	500	210	-	2580
CH_3O_2C	0.106	0.076	0.21	0.057

The reactivity pattern is consistent with electrophilic aromatic substitution. The slight *para* activation of Br and fairly strong *meta*-directing and deactivating effect of the CH_3O_2C group are consistent with the normal pattern, as is the strong *o,p* activation of the methoxy group. The cited reference reports correlation of these and other rates with σ^+ with $\rho = -4.4$. This would place the reaction in the relatively nonselective group, suggesting an early TS. The electrophilicity of the reagent derives from the weak O−O bond.

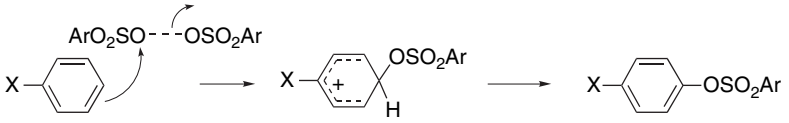

9.7. a. The strong activation of the hydroxy group will lead to bromination in the phenolic ring.

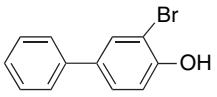

b. The reaction leads to desulfonation.

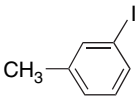

c. The *ipso*-directing effect of the silyl substituent is stronger than the *o,p*-directing effect of the methoxy group.

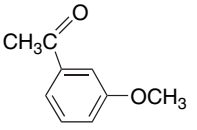

d. O-Protonation leads to the equivalent of a σ complex that can be stabilized by rearrangement and aromatization.

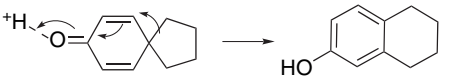

9.8. The dependence of the rate on the deuterium incorporation indicates an isotope effect. No significant isotope effect would be observed if the deprotonation step were fast, indicating that deprotonation is at least partially rate determining. The observed rate and isotopic distribution can be analyzed in terms of competing acylation at the deuterated (resulting in loss of deuterium) and undeuterated sites (resulting in retention of deuterium).

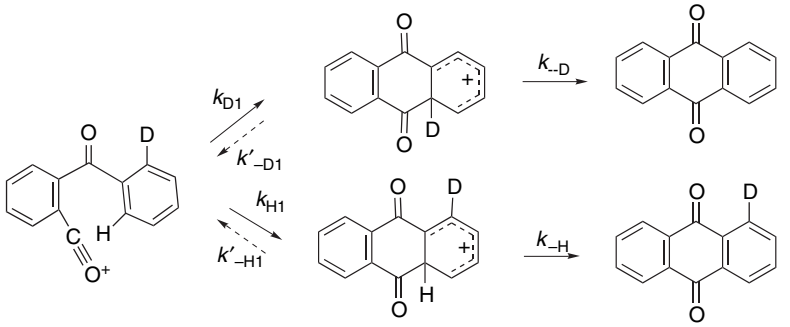

The observed kinetic isotope effect is 1.13. The fact that 60% of the deuterium is retained gives $k_{-H}/k_{-D} = 1.5$.

9.9. A mechanism involving generation and reaction of benzyne can account for the observed product.

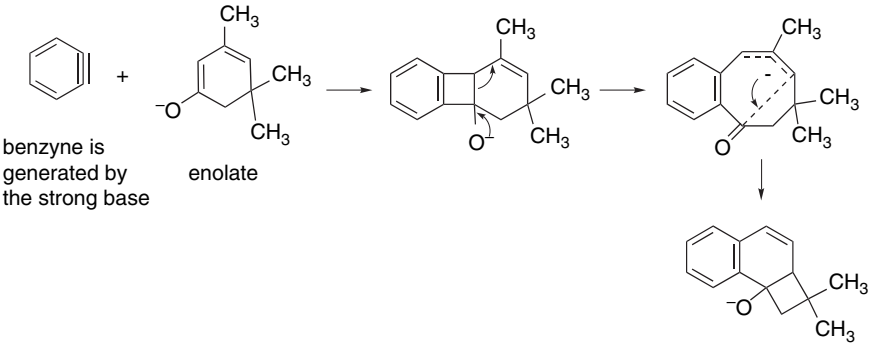

9.10. The boronic acid serves, at least in part, to trap the reaction product as a stable derivative. Most likely, it also exhibits a template or chelate effect by acting as a Lewis acid, not unlike the role of BF_3 and other Lewis acids in aldol addition.

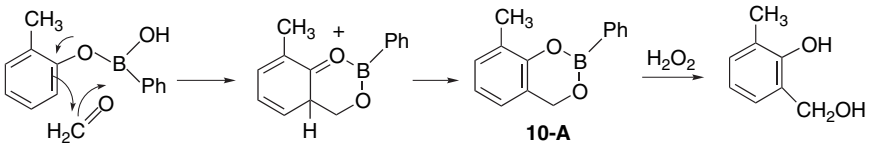

9.11. These results can be explained by initial cyclization of the allylic carbocation, followed by rearrangement to a more stable benzylic cation. Deprotonation of the two cations leads to products **11-C** and **11-D**, respectively.

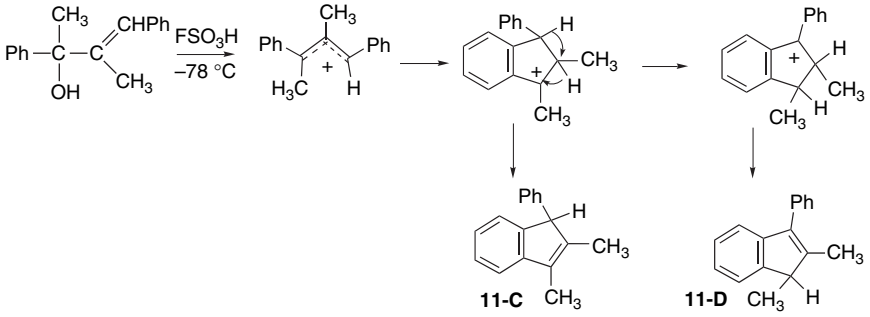

9.12. The reaction occurs in two steps. A normal isotope effect would be expected for rate-determining protonation. On the other hand, rate-determining dealkylation would be dependent on the extent of protonation and would be greater in the deuterated solvent. The results suggest that protonation is rate determining in the case of R = Ph, whereas dealkyation is rate determining for $R = CH_3$.

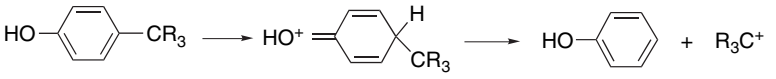

9.13. The activating effect of the methoxy group is presumably strongest in the substituted ring, accounting for **13-B** being the major product. Dealkylation is known for similar compounds and may involve a chelate structure. The preferred β-substitution in the unsubstituted ring may be the result of steric hindrance to deprotonation of the α-substituted intermediate (see p. 812).

9.14. The extent of rearrangement could be measured by an isotopic-labeling experiment that would distinguish between C(1) and C(4) or C(2) and C(3) of the butyl chain. These pairs of methylene groups become equivalent in **14-B**, but not in **14-A**. Intermediate **14-B** would be expected to be favored by ERGs. An experimental measurement done by using deuterium labeling indicated that with $X = OCH_3$, 69.5% of the product formed via **14-B** and 30.5% via **14-A**.

9.15. With the less reactive substrate, the formation of the σ complex is rate controlling and the terms describing formation of the active electrophile are not relevant. For the more reactive dimethoxybenzene, the formation of the active electrophile is rate determining and the concentration of the reactant does not appear in the kinetic expression.

9.16. The standard partial rate factor calculation yields the following results:

Halogen	f_o	f_m	f_p
F	0.054	0.00	0.78
Cl	0.030	0.002	0.14
Br	0.033	0.001	0.11
I	0.21	0.01	0.65

The data show that there is not a smooth trend among the halogen substituents. In terms of relative reactivity the order is F > I > Br ~ Cl, which must be the result of two or more opposing trends. Resonance stabilization should be in the order F > Cl > Br > I because of the importance of orbital overlap. On the other hand, the polar and polarization effects are in the opposite order I > Br > Cl > F. Resonance effects are dominant for F. For Cl and Br, the resonance and polarization effects are less important than the destabilizing polar effect. Reactivity is low, but the resonance effect does lead to *o,p* orientation. For I, the polar effect is smallest and polarization provides stabilization of the intermediate. A special feature of the data for F is the high *para*:*ortho* ratio. This is believed to be due to the strong polar effect of the F, which destabilizes the *ortho* transition state.

9.17.

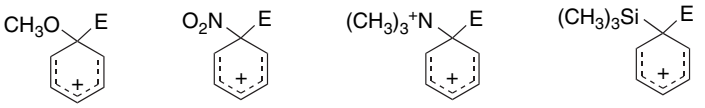

a. A methoxy or similar group should be slightly destabilizing by the polar effect, assuming that E is more electronegative than carbon. There could be a stabilizing anomeric interaction with the unshared electrons of the methoxy group and the σ^* orbital of the C−E bond.
b. A nitro or cyano group should be destabilizing by polar interactions but could be stabilized by an anomeric effect only if E were a potential σ donor such as a halogen.
c. A group such as trimethylammonio should be destabilizing on the basis of polar effects. Anomeric stabilization would be possible for electrophiles that are σ donors.
d. A group such as silyl would have a small polar stabilization and a strong hyperconjugative stabilization effect.

9.18. The decrease in the amount of **18-C** when deuterium is incorporated indicates that the deprotonation step is at least partially rate limiting. If the assumption is made that the rate of formation of **18-A** and **18-B** from their respective σ-complex precursors is unaffected by the isotopic substitution, the relative rates can be calculated.

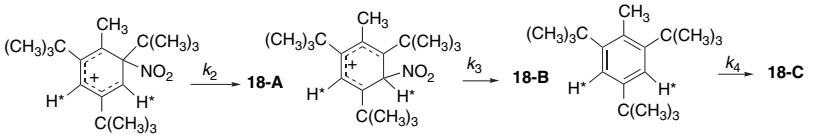

If k_2 and k_4 are assumed to be constant, the value of k_3 can be calculated from the product ratios:

$$\frac{k_{SH}}{k_2} = \frac{8.7}{40.2} = 0.216 \qquad \frac{k_{3D}}{k_2} = \frac{2.7}{42.4} = 0.0637 \qquad \frac{0.216}{0.0637} = 3.4$$
$$\frac{k_{3H}}{k_4} = \frac{8.7}{51.0} = 0.170 \qquad \frac{k_{3D}}{k_4} = \frac{2.7}{54.6} = 0.0494 \qquad \frac{0.170}{0.0494} = 3.4$$

The two independent calculations give the same value of 3.4. This is in the range that is consistent with a primary isotope effect.

9.19. a. These three examples indicate a preference for formation of six-membered rings relative to seven-membered rings. The second two cases involve endoergonic rearrangement of a tertiary cation to a secondary cation. The carbocation rearrangement must be faster than cyclization.

b. These cases suggest a strong preference for formation of six-membered rings over five-membered rings. There is no cyclization in reactions 1 or 4, where five-membered rings could be formed at primary or secondary carbons. Entry 2 suggests a "*gem*-dialkyl" effect favoring cyclization. However, the cyclization product is still a minor product. Entry 3 indicates facile formation of a six-membered ring at a primary carbon. Entry 5 suggests that a combination of favorable factors—a stable tertiary cation, an activating methyl group, and *gem*-disubstitution—can lead to cyclization forming a five-membered ring.

c. These reactions involve Lewis acid–mediated opening of epoxides to generate electrophilic intermediates. The first entry fails to form a five-membered ring by cyclization at an unsubstituted epoxide methylene group. The second entry fails to form a six-membered ring at an unsubstituted epoxide or a five-membered ring at the monosubstituted carbon. The third entry shows effective formation of a six-membered ring by attack at a monosubstituted epoxide carbon. In Entry 4, both six- and seven-membered rings are formed, the former requiring a hydride shift. Taken together these results suggest 6 > 7 > 5 as the order of preference for ring formation by intramolecular Friedel-Crafts reactions. Moreover, there are no *endo* cyclization products formed, even in Case 2, where a six-membered ring could be formed.

9.20. a. These reactions can be formulated as nucleophilic aromatic substitutions in which the 4-carbon of the 2,6-di-(*t*-butyl)phenoxide acts as the nucleophile, owing to the steric bulk around oxygen. The reactions might also be formulated as involving an electron transfer step.

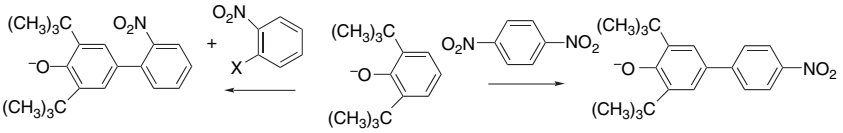

b. This result is best explained by intervention of a benzyne intermediate. The regioselectivity of the addition step is contrary to the EWG effect of the oxazoline ring and could be due to a chelation effect.

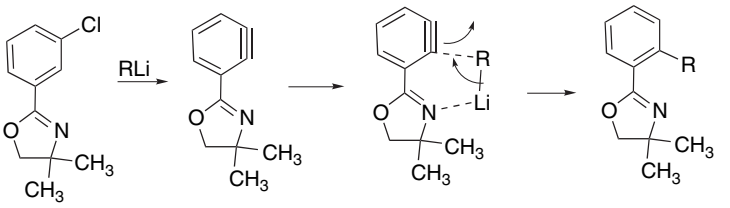

c. This is a vicarious nucleophilic substitution involving reaction at both the *o*- and *p*-positions.

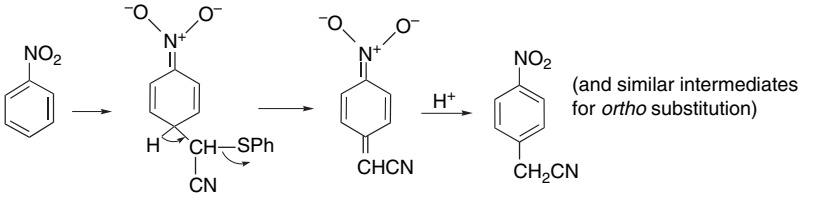

d. This product can be formed by two successive benzyne additions.

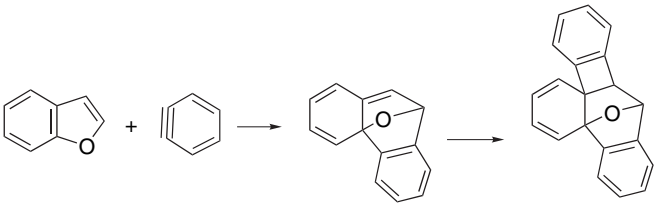

e. This reaction illustrates that a secondary carbocation cannot easily be formed from 3,3,3-trifluoropropene. Although the product might be formulated as an anti-Markovnikov protonation, it is likely that the mechanism is more complex. It has been suggested that most acid-catalyzed reactions of 3,3,3-trifluoropropene proceed through the 1,1-difluoroallyl cation generated by acid-catalyzed ionization. These reactions imply carbocation stabilization by the remaining fluorine substituents.

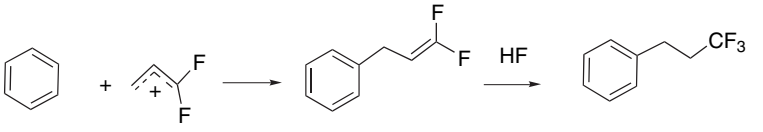

f. These results indicate that formation of six-membered rings is preferred to formation of five-membered rings, as is the case for Friedel-Crafts alkylation. The success of the acid chloride but not the carboxylic acid in the five-membered case suggests that a more reactive intermediate is available to the chloride. This could be a mixed anhydride with the Nafion-H sulfonic acid group.

9.21. These reactions are believed to proceed through an aryne intermediate, presumably generated as the solution warms. The *o*-cyano product can be generated by an intramolecular addition to the cyano group, followed by a cleavage reaction.

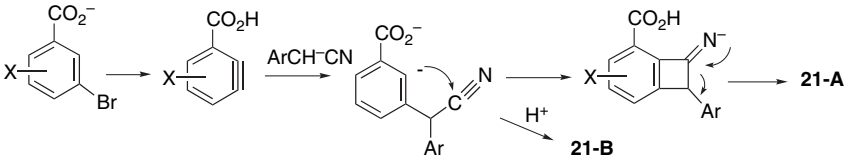

Chapter 10

10.1. a. Both the basis set orbital array and orbital symmetry correlation diagrams indicate that a disrotatory cyclization is not allowed. The disrotatory orbital array is a Hückel system with no nodes and four π electrons and is antiaromatic. For the disrotatory mode, a plane of symmetry is maintained. The ψ_2 orbital of the pentadienyl cation does not correlate with an occupied orbitals of the cyclopent-2-enyl cation. The reaction is forbidden.

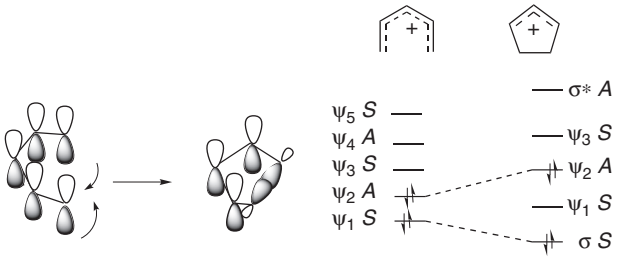

b. For the pentadienyl anion the number of π electrons is six. This means the disrotatory orbital array is aromatic. Furthermore, in the orbital symmetry diagram, ψ_3 is now filled and all filled orbitals correlate with ground state orbitals in the product. The reaction is allowed.

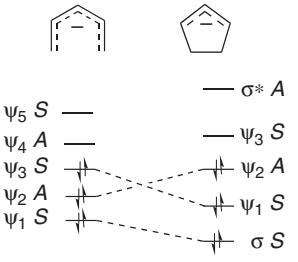

c. For the heptatrienyl cation there are six π electrons and no nodes, so the disrotatory orbital array is aromatic. The disrotatory mode maintains a plane of symmetry. The orbital symmetry diagram also shows correlation of the filled reactant orbitals with product orbitals, so this reaction is allowed.

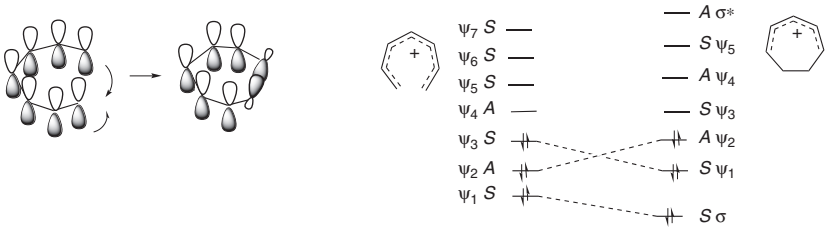

10.2. a.

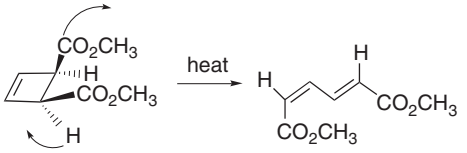

This cyclobutene ring opening is a conrotatory process and is allowed.

b.

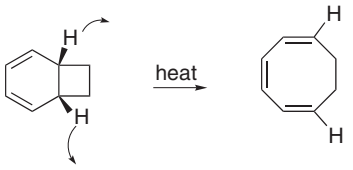

This is a six-electron ring opening and should be disrotatory. This leads to the *Z*,*Z*,*Z*-1,3,5-octatriene and is not geometrically constrained. The two compounds are reported to equilibrate on heating to 80°C.

c.

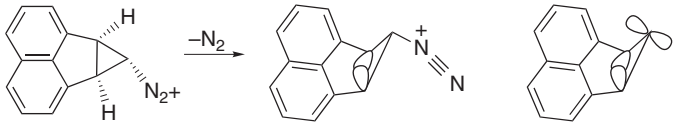

The diazonium group is in the *exo* orientation with respect to the naphthalene ring and the system is quite rigid because of the fused aromatic rings. The preferred ring opening is disrotatory, but the *exo* orientation of the diazonium group is not favorable for participation of the cyclopropyl orbitals, which would require an outward rotation of the C−C bonds to the aromatic ring. Outward rotation is precluded geometrically. For this reason, the diazonium ion is rather stable and resistant to ring opening. On treatment with HCl, it gives an unopened cyclopropyl chloride. Only when this chloride is heated with $AgClO_4$ at 70°C does ring opening occur.

d. Formally, this is a $[2\pi + 8\pi]$ suprafacial/suprafacial cycloaddition and is allowed. However, the donor dithiane ring, in conjunction with the strongly electrophilic tetracyanoethene, might well lead to a stepwise dipolar mechanism. The original report does not distinguish between the possibilities, but either reaction should be favorable.

e. This is an allowed 1,5-sigmatropic shift of hydrogen and the stereochemistry of the product follows from the cyclic transition structure.

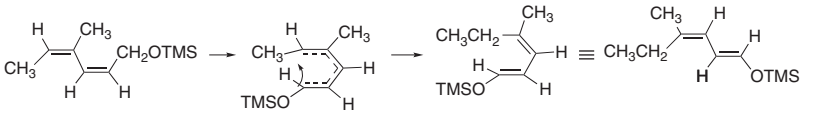

10.3. The observed product results from a disrotatory six-electron electrocyclization.

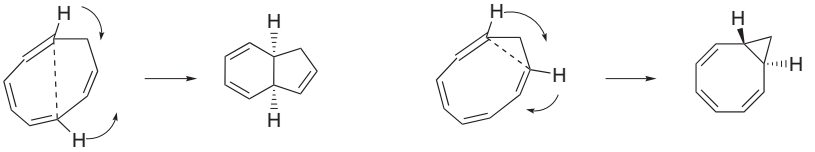

A conrotatory eight-electron electrocyclization is also allowed but this would lead to a more strained *trans* ring junction with a three-membered ring.

10.4. a. The *endo* isomer is more reactive because reaction can proceed with participation of the *anti* cyclopropyl orbital with a favorable disrotatory ring opening. The cyclopropyl orbital in the *exo* isomer is not positioned for participation.

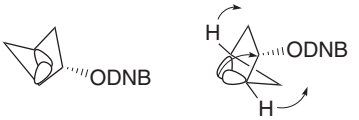

b. The anticipated chairlike TS for [3,3]-sigmatropic shift leads to the enantiomer. Note that the TS has a *center of symmetry.*

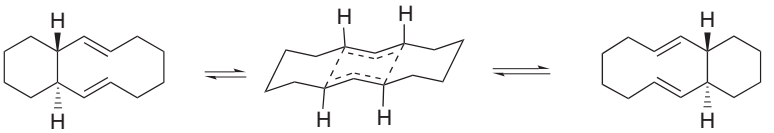

c. The observed stereochemistry is consistent with a retro $[2\pi + 4\pi]$ cycloaddition followed by conrotatory ring opening.

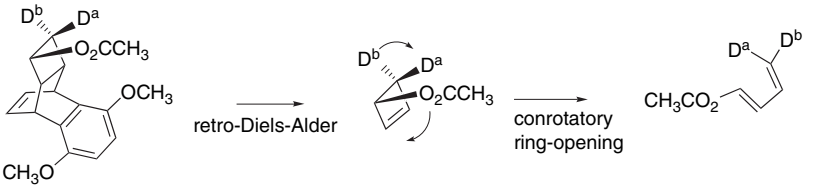

d. The ring opening of a cyclopropyl anion involving four electrons should be conrotatory. This is geometrically precluded by the fused ring system in **4-E**.

e. The heptatriene electrocyclization leads to the formation of a second benzenoid ring and therefore favors the observed product.

10.5. a.

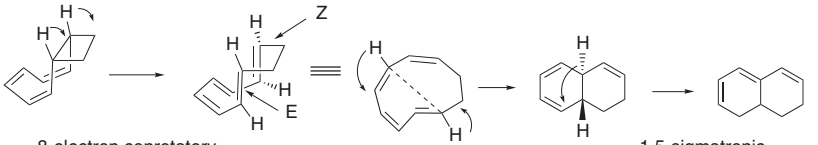

b.

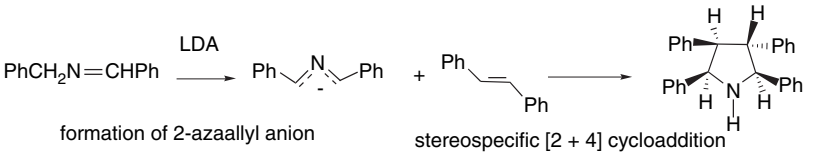

c. The preference for outward rotation of the hydroxy substituent leads to formation of the *E*-enol. An intramolecular 1,5-H transfer is precluded by the *E*-configuration and the tautomerization to the aldehyde presumably occurs by intermolecular proton transfer.

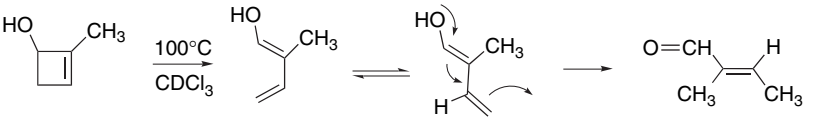

d.

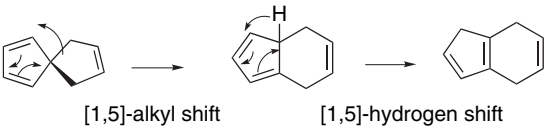

e.

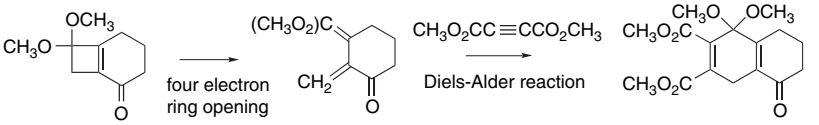

f

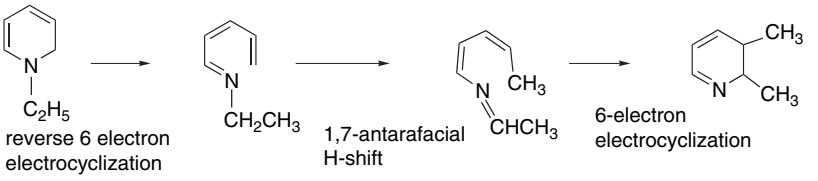

g.

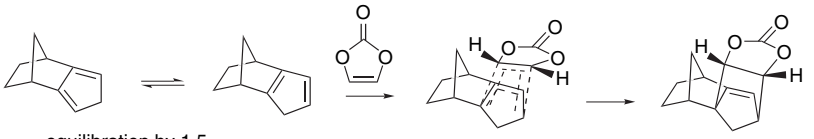

10.6. It has been suggested that a steric interaction between the aryl substituent and the ester group forces the former into a pseudoaxial position, leading to the observed stereochemistry.

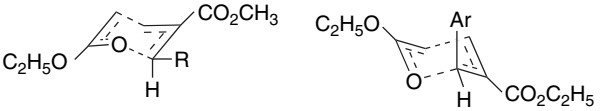

10.7. a. An *exo* [2 + 2] adduct is expected.

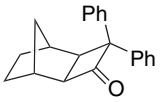

b. The donor effect of the ethoxy group controls the regiochemistry.

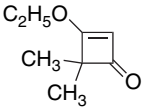

c. This compound undergoes the oxy-Cope rearrangement, with the final step being ketonization.

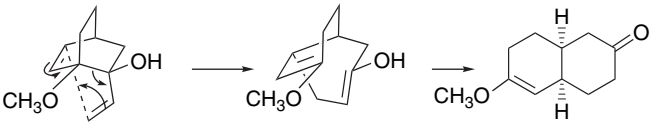

d. These conditions give a thio-Claisen rearrangement, with subsequent hydrolysis of the thioaldehyde.

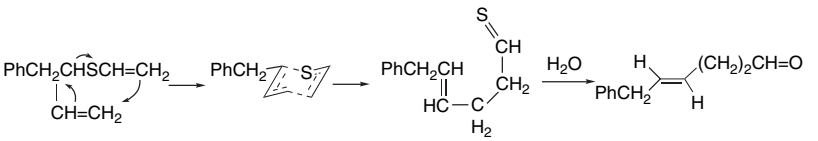

e. This reaction leads to ring expansion through a [2,3]-sigmatropic rearrangement of a sulfonium ylide.

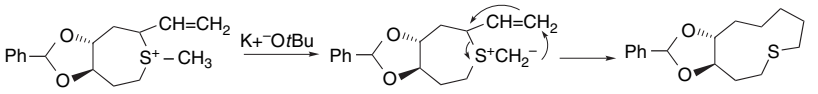

f. This reaction leads to two successive Diels-Alder reactions.

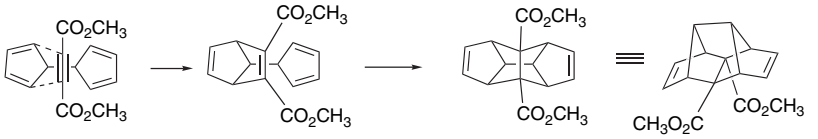

g. A Cope rearrangement is feasible and leads to a less strained cyclobutane.

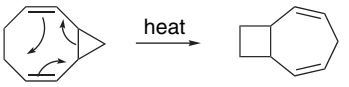

h. This [2 + 2] cycloaddition is antarafacial with respect to the ketene. Note that the *t*-butyl substituent is in a *cis* relationship to the C−C bond because of this stereoselectivity.

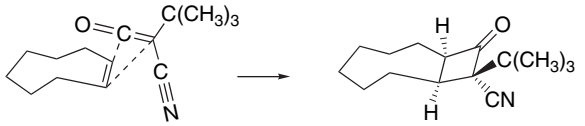

i. This intramolecular [2 + 2] ketene cycloaddition involves the 5,6-double bond rather than the exocyclic 3-methylene group.

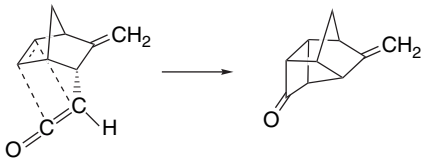

j. The ring opening should be conrotatory. The outward preference for rotation of the siloxy group and the inward preference of the formyl group predict the observed stereoselectivity.

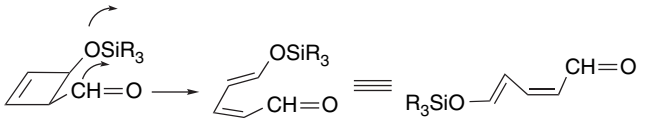

10.8. The failure of **10-B** to revert to **10-A** indicates that a high barrier, rather than an unfavorable equilibrium, is the cause of the nonreactivity. It is suggested that the shorter bridges imposes a transoid conformation that precludes optimal orbital overlap for [3,3]-sigmatropic shift, whereas the five-carbon bridge allows attainment of the cisoid conformation and permits rearrangement through a boatlike TS.

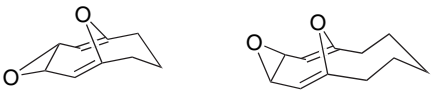

transoid cisoid

10.9. Since the bromine in both cyclooctatetraene and *E*-β-bromostyrene is attached to an sp^2 carbon, it is unlikely that direct ionization or substitution can occur. This is confirmed by the lack of reactivity of *E*-β-bromostyrene toward lithium iodide. The six-electron electrocyclization product 1-bromobicyclo[4.2.0]octa-2,4,7-triene has a cyclobutenyl structure that can ionize to a stabilized carbocation. This cation could be captured by iodide, accounting for the incorporation of iodide in the presence of lithium iodide. Subsequent conrotatory opening of the rearrangement product leads to *E*-β-bromostyrene.

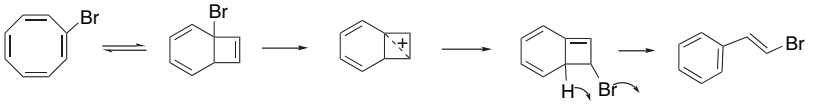

10.10. The reaction is suggested to proceed through formation of the enamine and corresponding iminium ion. The former would be an electron-rich diene and the latter an activated dienophile.

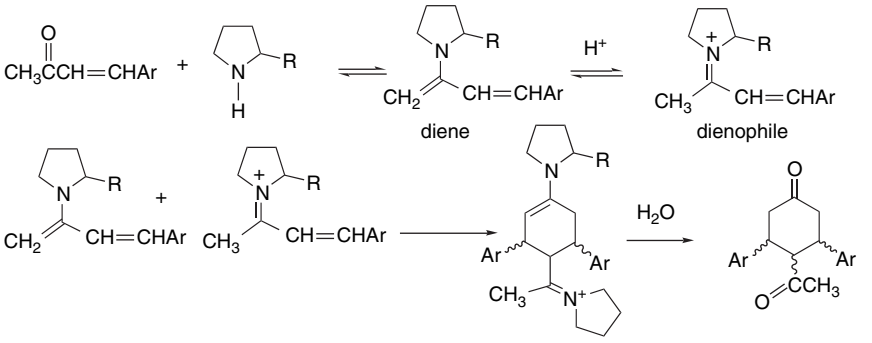

10.11. a. The reaction proceeds through an intramolecular Diels-Alder reaction involving a chelated transition structure with *endo* stereoselectivity.

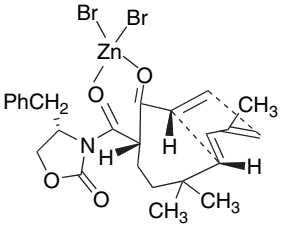

endo transition structure

b. The reaction is a 1,3-dipolar cycloaddition in which the regiochemistry is determined by the complementary electronic character of the reactants. The lithium cation organize the transition structure by coordination with the carbonyl and enolate oxygen.

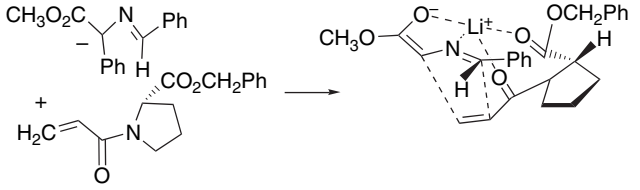

c. This is a 1,3-dipolar cycloaddition. The *o*-hydroxy can contribute a hydrogen bond that favors the transition structure leading to *cis* stereochemistry.

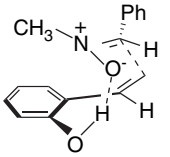

10.12. a. The reaction occurs by a six-electron electrocyclization, followed by a $[\pi 2_s + \pi 4_s]$ cycloaddition. Note that the reaction occurs by *endo* addition and that there is a preference for the substituted cyclobutadiene in the initial electrocyclization. This may reflect the stabilizing effect of the methyl substituent on the double bond.

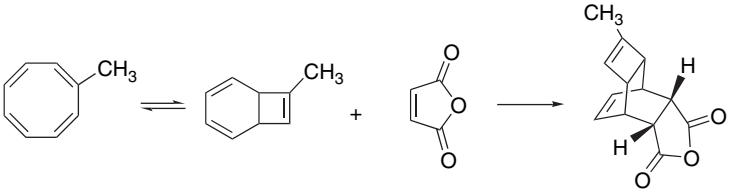

b. This is an intramolecular $[\pi 2_s + \pi 4_s]$ cycloaddition.

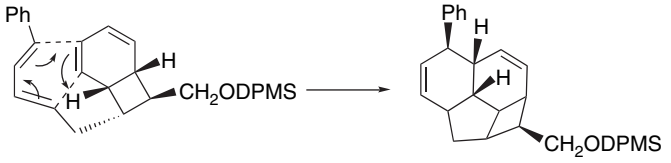

c. A conrotatory four-electron electrocyclic ring opening is followed by a $[\pi 2_s + \pi 4_s]$ cycloaddition.

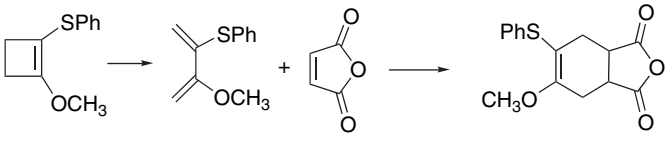

d. A conrotatory eight-electron electrocyclization is followed by a disrotatory six-electron electrocyclization.

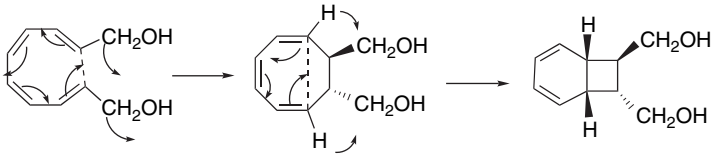

e. This is a [3,3]-sigmatropic rearrangement. The endocyclic double bond in the product is more stable than the exocyclic one in the reactant.

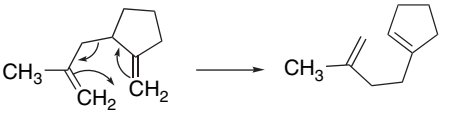

f. This reaction can occur by a [1,7]-sigmatropic shift of hydrogen and is presumably antarafacial.

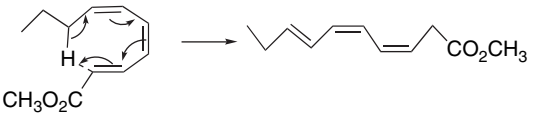

10.13. The reaction is a $[\pi 2 + \pi 2 + \sigma 2]$ process.

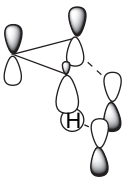

10.14. a. The stereochemistry is that expected for an *endo* transition structure.

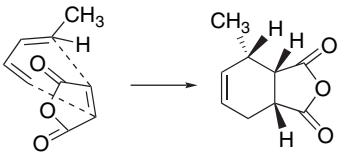

b. The regiochemistry is correctly predicted by FMO considerations and there is a 5:1 preference for the *endo-cis* stereochemistry.

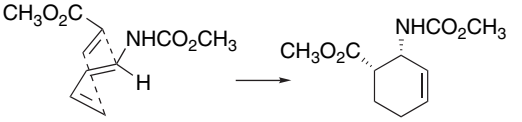

c. The isolated product results from elimination of pyrrolidine. The predicted regiochemistry is shown, but is obscured by the elimination of pyrrolidine. Some of the product is also aromatized by loss of hydrogen.

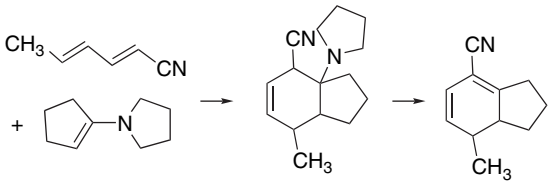

d. The regiochemistry results from reaction at the less stabilized of the two "enone" systems within the quinone. Note that the *cis* ring junction follows from the retention of the dienophile stereochemistry.

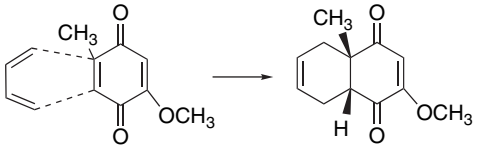

e. The reaction is 100% regio- and stereoselective and the *endo* transition structure is favored. Note also that the 1-phenylthio substituent controls the regiochemistry over the 2-methoxy group.

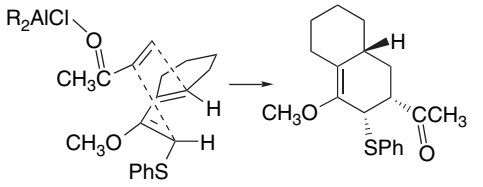

10.15. A prior ring opening would be conrotatory (eight electrons) and would be unfavorable for a *cis* ring junction, leading to an *E*-double bond. In the radical anion, the next highest MO is occupied and the disrotatory mode is favored. This mode is favorable for the *cis* ring junction, but not the *trans*. The most likely reaction sequence is electron transfer, opening of the *cis* radical anion, and a second reduction to the aromatic dianion.

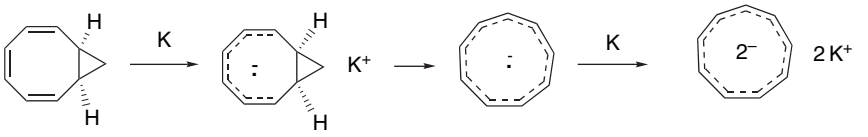

10.16. a. A Cope rearrangement interchanges the CH groups labeled a, b, and c.

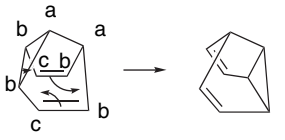

b. All of the CH groups become equivalent as the result of a sequence of Cope rearrangements that migrate the double bond around the five-membered rings.

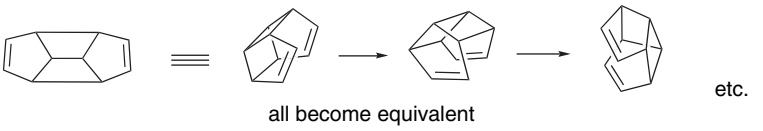

c. A *bis*-homo six-electron migration proceeds through the *bis*-cyclopropane intermediate. The six peripheral CH groups labeled "a" and the four internal CH groups labeled "b" interchange with one another as a result of this process.

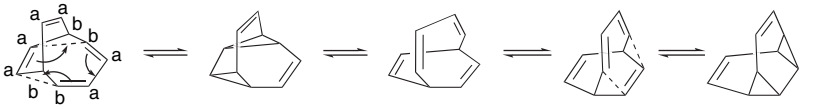

d. A Cope rearrangement interchanges the CH_2 groups labeled a and *a′* and the CH groups labeled b and c. However, the two faces of the ring remain nonequivalent.

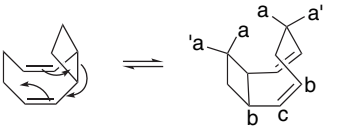

e. This Cope rearrangement interchanges all the CH_2 groups labeled a and also the carbons labeled b. The rather distorted geometry contributes to the relatively high temperature that is required.

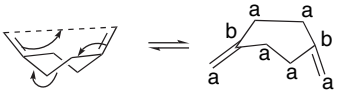

f. A 1,6-dioxa-Cope rearrangement interconverts the carbonyl carbon and oxygen with positions 1 and 6 of the dihydropyran ring.

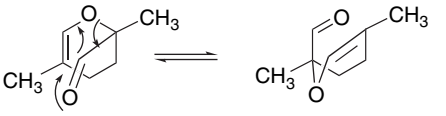

10.17.

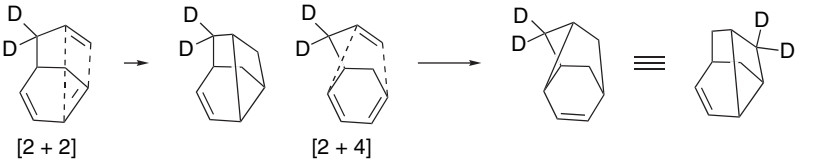

The results of the study show that the $[4+2]$ mechanism is followed.

10.18. The calculations indicate that the reaction is slowed by σ-donor substituents. A logical explanation for this is that such groups stabilize the pentadienyl cation more strongly than the cyclopentenyl cation, since they are at a nodal position in the latter cation. Alkyl groups would have the same effect and should retard the reactions. Conjugated EWGs should be weakly accelerating, since the polar effect would destabilize the reactant more than the product, but this would be counteracted by any conjugation with the cationic site. (See Section 4.4.1 for a discussion of the effect of π EWGs on carbocations.) The σ EWGs should destabilize the reactant more than the product and favor reaction.

10.19. a. This reaction occurs by [3,3]-sigmatropic rearrangement (oxy-Cope) and ketonization.

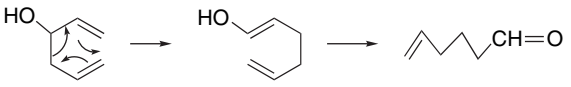

b. This reaction occurs by exchange to the vinyl allyl ether and [3,3]-sigmatropic rearrangement (Claisen rearrangement).

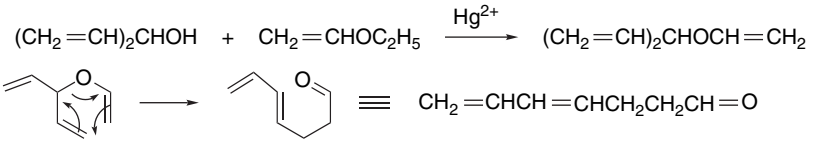

c. This product can be formed by conrotatory eight-electron ring opening of a *trans*-1,2-diacetyl derivative.

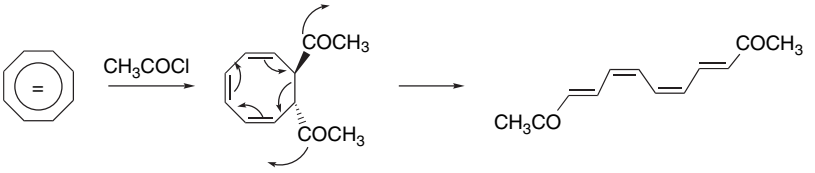

d. The product structure is consistent with cyclization of a pentadienyl cation generated by acid-catalyzed protonation and ionization of the hydroxy groups.

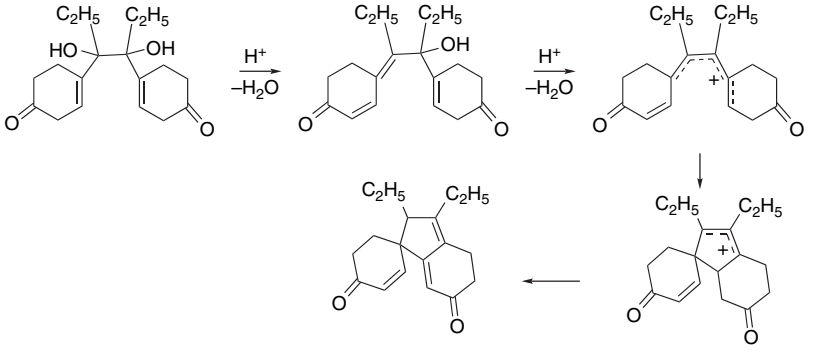

e. This is an oxy-Cope rearrangement.

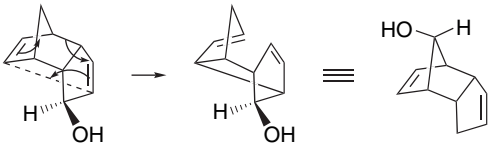

f. This reaction can occur by oxygen-protonation, followed by a two-electron electrocyclic ring-opening reaction.

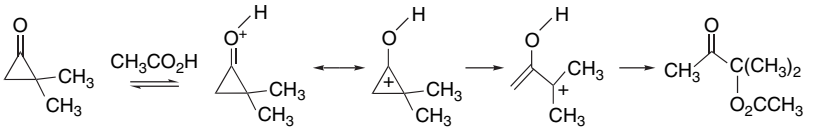

g. The retention of the *Z*-stereochemistry of the alkene indicates a concerted cycloaddition. A 1,3-dipole can be formed by opening of the epoxide and is stabilized by the cyano substituents.

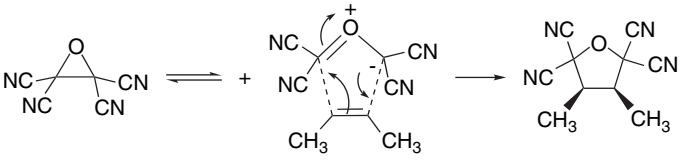

h. A reverse [2 + 4] cycloaddition (retro-Diels-Alder) accounts for this product.

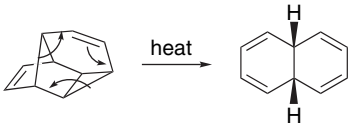

i. This is a [2,3]-sigmatropic shift of the sulfonium ylide, followed by aromatization and lactamization.

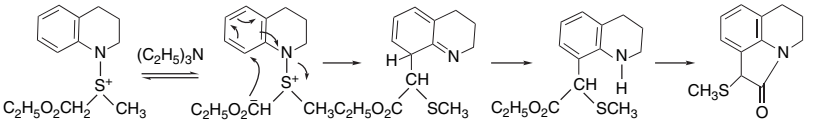

j. This reaction corresponds to an [8 + 2] cycloaddition.

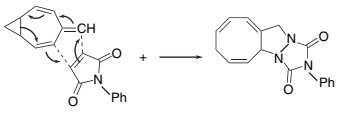

k. This reaction corresponds to a [6 + 4] cycloaddition. The stereochemistry indicates an *endo* transition structure. The final position of the double bonds is established by a [1,5]-sigmatropic hydrogen shift.

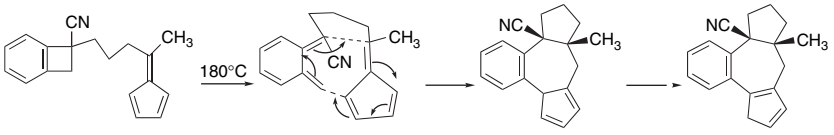

l. This reaction occurs by [2,3]-sigmatropic shift of the selenoxide intermediate, followed by solvolysis of the selenenate. Note the retention of α stereochemistry that occurs as the result of the suprafacial nature of the reaction.

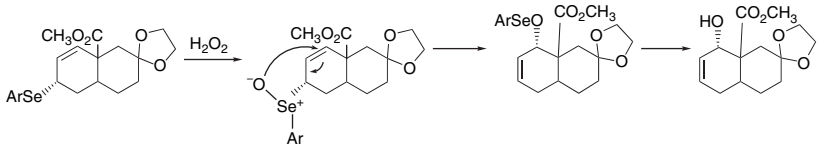

m. The reaction occurs by a [2,3]-sigmatropic shift of a sulfonium ylide.

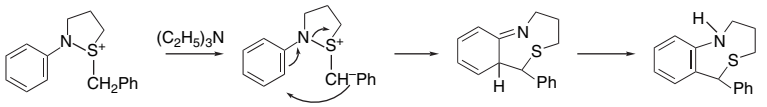

n. This is an intramolecular [2 + 2] cycloaddition.

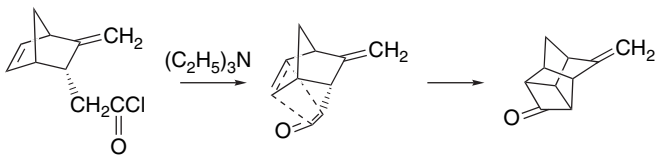

10.20. The planar all-*Z* cation, having eight electrons, would be expected to be antiaromatic. The large positive NICS value is in accord with this expectation. Structure **3**, with an *E* relationship can accommodate a Mobius twist, in which case the eight-electron system would be aromatic. The NICS value, which is in the strongly aromatic range, supports this. In order for scrambling of all atoms to occur, as indicated by the labeling data, the *E* relationship must not be fixed but must be available to each pair of carbons, by circulation around the ring.

The cation **8**, which gives rise to product, can be formed by a six-electron electrocyclization, which should be disrotatory.

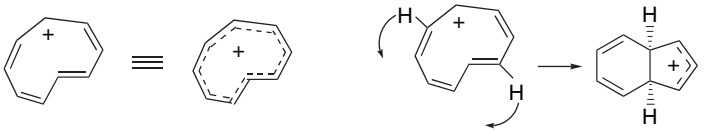

10.21. a. It is clear that the reaction is *kinetically controlled.* The $[2+4]$ adduct is substantially more stable than the observed $[2+2]$ adduct **2**. However the E_a for forming **2** is much lower. The same conclusion holds with the isomeric $[2+2]$ adduct **3**. It is only slightly less stable than **2**, but the E_a is substantially higher.

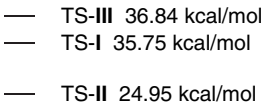

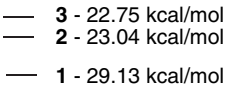

b. The transition structure shows considerable charge transfer, consistent with the description of the ketene $[2+2]$ cycloaddition given on p. 889. The TS leading to **2** delocalizes this positive charge over an allylic system, whereas it is more localized in **3**.

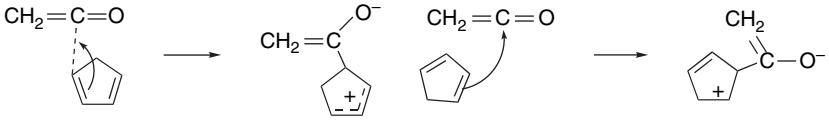

c. The TS **I** leading to **1** is very similar to a Diels-Alder TS. The bond formation is quite asynchronous. The initial bonding takes place primarily between the cyclopentadiene LUMO and the ketene HOMO, judging from the orbital separations shown in Figure 21Pc. The C=O π^* bond is not a direct participant in the $[2+4]$ TS. In the $[2+2]$ TS there is considerable charge transfer from the diene HOMO to the C=O π^* orbital. This orbital interaction has a smaller gap than the corresponding $[2+4]$ gap and, therefore, according to FMO theory, leads to greater TS stabilization.

11.1. a. *anti*-Markovnikov addition occurs in 93% yield.

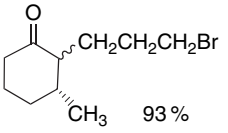

b. Radical addition of the 2-hydroxy-2-propyl radical is accompanied by lactonization and esterification.

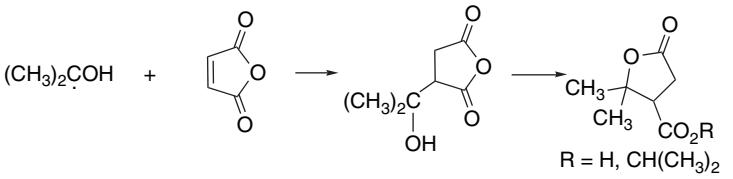

c. Intramolecular hydrogen abstraction leads to a γ-chloroalcohol that cyclizes to a tetrahydrofuran on treatment with base.

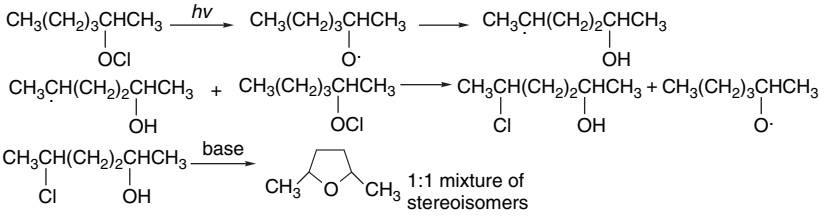

d. Radical chain addition of the aldehyde occurs.

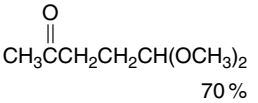

e. These conditions lead to allylic oxidation introducing a benzoyloxy group.

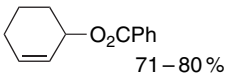

f. This reaction results in a transannular cyclization.

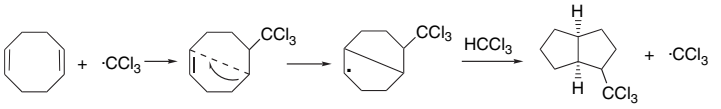

g. Oxidative decarboxylation and dimerization occurs in 43–56% yield.

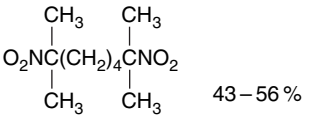

h. A radical chain addition of carbon tetrachloride occurs in 70% yield.

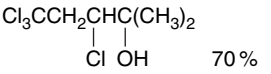

i. The product is the result of an $S_{RN}1$ substitution.

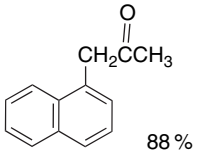

j. Anti-Markovnikov addition of the thiol occurs.

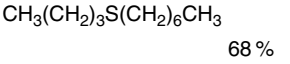

11.2. The cited source gives the *pri:sec:tert* selectivity for chlorination and bromination as 1:4.6:6 and 1:250:6300, respectively. The calculation of the ratio at positions **a**, **b**, **c**, and **d**, is as follows:

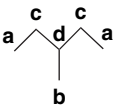

Chlorination: (6)1 + (3)1 + (4)4.6 + (1)6 = 33.4: 18%, 9.0%, 55%, 18%.
Bromination: (6)1 + (3)1 + (4)250 + 1(6300) = 7309: 0.08%, 0.04%, 13.7%, 86.2%.

11.3. The formation of 2-hexene can be accounted for by reversible H atom abstraction at the allylic position. The extent of reversible H atom abstraction in competition with addition increases with temperature. The radical chain addition of HBr to 2-hexene is not regioselective, as would be expected.

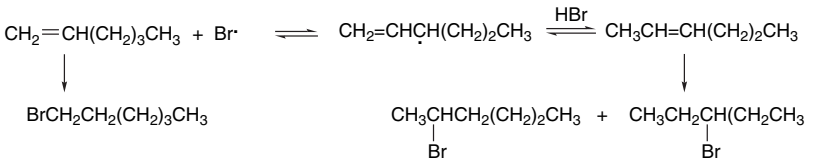

11.4. Both the 2- and 4-dioxolanyl radicals are expected to be nucleophilic in character because of the donor effect of the oxygens. The high-temperature conditions reduce the selectivity for the 2-position and increase the extent of fragmentation. The 2-substituted radical is more susceptible to fragmentation, since it leads to an ester.

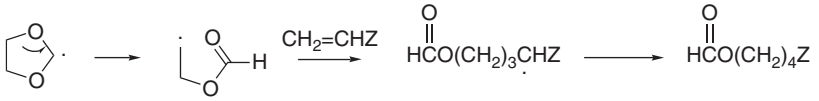

11.5. a. The retention of optical activity under these conditions is consistent with involvement of a bridged bromine radical. There would be no corresponding bridged intermediate in the case of fluorine. An alternative formulation based on recent computational work attributes this result to a lack of stereospecificity in the fluoro-substituted case (see p. 1028).

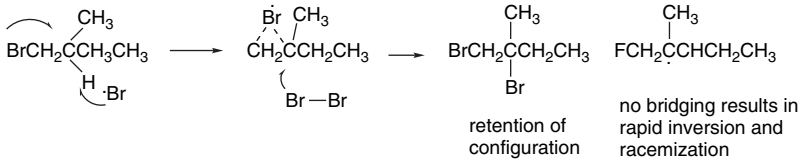

b. This stereoisomerization can result from reversible addition of bromine atom, which permits ring opening and stereoequilibration to the more stable *exo* isomer.

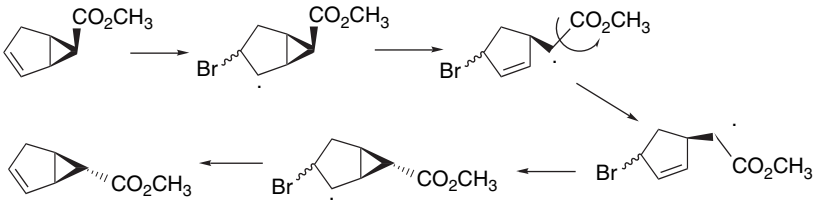

c. The stereoelectronic effect for interaction of the oxygen unshared electrons is more favorable in the case of the equatorial CH_3 group. This has the effect of weakening the axial C−H bond and results in a faster reaction.

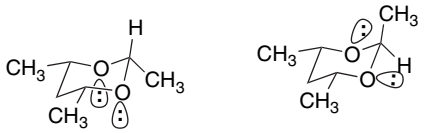

d. There are six possible sites of reaction, including the two sites **d** and **e** at C(3), which are diastereotopic by virtue of the adjacent stereocenter. The product of chlorination at **a** should retain chirality. The products of chlorination at **c** will be achiral because of the identity with the existing chloromethyl group. Products from reaction at **d**, **e,** and **f** do not involve the stereocenter and should retain the chirality in the reactant. The stereochemistry of the product at **b** will be dependent on the mechanism. Racemization at this site would indicate loss of stereochemistry in the presumed radical intermediate, and this is the outcome that is observed experimentally.

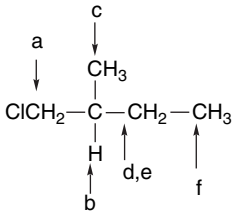

e. The radical resulting from hydrogen abstraction at the allylic position can give the 2-phenylethyl radical by a cyclopropylcarbinyl-type ring opening.

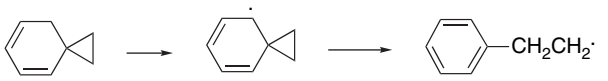

f. The formation of saturated products indicates that 5-*exo* cyclization follows the initial addition of the perfluoropropyl radical. The *cis* and *trans* isomers resulting from cyclization will give the same exocyclic elimination product.

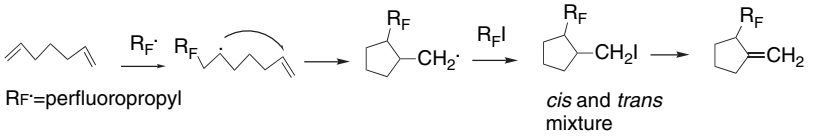

g. These results can be accommodated by an intramolecular shift of an H atom between the two rings. The resulting isomer can give rise to the cyclization product **5-D** and can form **5-E** and **5-F** by intermolecular iodine atom transfer.

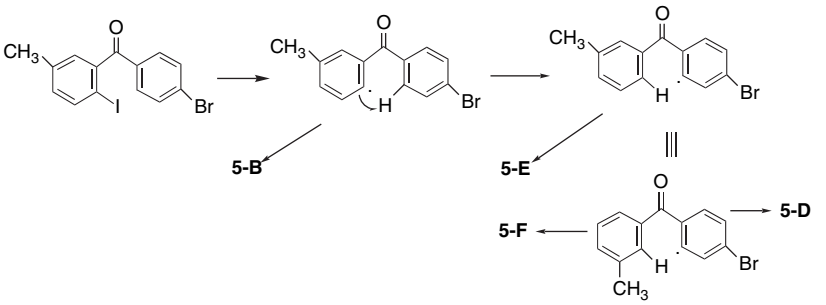

h. Product **5-H** can be formed by cage recombination without rearrangement. Products **5-I** and **5-J** result from an acyl group migration. Note that the acyl group migration occurs in preference to aryl group migration, which is consistent with the relative rate data given in Section 11.7.

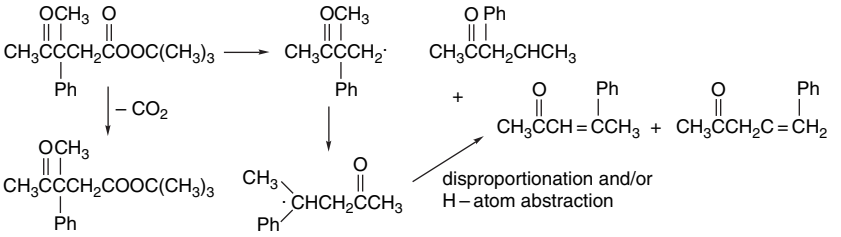

11.6. a. The cyclic product **6-B** arises by addition to the benzene ring. The unrearranged product **6-C** results from decarbonylation and hydrogen atom

abstraction. The rearranged product **6-D** can be formed via a spiro intermediate.

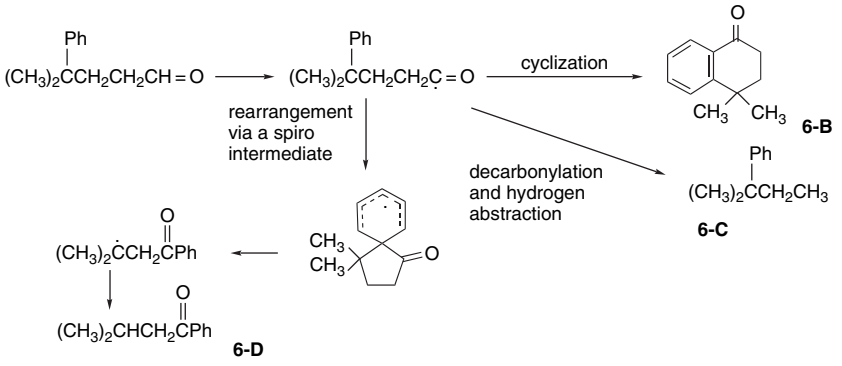

b. This cyclization can occur by a chain sequence involving selective abstraction of a benzylic hydrogen and *exo*-6 cyclization.

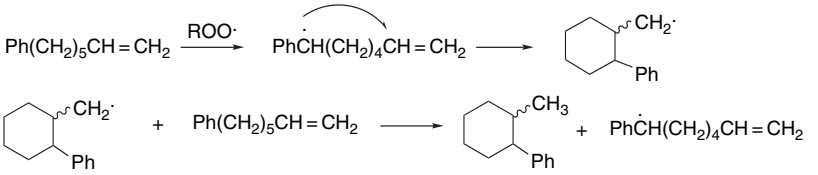

c. This reduction, occurs by a mechanism related to the $S_{RN}1$ mechanism. A tri-*n*-butylstannyl radical reduces the nitro compound to a radical anion that decomposes with loss of nitrite.

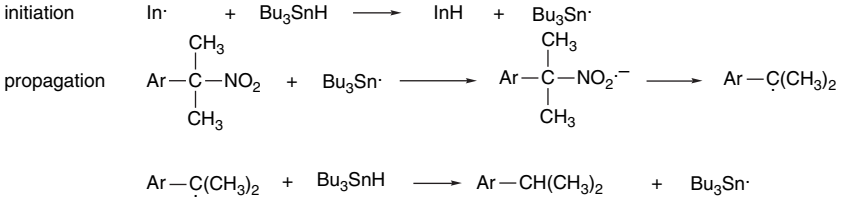

d. This reaction involves addition of the ethyl carbamyl radical and is initiated by one-electron reduction.

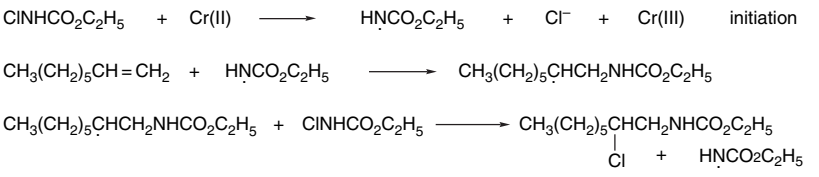

e. This is an $S_{RN}1$ reaction involving a pyridylmethyl anion as the nucleophile. The electron-accepting capacity of the pyridine ring is important to the effectiveness of the coupling between the radical and the anion.

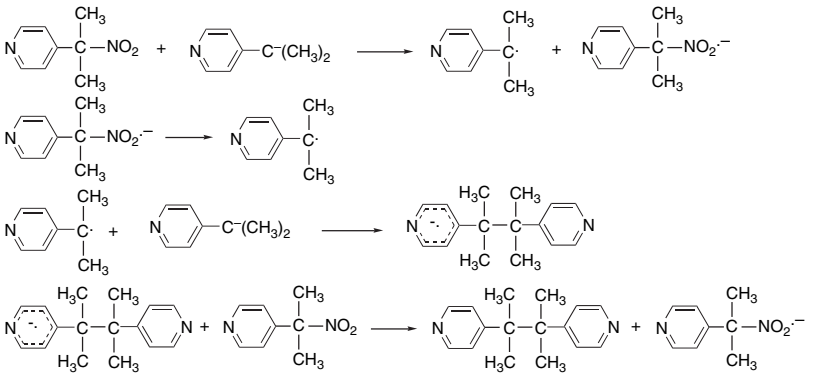

f. This is an electrolytic oxidation in which the initial alkoxy radical fragments. The 2-propyl radical is oxidized to a carbocation, which then reacts with the acetonitrile to generate the amide (Ritter reaction).

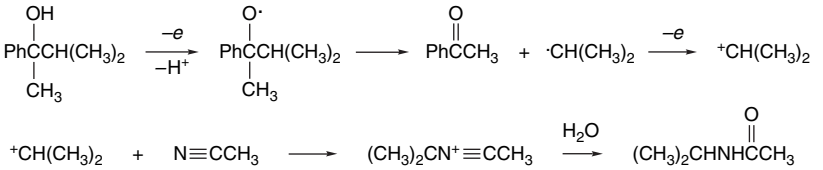

g. This reaction involves cleavage of the strained ring to a diradical that recyclizes to the more stable disubstituted exocyclic double bond.

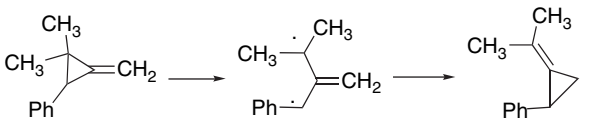

h. The reaction begins by attack of the phenylthiyl radical at the least hindered alkene carbon. The resulting intermediate is trapped by oxygen to give a peroxyl radical, which then adds at the second double bond by an 5-*exo* addition. The resulting radical is again captured by oxygen. The cycle is repeated by abstraction of hydrogen from the thiol.

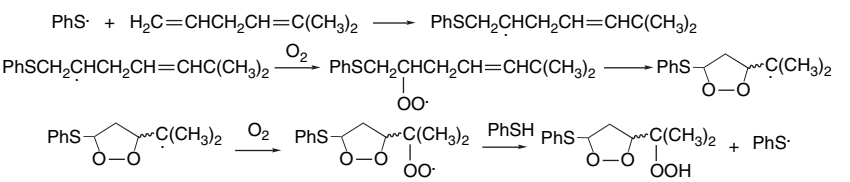

11.7. The equilibrium between the cyclopropylcarbinyl and 3-butentyl radicals can account for the label distribution (see p. 974, Figure 11.3 and Table 11.3, Entry 30). The equilibration of the *Z* and *E* labels involves rotation in the cyclopropylcarbinyl radical. The unequal deuterium distribution favoring that in the initial reactant at high concentration indicates that hydrogen abstraction is slightly faster than equilibration at the higher concentration.

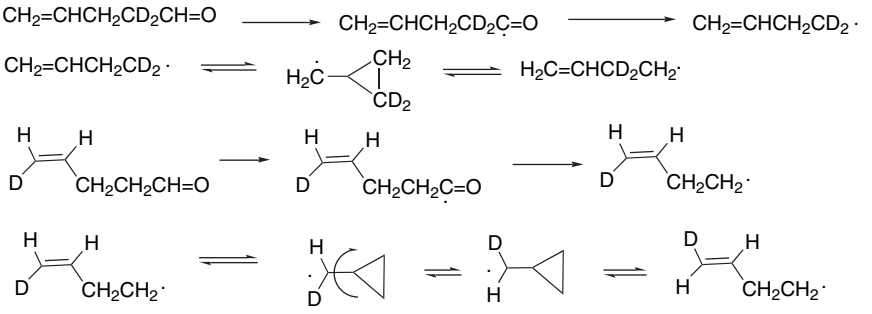

11.8. These results indicate that the *cis*-9-decalyl radical formed from **8-B** is conformationally distinct from the *trans*-9-decalyl radical formed from **8-A**. At low O_2 pressure, the *cis* radical is converted to the *trans* radical, which gives the 9:1 *trans*:*cis* product ratio. At higher O_2 pressure, successively more of the *cis* radical is trapped prior to the conformational change.

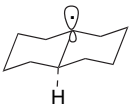

The radical formed from the *trans* reactant is conformationally preferred and reacts with O_2 with a 9:1 preference for *trans* product.

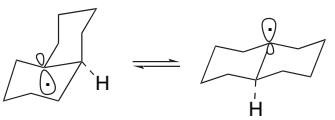

The conformationally distinct 9-decalyl radical formed from the *cis* peroxy ester is converted to the more stable *trans* radical at a rate that is competitive with capture by O_2.

11.9. a. Two possible propagation sequences follow. They differ in whether a sulfonyl radical or a trichloromethyl radical is the H-abstracting radical.

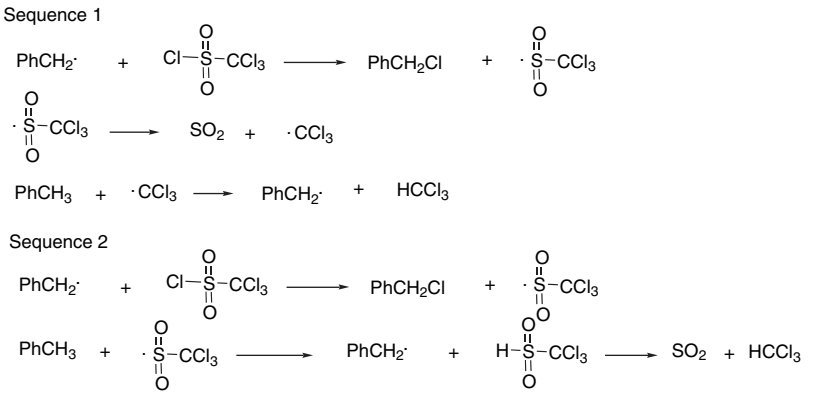

b. The bromination by bromotrichloromethane involves H abstraction by the trichloromethyl radical, which should show the same selectivity in both reactions. The data show that the reactions have different selectivity, indicating that different radicals are involved in H abstraction and favoring the second of the above sequences.

11.10. The unique feature of this reaction is the H-abstracting agent, which is the radical cation $R_2NH^{\cdot+}$. This positively charged radical avoids the functional groups, which are protonated in the strong acid. The $\omega - 1$ selectivity reflects the preference for abstracting a secondary, rather than primary, hydrogen.

11.11. a. The spectrum consists of five equally spaced triplets, indicating that the four terminal and two internal hydrogens are equivalent. The coupling constants are 7.6 G and 2.9 G. According to the McConnell equation (p. 971), the spin density is proportional to the splitting constants. This indicates 0.28*e* on the internal carbons and 0.72*e* on the terminal carbons.

b. As there is a barrier to rotation in the allyl radical, the terminal hydrogens **a** and **b** are nonequivalent and give rise to an 18-line spectrum. The terminal hydrogens give rise to triplets with large splitting, whereas the C(2) hydrogen has a much smaller splitting.

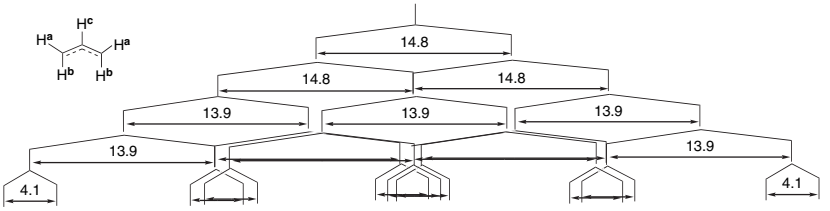

11.12. a. The reaction involves acyl radical generation and decarbonylation. The rearranged product is the result of a phenyl group migration.

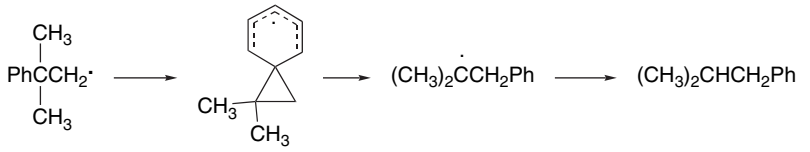

b. The reaction is initiated by acyl radical generation and decarbonylation. The major product is formed by phenyl group migration followed by hydrogen abstraction.

c. The hydrogen abstraction in this chain process is done by the *t*-butoxy radical. The product is the result of bromine atom rearrangement.

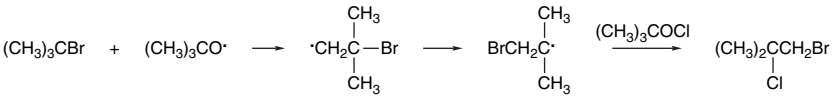

d. The rearrangement occurs by a ring expansion through a cyclopropylcarbinyl type rearrangement.

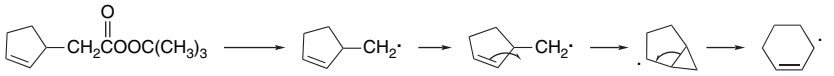

e. This transformation involves a phenyl group migration. The highly substituted nature of the alkene leads to elimination of the hydrogen atom, in preference to substitution.

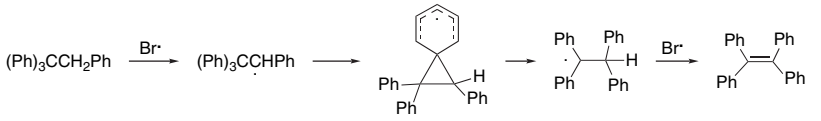

11.13. The reaction can begin by peroxide cleavage and fragmentation to diradical **13-D**. Intramolecular recombination gives intermediate **13-E**. Decomposition of this peroxide gives intermediate **13-F**, which can recombine after loss of one (**13-G**) or two (**13-H**) molecules of CO_2 by decarboxylation.

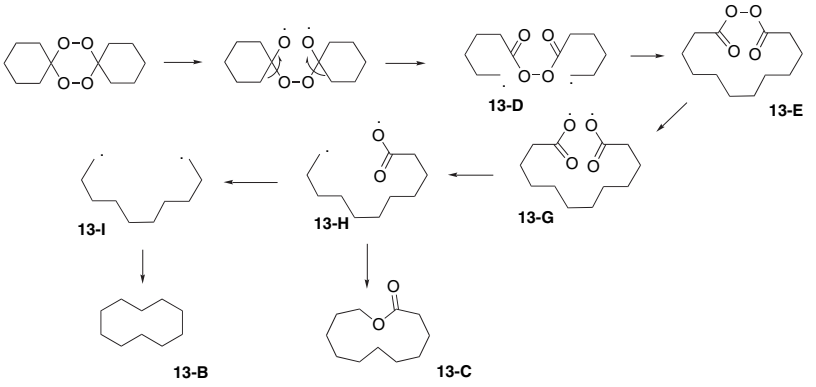

11.14. The product distribution reflects competition between H abstraction from the methyl group and ring cleavage. Bromine reacts entirely by ring cleavage at the more substituted bond, whereas chlorine attacks mainly the C−H bond. Furthermore, the ring opening by Cl_2 is nonselective. The C−H bond of the methyl group is somewhat weaker than the ring C−H groups, which accounts for the preferential chlorination at the methyl group. This difference is due to the small endothermicity of the C−H abstraction by Br·.

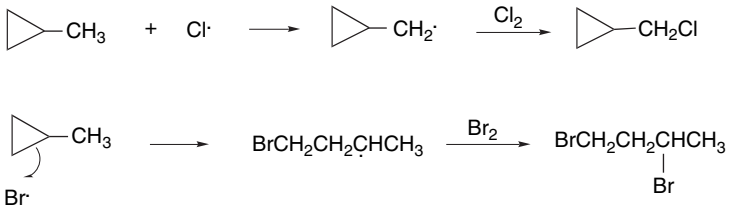

11.15. The cyclization product must form at the radical stage. The hydrocarbon is a mixed coupling product with methyl derived from acetate. The ester arises from a rearranged carbocation. The rearrangement most likely occurs at the carbocation rather than at the radical stage.

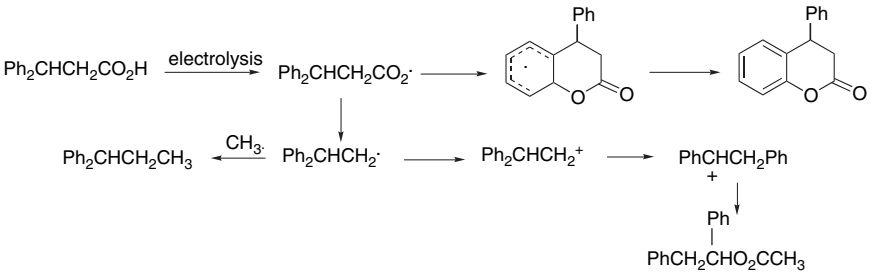

11.16. a. Although this reaction involves an anion-radical coupling, it is not an $S_{RN}1$ chain mechanism. The $Fe(CN)_6^{3-}$ oxidant is used in excess and oxidizes both the nitronate anion and the product of the radical-cyanide coupling.

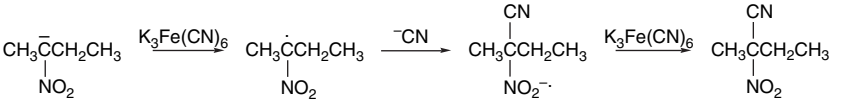

b. This reaction occurs by an $S_{RN}1$ chain process. The dialkyl phosphite anions are good electron donors as well as nucleophiles. A noteworthy feature of the reaction is the elimination of sulfinate rather than nitrite ion from the intermediate radical anion.

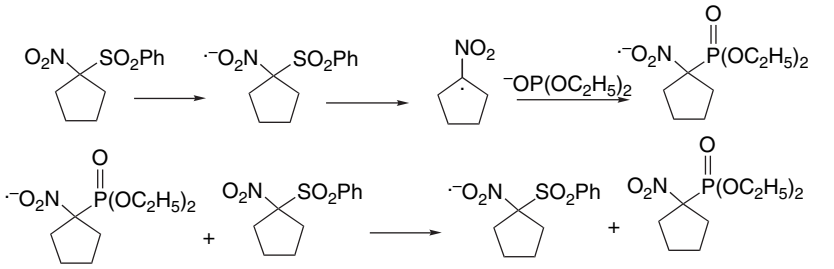

c. This reaction, which is initiated by photolytic decomposition of the organomercury compound, can continue by a $S_{RN}1$ radical chain mechanism.

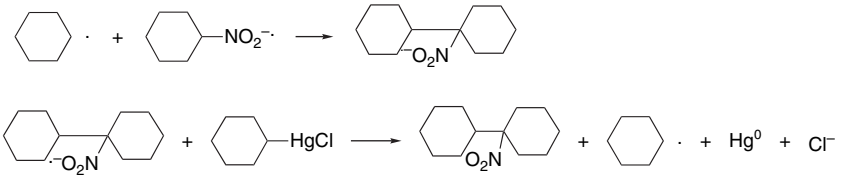

11.17. The α position is potentially stabilized by capto-dative interaction between the amino and ester substituents. The order of reactivity suggests that substitution

is destabilizing. It has been suggested that the α-alkyl substituent inhibits the planarity required for capto-dative stabilization.

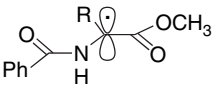

11.18. Application of the relationship $BDE = PA + IP - IP_H$ gives the following BDE and RSE relative to methyl are obtained. The results are in generally good agreement with those in Table 3.20, showing substantial stabilization for the benzyl and allyl radicals and destabilization for the vinyl and cyclopropyl radicals. All of the cyclic polyenes show substantial stabilization in the order $7 > 5 > 3$, which indicates that there is no aromatic/antiaromatic relationship for the conjugated cyclic radicals. According to HMO orbitals, the SOMO orbital is antibonding for the seven- and three-membered rings, but slightly bonding for the five-membered ring. The apparent stabilization order is consistent with HMO calculations, which give 1.0β, 1.85β, and 2.54β as the delocalization energy for the cyclopropenyl, cyclopentadienyl, and cycloheptatrienyl radicals, respectively.

	BDE	RSE
$PhCH_2—H$	87.4	16.6
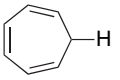	76.4	27.6
	83.4	20.6
	90.4	13.6
$CH=CHCH_2—H$	90.4	13.6
	105.4	–1.4
$CH_2=CH—H$	111.4	– 7.4

11.19. a. This reaction can occur by thiyl radical addition, cyclopropylcarbinyl radical opening, addition to methyl acrylate, a 5-*exo* cyclization and elimination of the thiyl radical.

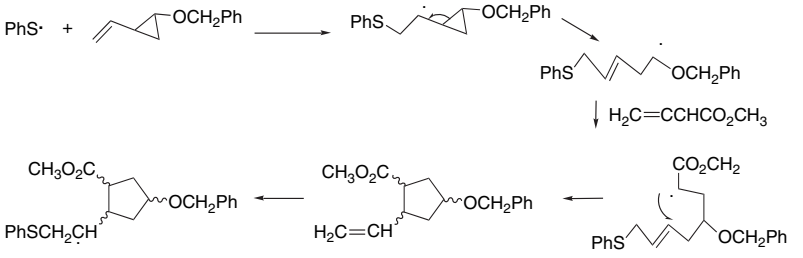

b. The addition of a dimethyl malonyl radical to the double bond is followed by a rearrangement via a cyclopropyloxy radical (acyl group migration).

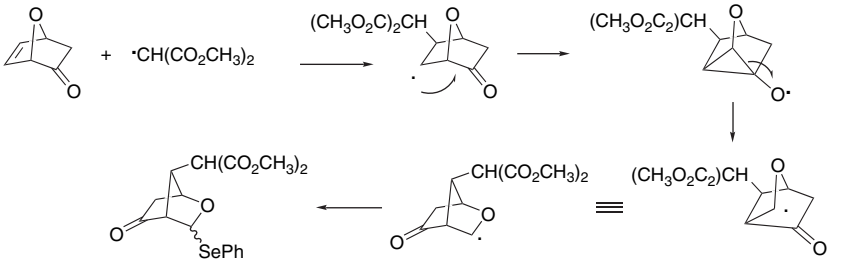

11.20. According to the computations the fragmentation of the 1–4 bond is favored for the bicyclo[2.1.0]pent-2-yl radical **1**. It is thermodynamically favorable and has a low activation energy. Rupture of the 1–4 bond relieves the strain in both rings. The reaction is a cyclopropylcarbinyl ring opening.

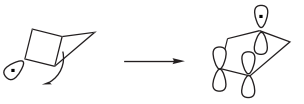

1 **1c**

None of the fragmentations of the bicyclo[2.1.0]pent-1-yl radical **2** are computed to be favorable in terms of $\Delta H^{\ddagger}$. There is poor alignment of all three β, γ bonds.

2

Fragmentation of the bicyclo[2.1.0]pent-5-yl radical **3** is calculated to be thermodynamically and kinetically favorable. It relieves the strain in both rings.

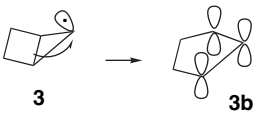

3 **3b**

There is poor overlap with the β, γ bonds in both the 1- and 2-bicyclo[1.1.1]pentyl radicals **4** and **5** and although the ring openings are thermodynamically favorable, they have significant kinetic barriers. The later (1995) computations indicate a destabilization of the fragmentation transition state by antibonding interactions in these radicals.

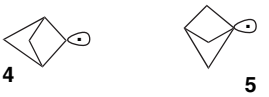

4 **5**

11.21. The stereoequilibration must involve rupture of a cyclopropyl bond. This 1,3-diradical must have a sufficiently long lifetime to permit bond rotation. Cleavage of the C(1)−C(4) bond would generate a diradical that can fragment to the 1,4-diene product. The bicyclo[3.2.0]heptane derivatives must form by hydrogen abstraction. The fact that there is no intermolecular deuterium scrambling means that the reaction must occur by an intramolecular process. This indicates that the 1,4-diradical has a finite lifetime.

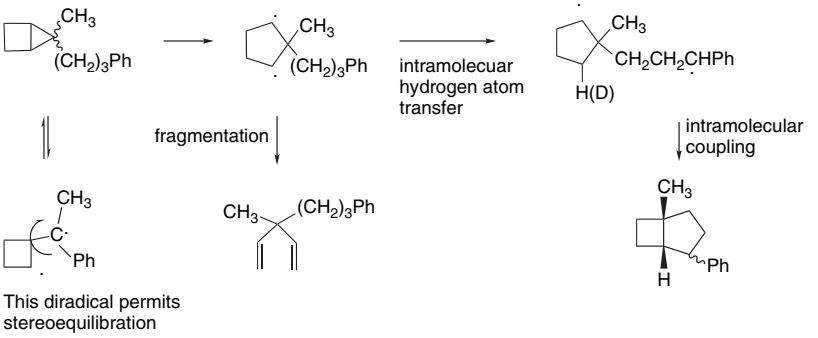

Chapter 12

12.1. This issue could be approached by isotopic labeling in the side chain to determine if the two methylene groups become equivalent, as required by the intermediate. Use of ^{14}C labeling indicated no interchange of the two carbons, ruling out the symmetrical bridged radical.

12.2. a. Orbital symmetry considerations predict a conrotatory ring opening and this is observed.

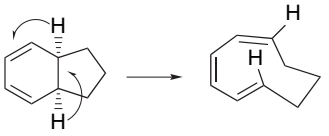

b. Photolysis would be expected to lead to photocyclization of the two vinyl substituents. Two modes are possible and the head-to-tail mode predominates by 10:1.

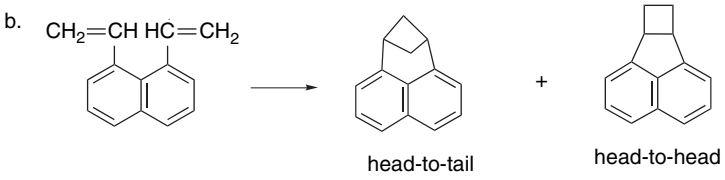

c. The product results from disrotatory electrocyclization.

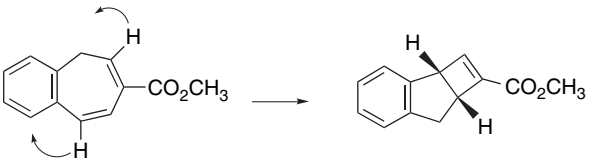

d. The product results from conrotatory opening of the cyclohexadiene ring.

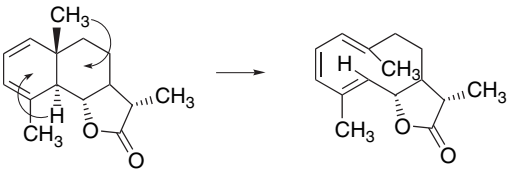

e.,f. The reactions are disrotatory electrocyclizations.

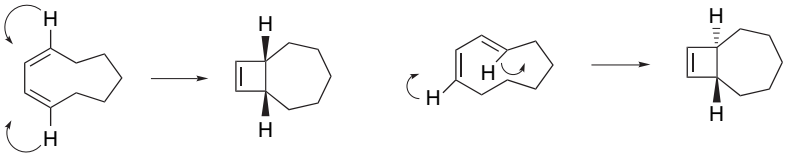

12.3. a. This result indicates that there is a triplet state accessible by photosensitization and that, as with simple alkenes, rotation can take place at one of the double bonds, leading to formation of the enantiomer.

b. **3-C** is the product of disrotatory electrocyclization, whereas **3-B** results from the conrotatory diene → triene interconversion. The triene absorbs much more strongly than the diene at 300 nm and therefore is a minor component of the photostationary state, allowing the reaction to proceed to the electrocyclization product.

c. The reaction is proposed to occur by photocyclization of a quinodimethane intermediate generated by acid-catalyzed opening of the dioxolane ring. This intermediate can undergo an electrocyclization. After ketonization, a new quinodimethane intermediate is formed, which can lead to reclosure of the dioxolane ring.

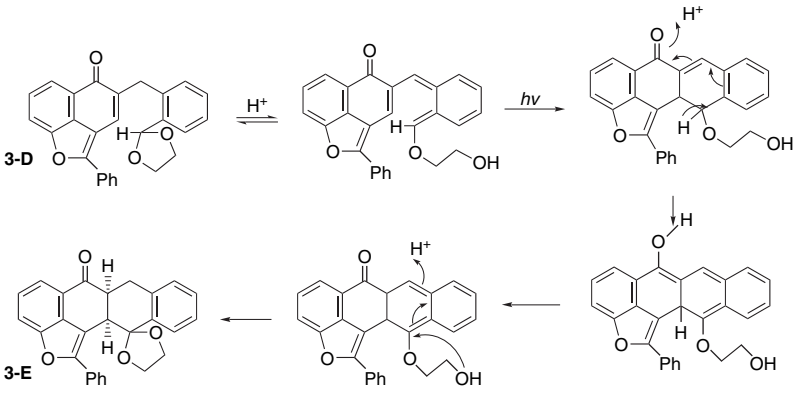

12.4. a. The initial step is α-cleavage. The products are then formed by intramolecular hydrogen atom abstraction, leading to the conjugated dienal, and a 3,5-pairing that gives rise to a ketene intermediate that is trapped as the ester.

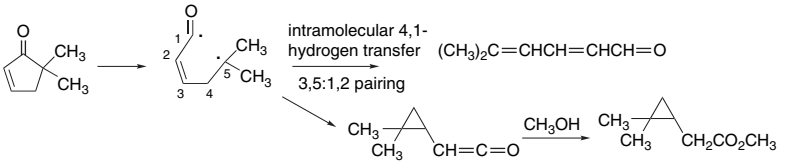

b. This is an intramolecular addition of the alkene to the aromatic ring with 2,6-pairing.

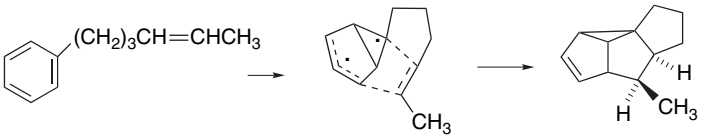

c. This product results from intermolecular hydrogen atom abstraction, followed by radical recombination.

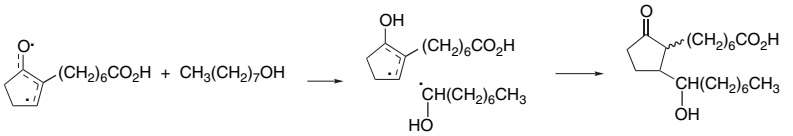

d. This rearrangement can occur by 5,6-cleavage followed by 3,6-coupling. The distribution of the trideutero methyl groups indicates that the reaction proceeds through a diradical intermediate that is sufficiently long-lived for free rotation of the isopropyl group.

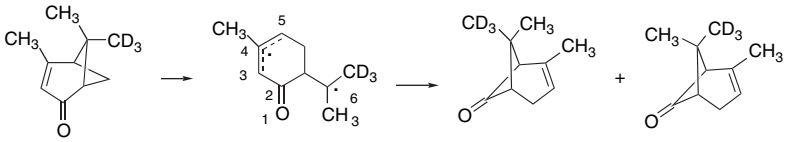

e. This ring expansion and nucleophilic addition can be formulated as occurring through an oxacarbene species.

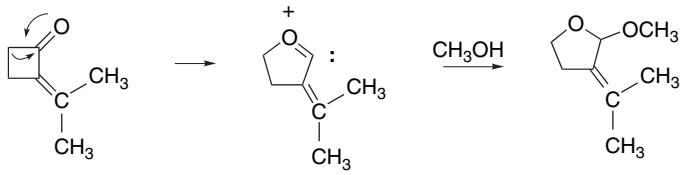

f. The altered course of the reaction in acidic solution indicates that the reaction may proceed through a protonated intermediate. In neutral solution the reaction results from a [2 + 2] electrocyclization.

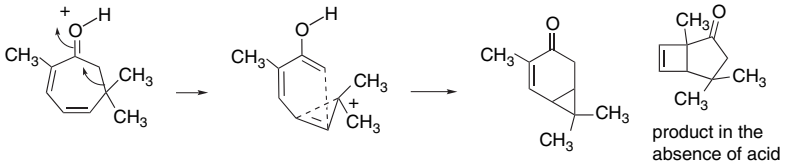

g. This rearrangement reaction has been proposed to occur via an initial bonding between the aromatic ring and the terminal carbon of one of the ethylene groups.

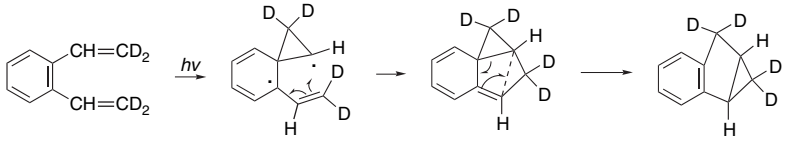

h. The product results from 1,5:2,6-pairing in the initial triene system. It is an intramolecular example of the bicyclo[3.1.0]hex-2-ene ring closure seen in acyclic analogs.

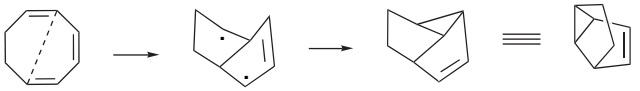

i. This is an oxa-di-π-methane rearrangement.

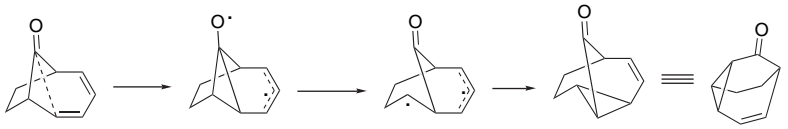

j. This is an oxa-di-π-methane rearrangement.

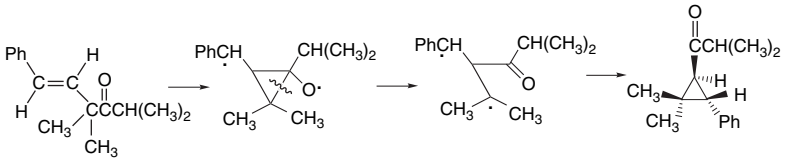

k. This transformation occurs by intramolecular hydrogen atom transfer and 1,4-diradical cleavage. Although the oxygen appears to be in close proximity to the hydrogen, the alignment is not ideal and the reaction has a relatively low quantum yield.

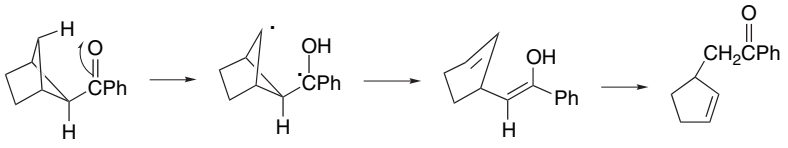

l. This reaction can occur by a six π-electron electrocyclic ring opening, followed by addition of water to the ketene that is produced. It is not clear from the original report if the *Z*-configuration of the 3,4-double bond is retained.

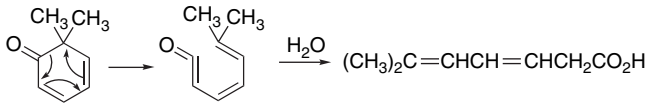

m. This reaction involves α-cleavage, followed by decarbonylation and fragmentation of a cyclopropyl diradical.

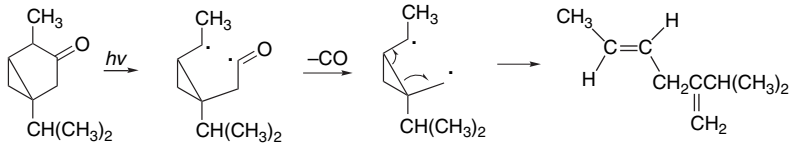

n. This product can be formed by a [2 + 2] addition of dimethyl acetylenedicarboxylate to the benzene followed by an electrocyclic opening of the cyclobutene ring. The ring opening must be disrotatory and can be regarded as a thermal opening of the cyclohexadiene ring or a photochemical opening of the cyclobutene ring. This facet of the reaction does not seem to have been established.

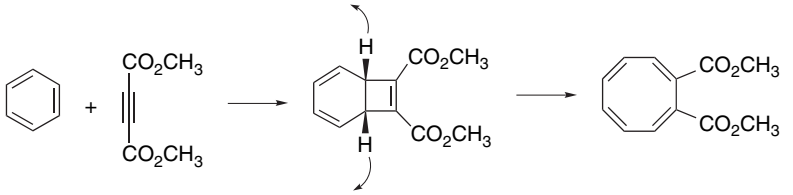

o. This reaction is believed to occur through an oxetene intermediate formed by a Paterno-Buchi reaction with the alkyne. The ring opening, which is highly favored thermodynamically, is probably a thermal reaction.

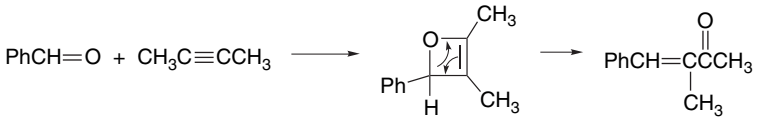

12.5 These reactions can be expected to proceed by protonation of the strained *E*-cyclohexene structure. The authors suggest intramolecular participation in this process, leading to the observed stereoselectivity. The regiochemistry can also be interpreted in terms of ring opening of an oxonium ion intermediate. The major product is the 4-acetoxy isomer, which corresponds to the favored diaxial opening of a three-membered ring. The original formulation involved

participation by the methoxy oxygen, but a similar mechanism involving the carbonyl oxygen might also be feasible.

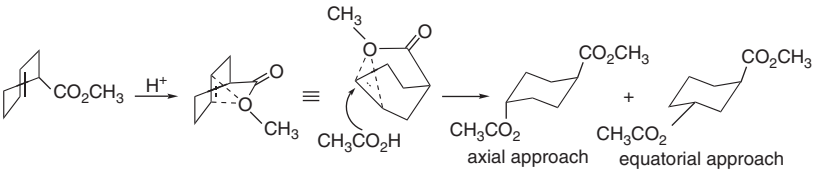

12.6. The product can be formed by an α-cleavage, followed by an intramolecular hydrogen atom transfer. The isotope effect is 1.07, which is quite small for a primary effect. The low value indicates a very early transition state, which would be expected for a reaction involving the weak C−H(D) bond β to a radical.

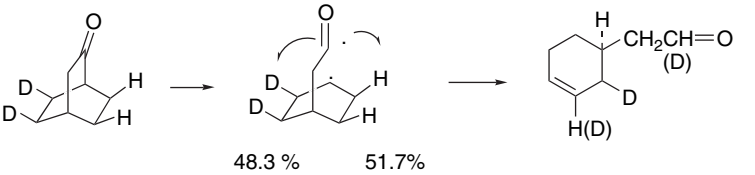

12.7. The contrast between the direct and photosensitized reactions suggests that the di-π-methane rearrangement in this case involves the triplet state. The transformation to benzocyclooctatetraene occurs via bridging between the aryl and vinyl groups. The minor route leading to 3,8-di-labeling proceeds by vinyl-vinyl bridging. The di-π-methane rearrangement could proceed by vinyl-vinyl or vinyl-benzo bridging. The isotopic labeling shows that the former is preferred.
Benzocyclooctatetraene formation:

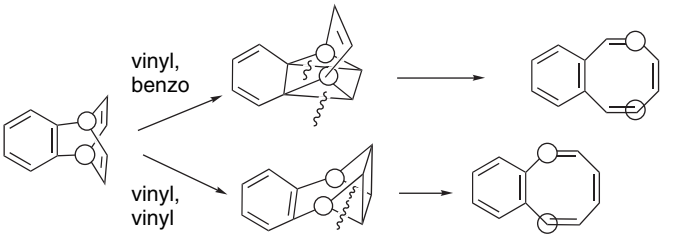

Benzosemibullvalene formation:

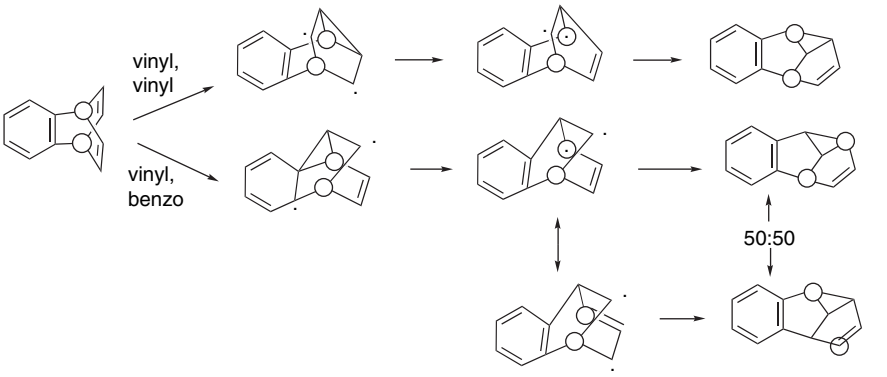

12.8. The total quantum yields, 1.04 and 0.99, account for all the photochemistry. The racemization provides a measure of the extent of back transfer of hydrogen from the intermediate diradical. The alcohol evidently extends the lifetime of the radical, perhaps by solvation, so that fragmentation becomes dominant.

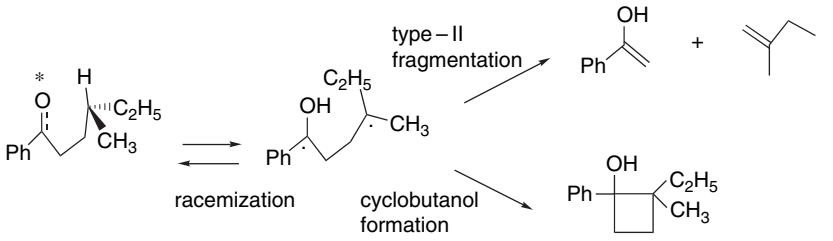

12.9. As shown in Figure 12.P9, the T_1 state is generally lower in energy than the S_1 state and relaxes to a higher-energy point on the S_0 surface. As a result, the shift is greater for phosphorescence than for fluorescence.

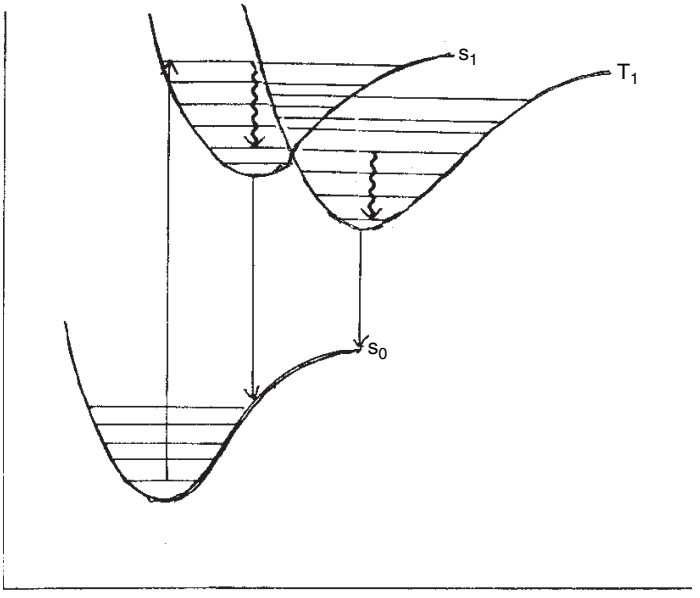

Fig. 12.P9. Diagram showing the relationship between fluorescence and phosphorescence.

12.10. This difference can be accounted for by the differing orientation of the side chain in the two stereoisomers. Assuming an $n - \pi^*$ transition, the electron deficiency is in the plane of the carbonyl bond. The *cis* side chain is favorably oriented toward the oxygen for facile hydrogen transfer and fragmentation. The *trans* isomer is less favorably oriented. The racemization presumably occurs by

α-cleavage and recombination, unless there is a nonphotochemical enolization mechanism operating.

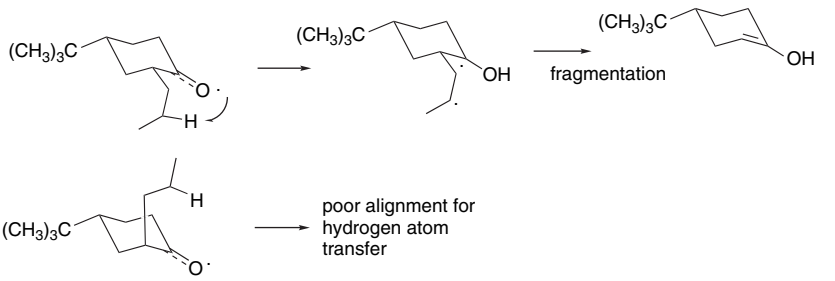

12.11. This example provides a good illustration that the reaction does not proceed through a thermally equilibrated excited state, since both isomers would give rise to the same 90° minimum energy structure. The results are consistent with the ideas discussed in connection with the butadiene energy surface (p. 1140), which indicate that conical intersections determine efficiency of product formation. There should be more of the *s-cis* conformation present for the *E*-isomer, since the methyl group causes steric interactions in the *s-cis* conformation of the *Z*-isomer. The *s-cis* conformation is required for cyclization. Formation of the dimethylcyclopropene product requires 2,4-bridging and a hydrogen shift. The 2,4-distance is not as sensitive to the rotational change.

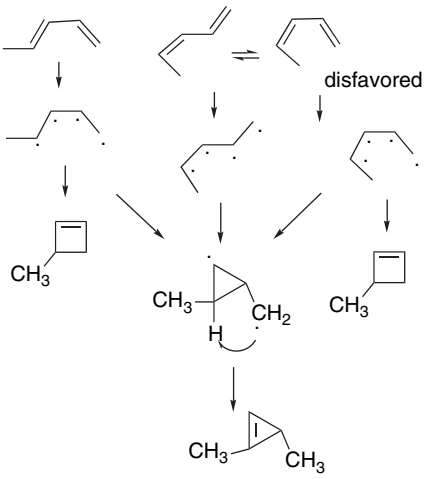

12.12. The first step is an internal [2 + 2] cycloaddition. The second step can occur by a reaction sequence that initially resembles a di-π-methane rearrangement but then undergoes an acyl shift prior to cyclopropyl diradical fragmentation. The acid-catalyzed step is a reverse aldol addition triggered by protonation of the enol ether.

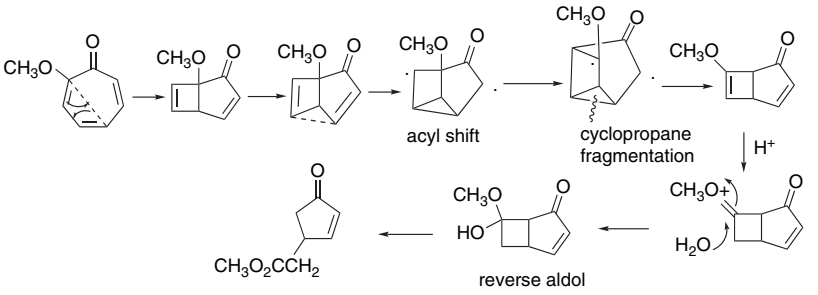

12.13. Cyclobutane formation can occur by a C(4)−C(5) bond fragmentation. This would be facilitated by the radical-stabilizing aryl substituents. The observed racemization is consistent with an achiral intermediate and inconsistent with a concerted process. The phenyl migration product **E** can be formed by a 3,4-hydrogen shift. Product **F** can result from the di-π-methane (type B) cyclohexenone rearrangement. This mechanism is not available to compound **B**, which has only a saturated substituent at C(4).

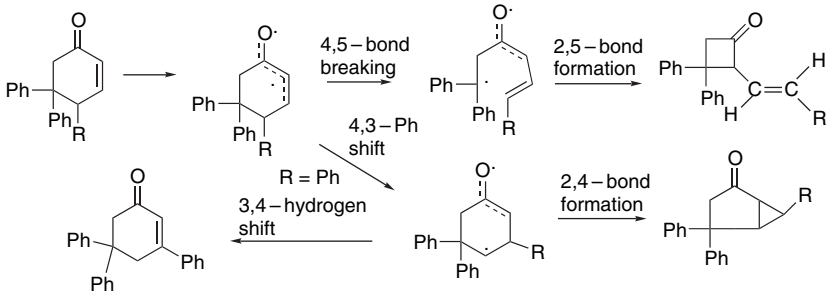

12.14. This is the stereochemistry predicted by a concerted migration process.

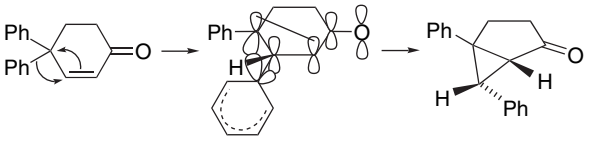

12.15. A cyclohexadiene → hexatriene conversion/reversion accounts for the photochromic behavior. Although the product is enolic, and could conceivably revert to a less conjugated dione, the β-carbonyl group is presumably effective at stabilizing the enol form.

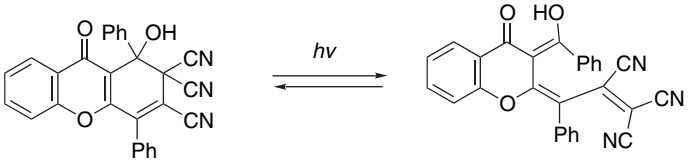

12.16. These results are consistent with conformational control of the reactivity of the excited state and diradical intermediates. The two *t*-butyl derivatives will be overwhelmingly in the conformations shown. The axial benzoyl group is

favorably disposed for hydrogen abstraction and recombination to a cyclobutanol. The equatorial benzoyl group is less well positioned for hydrogen abstraction and reacts by α-cleavage and partial recombination. The unsubstituted system has both conformers present and can follow both reaction pathways.

Hydrogen-abstraction/recombination pathway for axial benzoyl.

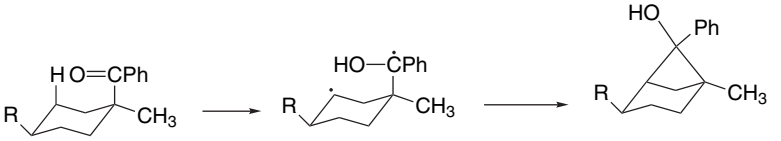

α-Cleavage and recombination pathway for equatorial benzoyl.

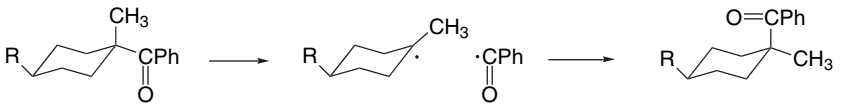

12.17. The azo compounds have a concerted mechanism available for formation of the barrelene structures **17-C** and **17-E**. Thus they are not necessarily good models for a singlet diradical. The photosensitization results indicate that the *T* excited state provides access only to the semibullvalenes **17-D** and **17-F**. The direct photolysis results might suggest that the *S* state could give rise to both products or that there is $S \rightarrow T$ intersystem crossing. These issues have not been definitively established, but in the original paper the authors comment on the "tight" and "loose" character of the *S* and *T* excited states, respectively. The *S* structure can be depicted as a singlet cyclopropyl diradical and the triplet as an allylic radical.

12.18. The difference between the direct and photosensitized reactions suggest that **18-A** and **18-C** are triplet products, whereas **18-B** is a singlet product. Products **18-A** and **18-C** can be accounted for by the di-π-methane mechanism, with **18-C** being formed by fragmentation rather than recombination. Product **18-B** can result from a phenyl migration resulting from vinyl-phenyl bridging. An alternative di-π-methane product, **18-D**, is missing, presumably because of the preference for formation of the aryl stabilized diradical.

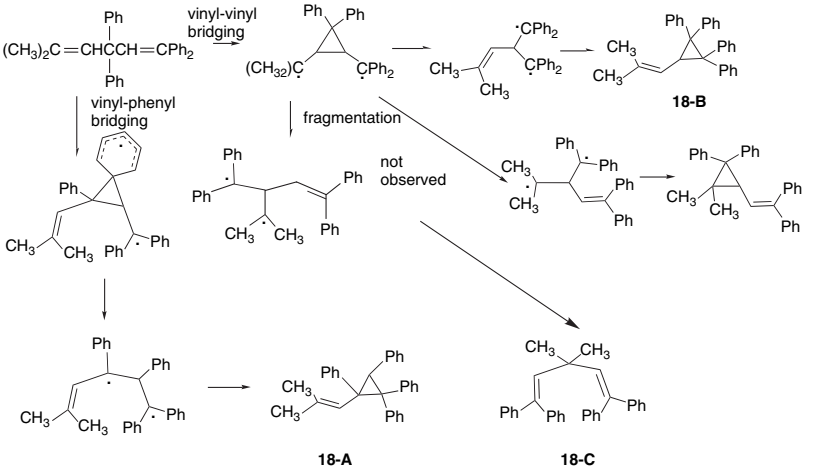

12.19. These products can all be accounted for by an initial β-hydrogen abstraction, followed by alternative rebonding patterns.

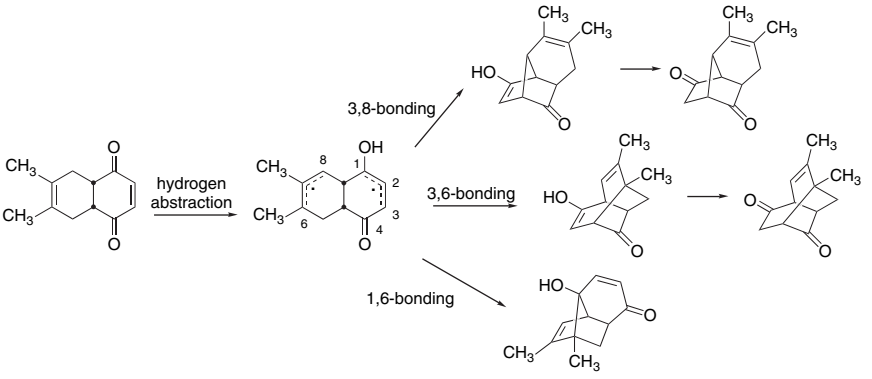

12.20. Although the difference in composition is not extreme, the results suggest that the sensitized triplet reaction gives more of the more stable *exo* product. This could be described in terms of a tighter excited state (or conical intersection) leading to a dominance of the *endo* isomer, whereas a looser more flexible (and longer-lived) triplet state adopts a geometry influence by the relative stability (strain) of the two structures.

12.21. These data show some very strong directive effects for quite similar substituents. The guiding principle for regioselectivity in the di-π-methane rearrangement is the radical-stabilizing effect of the substituents. Beyond that, it has been suggested that there is a polar effect as well, indicating that there is some increase of electron density in the cyclopropyl diradical intermediate, in which case EWG > ERG. For the two monosubstituted cases, the radical-stabilizing and EWG effects would be synergistic and complete selectivity is observed. The CO_2CH_3 > $CON(CH_3)_2$ and $CSOCH_3$ > CO_2CH_3 selectivities can be rationalized by the greater EWG effect of the amide and the greater radical stabilizing effect of $CSOCH_3$. The radical-stabilizing effect of phenyl is evident in

the last entry. The very high regioselectivities are quite impressive, especially considering that they are directing the reactivity of highly reactive species.

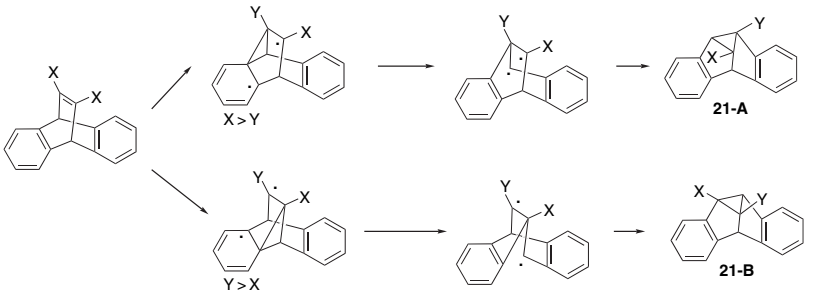

12.22. This reaction has been shown to be quite general for enynes and is not restricted to the cyclic example shown. It has been suggested that it might proceed through cycloaddition to a cyclobuta-1,2-diene.

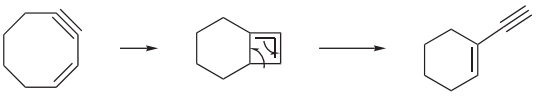

12.23. These results can be explained by conformational control of competing hydrogen abstraction and fragmentation. In the unsubstituted compound the benzoyl substituent will occupy an equatorial position and hydrogen abstraction is not favored. As a result, fragmentation occurs, leading to the observed ring-opened product. When an alkyl substituent is present, the benzoyl group can occupy an axial position, which is favorable for H abstraction from C(4). This leads to cyclobutanol ring formation and eventually, to the rearranged product.